THE INSTITUTE & FACULTY OF ACTUARIES

SA0 THESIS

Cause-of-Death Mortality Modelling and Population Projection in Kenya

---

Titus Kipkoech ROTICH, PHD

Research School of Finance, Actuarial Studies and Statistics
College of Business and Economics
THE AUSTRALIAN NATIONAL UNIVERSITY

A thesis submitted for SA0 of The Institute & Faculty of Actuaries

April, 2025

Declaration of Authorship

I, Titus Kipkoech ROTICH, declare that this thesis titled, "Cause-of-Death Mortality Modelling and Population Projection in Kenya" and the work presented in it are my own. I confirm that:

- This work was done wholly by me.
- Where I have consulted the published work of others or quoted from their work, this is always clearly attributed, and the source is always given. With the exception of such quotations, this thesis is entirely my own work.
- Where the thesis is based on work done by myself jointly with others, I have made clear exactly what was done by others and what I have contributed myself.

Titus Kipkoech ROTICH

Abstract

Life expectancy in Sub-Saharan Africa has risen sharply over recent decades, with Kenya experiencing annual increases of 0.88 years over the last two decades. However, mortality modelling and forecasting for the region remain underexplored, exacerbated by limited availability of age-specific mortality data. This dissertation addresses these challenges by applying a novel approach to cause-of-death (CoD) mortality modelling using Kenyan data from 1990 to 2017.

A constrained penalised splines (CPS) model is applied, offering flexibility to incorporate expert judgment and historical trends, thereby improving forecast accuracy, particularly for causes with irregular mortality patterns. Compared to conventional models such as the Lee-Carter (LC) and penalised splines (PS) models, the CPS model demonstrates versatility and coherence in reconciling individual CoD and aggregate mortality projections. Additionally, measures of lifespan, mean lifespan and lifespan variation are calculated, with projections indicating an average life expectancy of 73.3 years, surpassing United Nations estimates of 70.0 years.

Population projections are derived using the population equilibrium equation and compared against official estimates from the Kenya National Bureau of Statistics, further validating the model's robustness. Projected population pyramids are presented.

These findings underscore the utility of CoD modelling in providing a deeper understanding of mortality drivers and improving projections relevant for public health planning and life insurance product development. By presenting a transparent methodology for mortality data preparation, extrapolation, and forecasting, this research contributes valuable insights and practical tools for mortality modelling in low- and middle-income countries.

Contents

List of Figures

List of Tables

Chapter 1

Introduction

Mortality investigation has been the centrepiece of most actuarial research in recent decades. Given unprecedented improvements in mortality experience, actuaries, alongside demographers, have put substantial effort into modelling and forecasting mortality with an acceptable level of precision.

One of the main risks faced by life insurers is mortality risk. Most studies have focused on measuring and forecasting mortality trends, intending to price for it accurately. Mortality trends are also vital in government planning and budgeting. For example, Tuljapurkar et al. (2000) noted that the financing of healthcare especially at old ages, would be driven by ageing baby boomers and primarily by a sustained increase in human lifespan.

For instance, the life expectancy in sub-Saharan Africa has sharply increased from 50.45 years in 2000 to 61.27 years in 2017, translating to an approximately 0.64 yearly increment (WB, 2020). Kenya has experienced one of the fastest life expectancy increases within this region, with a 0.81 yearly increment over the same period. As people continue to live longer, the uncertainty on the implications of an ageing population increases, as does mortality forecasting uncertainty (Horiuchi & Wilmoth, 1997).

This issue is further exacerbated by irregularities in mortality patterns and improvements over time (Tuljapurkar & Boe, 1998), a phenomenon explored by Tuljapurkar et al. (2000) in an analysis of mortality patterns from the seven most economically developed countries, the G7,[1] over 5 decades from 1950-1994.

Mortality modelling has a direct and vital application in population projection as well. Being able to forecast population changes accurately is important for resource allocation as well as for anticipating and planning future healthcare needs (Vollset et al., 2020). Given that mortality, fertility, and migration are key drivers of any population change, an improvement in mortality modelling precision often directly translates to a significant improvement in the precision of population projections.

Arguably, mortality modelling is a centrepiece in population projections, which are crucial elements of government budgeting and tracking development. Since population estimates

[1] Canada, France, Germany, Italy, Japan, United Kingdom (UK) and United States of America (USA).

are commonly used as the denominator in most economic, demographic, and epidemiological indicators, their accuracy is essential.

Most government agencies, commonly the National Bureau of Statistics, produce population projections that aid the government in budgeting, planning, and resource allocation. However, these projections are sometimes based on over-simplified approaches, such as linear extrapolation. While these estimates may serve general purposes, some applications require more accurate estimates.

For instance, the accurate estimation and projection of mortality trends and population by age and gender are critical in healthcare financing because healthcare costs vary substantially across age and gender. A country with an ageing population spends significantly more on healthcare than a youth-populated country, all other factors being equal. Additionally, analysing mortality by cause of death can provide insights into progress in achieving global goals such as the elimination of malaria (see World Health Organisation [WHO], 2019), informing policy and targeted funding requirements.

In contrast, inconsistent methods of mortality and population estimation and projection may provide a false alarm of a decline or increase in such indicators. Changes may, for example, be purely due to overestimation or underestimation, affecting the tracking of development goals such as the rallying for universal healthcare coverage (UHC) by 2030 (see WHO, 2019).

In addition to the factors stipulated by Tuljapurkar et al. (2000), recent mortality studies have focused on older adults due to significantly reduced mortality at younger ages (Andreev, 2004) and rapid improvements at older ages (Terblanche & Wilson, 2015a). These studies assume the availability of mortality data, but there is a paucity of research for cases without sufficient data. Additionally, most mortality studies have been based on developed countries, with limited literature on developing countries.

Given global policies and goals such as UHC (WHO, 2019), the need for accurate models that reflect developing countries' circumstances is becoming increasingly important. While mortality data for younger and adult ages can be obtained or estimated for developing countries, older age ranges present the biggest challenge due to a lack of reliable mortality data, and proxies for their approximations are often either unavailable or highly unreliable.

Various models have been applied to mortality modelling and forecasting, leveraging trends underlying observed mortality improvements (e.g. see Booth & Tickle, 2008; Cairns et al., 2008, 2009; Dowd et al., 2010, among others for a detailed review). These models have been extended to cause-of-death (CoD) mortality to identify the key drivers of mortality improvements observed in all-cause mortality (see Li et al., 2019, and references therein). However, while forecast reconciliation approaches attempt to reconcile all-cause and CoD mortality forecasts (Hyndman

et al., 2011; Wickramasuriya et al., 2018, see methodology review), they sometimes produce implausible forecasts due to rigid modelling structures.

Incorporating expert opinion on past mortality patterns and anticipated future medical breakthroughs could significantly improve the accuracy of CoD forecasts. Recently, methods that combine well-established smoothing models with prior demographic information have been proposed (see Camarda, 2019, for a comprehensive methodology review). When applied to all-cause mortality, these methodologies result in improved forecasts with plausible age profiles and time trends (Camarda, 2019). This thesis investigates whether applying Camarda's methodology to CoD mortality, alongside forecast reconciliation approaches, improves mortality forecast and population projection accuracy.

CoD mortality modelling has garnered increased research attention due to its potential to provide deeper insight into mortality drivers. However, modelling mortality by cause introduces noise into the model (Li et al., 2019). A balance between noise and the amount of information harnessed by cause-specific modelling is necessary.

This thesis makes several contributions to the literature and actuarial practice. Firstly, it develops methodologies to address data availability challenges for older adults in developing countries, using Kenya as a case study. We propose methods for imputing missing demographic data. By applying Camarda (2019)'s Constrained Penalised Splines (CPS) model to CoD, we demonstrate that constraining future CoD mortality patterns within plausible age profiles and time trends improves forecast accuracy for mortality causes with irregular patterns. Additionally, applying CPS to individual causes and aggregate mortality, and subsequently applying forecast reconciliation approaches ensures forecast coherence. To the best of our knowledge, this is the first study applying this methodology to CoD mortality data and to Kenyan data.

Most recent mortality research focuses on developed countries, with limited literature on developing countries. Given UHC goals (WHO, 2019) and rapid life expectancy changes in developing countries (WB, 2020), the need for accurate models tailored to developing countries is crucial. Infant mortality remains persistently high in these countries compared to developed countries (see Figure 1.1[2]), necessitating appropriate mortality models. Using a modified age domain basis, and following common life table practice (Chiang, 1984), we separate infant mortality from other ages, leading to more accurate infant mortality modelling.

Finally, we apply the CPS model to calculate two lifespan measures. We show that applying CPS models leads to an increase in projected average life expectancy by 3.3 years (to 73.3) compared to the United Nations (UN) estimate of 70.0, with potential implications for government costs and policy settings. We illustrate an application of the proposed CoD model by estimating a

[2]Combined infant mortality per a thousand live births in Kenya and five other countries: Australia, Nigeria, South Africa (SA), United Kingdom (UK) and the United States of America (USA) from 1960 to 2019. Data Source: (The World Bank, 2021).

population projection model for Kenya, producing future population estimates and offering policy recommendations.

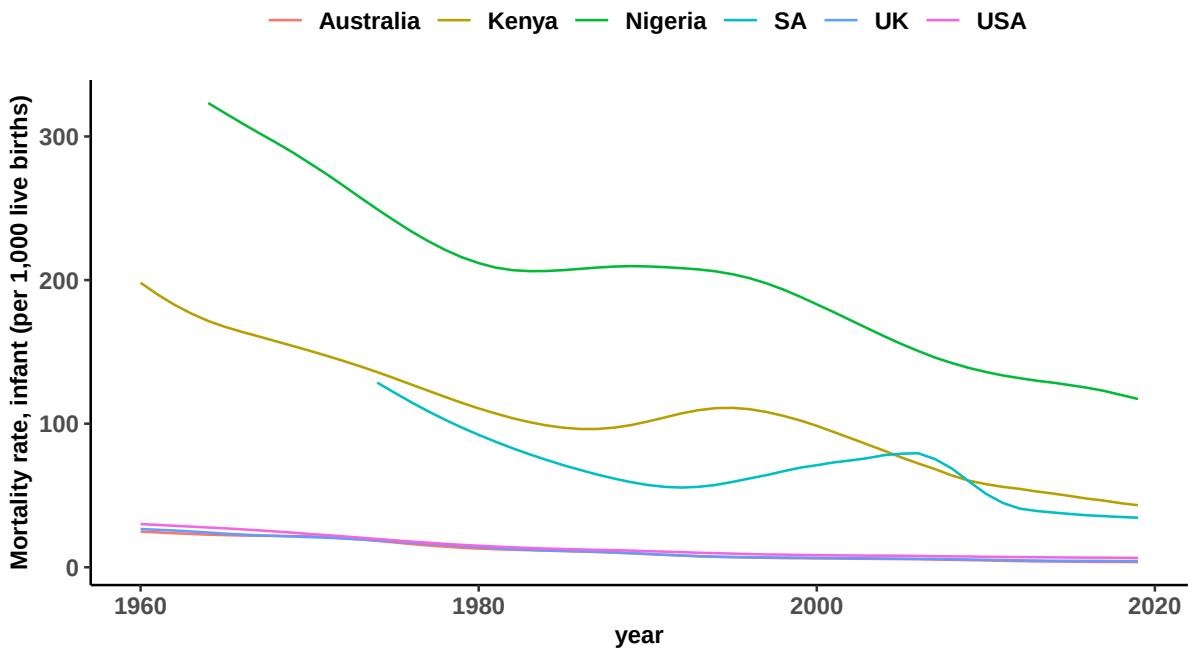

FIGURE 1.1: Infant mortality per a thousand live births. Data Source: (The World Bank, 2021).

The rest of this thesis is structured as follows. Chapter (2) outlines the data sources and methodologies employed in this study. Specifically, Section (2.1) describes the data used and the classification of CoD adopted. Since the data obtained were not initially in a suitable format for mortality modeling, Section (2.2) discusses the preprocessing techniques applied. Additionally, given the limited availability of data at older ages, this Section also details the methods used to estimate mortality rates in these age groups. Finally, we introduce the models employed for estimating and forecasting mortality in Kenya.

Chapter (3) presents the results of the preliminary analysis of Kenyan mortality, as well as the outcomes of the mortality modeling and forecasting process. This Chapter begins with an exploration of historical mortality and population trends in Kenya, including the use of Lexis diagrams to visualize demographic changes over time. This is followed by an analysis of cause-specific mortality trends to examine how different causes of death have evolved.

An important aspect of mortality modeling involves assessing potential structural changes in mortality patterns before fitting the models. This is addressed in Section (3.1.5). Next, in Section (3.2), we describe the CoD mortality modeling process, starting with the selection of an appropriate fitting period and proceeding with model estimation based on the approaches discussed in Chapter (2). These models are then evaluated using out-of-sample performance

measures, with results presented in Section (3.2.3). Based on these assessments, the most suitable models for forecasting CoD mortality in Kenya are selected, as discussed in Section (3.2.4).

Using the selected models, we generate CoD mortality forecasts for Kenya, with results detailed in Section (3.3). One key application of mortality modeling is population projection, which is one of the primary objectives of this thesis. Accordingly, we apply our models to project Kenya's population up to 2042, as discussed in Section (3.4). To facilitate visual inspection of projected demographic changes, we construct population pyramids. Additionally, we compare our projections with those produced by the United Nations, analyzing results separately for males and females.

A major contribution of this thesis to the literature and actuarial practice is the application of the CPS model to CoD mortality modeling. Specifically, we explore the use of constraints in mortality models to incorporate expert judgment regarding mortality patterns and age profiles. The implications of these constraints are examined in detail in Chapter (4). We demonstrate how constraints can be appropriately selected to replicate the outcomes of more restrictive models, such as the Lee-Carter model, or more flexible approaches, such as P-splines.

Finally, Chapter (5) provides a summary of the key findings, discusses their practical applications, outlines the limitations of this research, and proposes avenues for future research.

Chapter 2

Data and Methodology

This chapter presents the data sources and methods used in this thesis. The chapter is organised as follows: First, Section 2.1 discusses the data sources for our research and outlines the CoD classification utilised. Next, Section 2.2 provides a summary of the methods utilised.

2.1 Data

This section describes the data. Firstly, we provide a list of the data sources considered in Section 2.1.1, with a justification for the ultimate data source used. A description of the CoD data used in our analyses is then outlined in Section 2.1.2. We conclude this section with a detailed discussion of the CoD classifications of the data obtained in Section 2.1.3.

2.1.1 Data Sources

Data for both males and females were utilised. The data sources considered for this study included United Nations' Population Division (UNPD, 2019), WB (2019), Knoema (2018), Kenya National Bureau of Statistics (KNBS, 2020), sourceAFRICA (2018), the GBD (2017), openAFRICA (2020), and the WHO (2020) databases. Other than the GBD, the other sources' data were non-replicable due to either a lack of transparency on assumptions and methodology or a high level of subjectivity applied to the process of collating the data and providing the estimates.

Therefore, data from the GBD are preferred because they are replicable, and the process used in estimating the data is transparent in comparison to all the other possible data sources that we have already outlined.[1] In addition, uncertainty intervals are also provided for the estimates, making it easy to check the reliability of the methods and the data. The GBD committed to the GATHER[2] (Stevens et al., 2016). Finally, the CDC Kenya uses GBD data as the source for its

[1] The GBD (Global Burden of Disease) is a project led by the Institute for Health Metrics and Evaluation (IHME) at the University of Washington. The IHME is an independent global health research organization that provides comparable measurements of the world's most important health problems and evaluates the strategies used to address them (of Washington, 2021). The data used in this research is publicly available and can be accessed through the Global Health Data Exchange (GHDx; GBD, 2017). The GBD project collects and collates data on causes of death and non-fatal health outcomes from various sources, including vital registration systems, verbal autopsy studies, and disease-specific registries. More information on the data collection methods and assumptions can be found in the GBD documentation (Institute for Health Metrics and Evaluation [IHME], 2021).

[2] **G**uidelines on **A**ccurate and **T**ransparent **H**ealth **E**stimates **R**eporting.

"Top 10 Causes of Death in Kenya" list. Data from the other sources were also obtained and used for reasonableness checks and filling in data gaps that existed.

2.1.2 Cause-of-Death Data

By-cause data for the full list of causes of death in Kenya were obtained from the GBD. Data over 28 years, from 1990 to 2017, were utilised in this research. The death data are available in the following age groups: birth, early, late, and post-neonatal, 1-4 age range, 5-year age intervals from 5 to 94 years, and a final open interval of 95+ years.

Moreover, population counts data are available in the intervals: birth, early, late, and post-neonatal, single-year age intervals from 1 to 94 years, and a final open interval of 95+ years.

Death data were obtained on the aggregate and specific cause of death levels. The data were cut off at age 90, since, beyond this age, most data would be unreliable. Normally, yearly data are estimated using records such as surveys and censuses. The figures reported in these records, especially for older adults, are known to be overstated (see Andreev, 2004). Hence, most population data use an open age interval at very old ages.[3]

2.1.3 Cause-of-Death Classification

Population and CoD data for Kenya were obtained from 1990 to 2017 for males and females. The data were obtained from the GBD with four CoD classifications. The first level has three broad CoD categories: Communicable, maternal, neonatal, and nutritional diseases (category I), non-communicable diseases (category II), and injuries (category III).

This first level presents a high-level aggregation of various causes, so it may not result in meaningful CoD analysis. The second level has 22 intermediate CoDs (see Table 2.1). We used this list for our initial exploratory analysis. The third level has 169 more granular CoDs, while the full list of CoDs, the fourth level, has 293 CoD categories. The full list was eventually used in this study for CoD modelling and forecasting.

Nonetheless, the data could not be directly used for mortality modelling in the form it was obtained. Therefore, we used preprocessing procedures to clean (see Section 3.1.1) and prepare the data for modelling in Section 3.1.3. Subsequently, a simplified preliminary analysis was undertaken on these data to understand some basic features inherent in the dataset, as discussed in Section 3.1.

[3] That is, the progressive unreliability of demographic data with age.

TABLE 2.1: The second level of CoD classification based on GBD

Category	Causes of Death
I	HIV/AIDS and sexually transmitted infections; Respiratory infections and tuberculosis; Enteric infections; Neglected tropical diseases and malaria; Other infectious diseases; Maternal and neonatal disorders; Nutritional deficiencies
II	Neoplasms; Cardiovascular diseases; Chronic respiratory diseases; Digestive diseases; Neurological disorders; Mental disorders; Substance use disorders; Diabetes and kidney diseases; Skin and subcutaneous diseases; Sense organ diseases; Musculoskeletal disorders; Other non-communicable diseases
III	Transport injuries; Unintentional injuries; Self-harm and interpersonal violence

2.2 Methodology

This section offers a high-level summary of the methods utilised. We include their mathematical forms and the necessary constraints, if any. Additionally, we state the shorthand notations used for these models.

2.2.1 Cause of Death Data Preprocessing

Each dataset was split by gender to obtain data for males and females separately. The aim was to accurately model mortality by fitting appropriate models to cause-specific mortalities for the respective genders.

We required single-year-age data for modelling. Although the aggregation of data in age groups reduced the noise in the deaths data, Gelman and Auerbach (2016) established that these aggregations introduce biases to mortality tables emanating from the evolution of the age structure of the inner population within any particular age interval.

We, therefore, wanted to disaggregate the mortality data into single-year ages to exploit age-specific mortality patterns for understanding the overall mortality structure. To do this, the constrained cubic splines method discussed by McNeil et al. (1977) and later utilised by Wilmoth et al. (2017) in the development of HMD data, was utilised[4] with a few modifications. The following steps were substituted:

a) First, the count for $x = 0$ was obtained by summing the late and post-neonatal death counts.

b) Then, deaths between ages 1 and 2 were explicitly calculated as

$$\frac{Y(5) - Y(1)}{2}$$

where $Y(.)$ is the cumulative death counts as defined in McNeil et al. (1977).

[4]To be consistent with literature.

c) Once the death count for age 0 was obtained, the cumulative sum was calculated as described in McNeil et al. (1977). The ages were chosen as $0, 1, 4, 9, \cdots, 94,$ and 100, where age 100 represented the cumulant of the open interval. In addition, a monotonicity constraint was applied to the estimated spline by applying derivative constraints to the interpolant and extending de Boor-Swartz's monotonicity limit, as described by Hyman (1983).

d) This process was iteratively repeated until the trace-minimising values of coefficient c (which monotonically increased values of y) were obtained.

e) The coefficients estimated were then used to estimate $\hat{Y}(x)$ at single ages $x = 0, 1, \cdots, 100$, and the corresponding death estimates $\hat{D}(x)$ calculated as the difference:

$$\hat{Y}(x+1) - \hat{Y}(x)$$

The "constrained cubic spline" referred to the increasing monotonicity.

After acquiring our age-specific death counts, we used these numbers to calculate the mortality rates for modelling. Period death counts are required to calculate the mortality rates $m(x,t)$, so lexis diagrams were utilised as shown in Figure 2.1.

To estimate the period death counts[5] used to calculate the period central death rate, we needed to evaluate the sum:

$$D(x,t) = D_L(x,t) + D_U(x,t) \tag{2.1}$$

Assuming that deaths occur uniformly throughout any year, it was reduced to

$$D(x,t) = \frac{1}{2}\left(D_E(x,t) + D_E(x-1,t)\right) \tag{2.2}$$

where $D_L(x,t)$ and $D_U(x,t)$ are the cohort deaths as shown in figure (2.1).

2.2.2 Exposure Data Preprocessing

This research inherently assummed that deaths, and hence death counts, occurred following a Poisson distribution. Thus, exposures were assumed to be central exposures. We, therefore, estimated these exposures from the population data. Given the population data, the exposures were estimated as (see Figure 2.1ii and Appendix E of Wilmoth et al. (2017)):

$$E(x,t) = \frac{1}{2}\left(P(x,t) + P(x,t+1)\right) + \frac{1}{6}\left(D_L(x,t) - D_U(x,t)\right) \tag{2.3}$$

$$= \frac{1}{2}\left(P(x,t) + P(x,t+1) + \frac{1}{6}\left(D_E(x,t) - D_E(x-1,t)\right)\right) \tag{2.4}$$

[5] Henceforth just referred to as death counts.

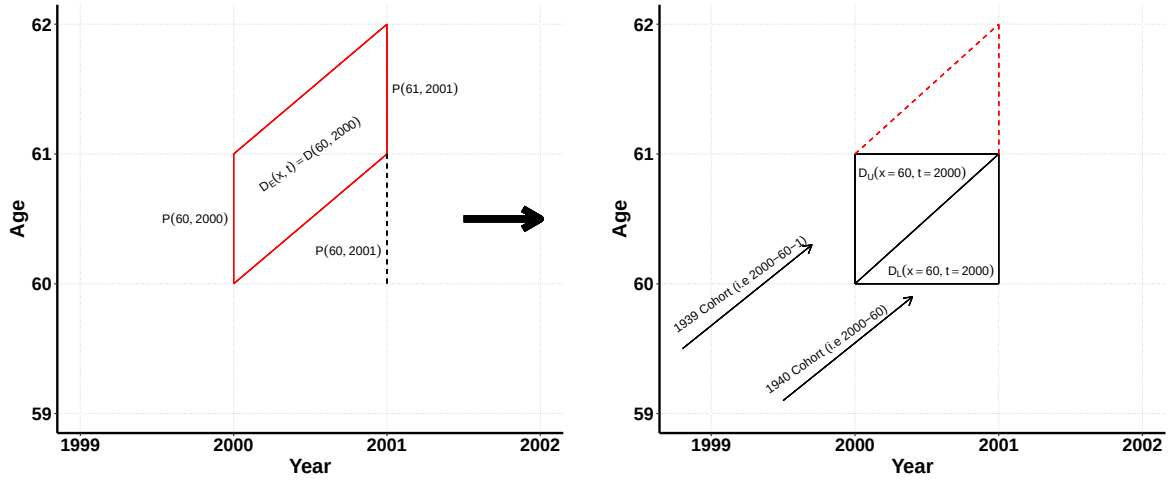

(I) Estimated death counts, 2000 (II) Period death counts, 2000

FIGURE 2.1: Lexis diagrams

for all ages and where deaths were total deaths from all causes. $P(x,t)$ denotes the population aged x at time t. This approximation implied that the period of investigations was 1 year less than the original period of data obtained.

However, for ages above 90, population estimates were first calculated using the extinct cohort method (see Thatcher et al., 2002; Vincent, 1951) before the above formula was applied to estimate the respective exposures. Due to limited data, the extinct cohort could only be applied to the 1906 cohort and earlier. Thus, for later cohorts, projected survivor ratio (SR) method was used (see Depoid, 1973; Thatcher, 1993). In this research, the SR, R_x^c, for cohort c at age x were calculated as follows:

$$R_x^c = \frac{P_{x,t}^c}{P_{x-k,t-k}^c} \tag{2.5}$$

where $P_{x-k,t-k}^c$ is cohort population k years ago.

Next, we discuss the methods used to fit the stochastic models.

2.2.3 Stochastic Mortality Models

Here, we outline the stochastic models used in this research.[6,7] The three types of models considered were the LC model (Lee & Carter, 1992), the Renshaw-Haberman model (Renshaw & Haberman, 2006) and the Plat model (Plat, 2009).

[6]Parameter transformations to ensure unique solutions, as well as any parameter contraints have been exhaustively discussed by Villegas et al. (2018).

[7]A more detailed discussion on the stochastic mortality models considered in this research can be found in Appendix A.1.

2.2.3.1 Lee-Carter Model

The LC model is given by:

$$\texttt{log}(m(x,t)) = \alpha_x + \beta_x k_t \tag{2.6}$$

Where k_t is modelled using a random walk with drift (RWD), given by

$$k_t = \delta + k_{t-1} + \varepsilon_t \tag{2.7}$$

Where $\varepsilon \sim N(0, \sigma^2)$ and δ is the drift. $m(x,t)$ is the central rate of mortality at age x and time t. We denoted this model as LC.

2.2.3.2 Renshaw-Haberman Model

The RH model is given by:

$$\texttt{log}(m(x,t)) = \alpha_x + \beta_x^{(1)} k_t + \beta_x^{(0)} \gamma_{t-x} \tag{2.8}$$

Where k_t and γ_{t-x} are modelled using ARIMA processes.

Of interest in this research were two cases of this model: The case where $\beta_x^{(0)} = 1$ and $\beta_x^{(1)} = \beta_x$ which we denoted as RH and the case where $\beta_x^{(1)} = \beta_x^{(0)} = 1$ which we denoted as APC.

2.2.3.3 PLAT Model

The PLAT model is given by

$$\texttt{log}(m(x,t)) = \alpha_x + k_t^{(1)} + (x - \bar{x}) k_t^{(2)} + (x - \bar{x})^+ k_t^{(3)} + \gamma_{t-x} \tag{2.9}$$

This model was denoted as PL.

2.2.4 Constrained Penalised Splines (CPS) Model

A key contribution of this thesis is the application of the CPS model to CoD mortality modeling. The CPS model builds upon the Penalised Splines (P-splines) framework. Therefore, we first introduce P-splines to establish a foundational understanding before discussing the constraints applied to form the CPS model.

When using P-splines, it is assumed that data on the number of deaths observed at each age and year are available alongside their exposures. In matrix notation, this can be represented as:

$$\boldsymbol{Y} = \begin{pmatrix} y_{11} & y_{12} & \cdots & y_{1n} \\ y_{21} & y_{22} & \cdots & y_{2n} \\ \vdots & \vdots & \ddots & \vdots \\ y_{m1} & y_{m2} & \cdots & y_{mn} \end{pmatrix} \qquad \text{and} \tag{2.10}$$

$$\boldsymbol{E} = \begin{pmatrix} e_{11} & e_{12} & \cdots & e_{1n} \\ e_{21} & e_{22} & \cdots & e_{2n} \\ \vdots & \vdots & \ddots & \vdots \\ e_{m1} & e_{m2} & \cdots & e_{mn} \end{pmatrix} \tag{2.11}$$

where **Y** and **E** are matrices of deaths and exposures observed for m ages, $1, 2, \cdots, m$, and n years, $1, 2, \cdots, n$, respectively. It is also assumed that deaths occur following a Poisson distribution such that:

$$y_{ij} \sim Po(\mu_{ij} e_{ij}) \qquad \text{where} \qquad \mu_{ij} = \frac{y_{ij}}{e_{ij}} \tag{2.12}$$

The objective is to obtain a smoothed estimate of μ_{ij}, $\widehat{\mu}_{ij}$. The expected number of deaths, using logarithm as the link function, can be expressed as:

$$\texttt{log}(\mathbb{E}[y]) = \texttt{log}(\mathbf{e}) + \texttt{log}(\boldsymbol{\mu}) = \texttt{log}(\mathbf{e}) + \boldsymbol{\eta} \tag{2.13}$$

Where $\texttt{log}(\mathbf{e})$ is the offset and $\boldsymbol{\eta}$ a linear predictor such that, in the usual GLM context:

$$\boldsymbol{\eta} = \boldsymbol{X}\boldsymbol{\alpha} \tag{2.14}$$

The basis functions, **X**, are predetermined to fit the data with some estimated coefficients $\boldsymbol{\alpha}$.

Defining **B** as a banded matrix of k B-splines, $\{B_1(x), B_2(x), \cdots, B_k(x)\}$, the linear predictor can be rewritten as:

$$\eta = \boldsymbol{B}\alpha \tag{2.15}$$

Suppose the estimated regression matrices of B-splines for the marginal models are $\boldsymbol{B_y}$[8] for the columns and $\boldsymbol{B_a}$[9] for the rows, then the two-dimensional regression matrix is given by the Kronecker product:

$$\boldsymbol{B} = \boldsymbol{B_y} \otimes \boldsymbol{B_a} \tag{2.16}$$

[8] That is over years $1, 2, \cdots, n$.
[9] That is over ages $1, 2, \cdots, m$.

With $y \times a$ regression coefficients, α, which can be used to build a forecasting model by applying a penalised log-likelihood approach. To incorporate prior mortality knowledge or expert judgement as to whether specific observed mortality patterns reflect historic circumstances that are not expected to persist into the future, constraints on the time and age domains can be imposed.

On the age domain, the constraint is obtained by calculating the relative derivative:

$$\frac{\frac{\partial}{\partial a}\widehat{\boldsymbol{\mu}}}{\widehat{\mu}} = \frac{\partial}{\partial \boldsymbol{a}}\log(\widehat{\boldsymbol{\mu}}) = \frac{\partial}{\partial \boldsymbol{a}}\widehat{\boldsymbol{\eta}} = \left(\boldsymbol{B}_{n_1} \otimes \frac{1}{h}\left[{}^{q-1}\boldsymbol{B}_a^{\vee} - {}^{q-1}\boldsymbol{B}_a^{\vee-1}\right]\right)\widehat{\boldsymbol{\alpha}} \tag{2.17}$$

Where n_1 are the observed years, h the distance of the knots, $\vee$ the position of the B-splines in $\boldsymbol{B}_a$, and q the degree of the spline polynomials. On the time domain, similar arguments are made leading up to:

$$\frac{\frac{\partial}{\partial n_1}\widehat{\boldsymbol{\mu}}}{\widehat{\mu}} = \frac{\partial}{\partial \boldsymbol{n_1}}\log(\widehat{\boldsymbol{\mu}}) = \frac{\partial}{\partial \boldsymbol{n_1}}\widehat{\boldsymbol{\eta}} = \boldsymbol{D}_{n_1}^{n_1}\widehat{\boldsymbol{\alpha}} \tag{2.18}$$

computed over $\boldsymbol{B}_y$. $\boldsymbol{D}_{n_1}^{n_1}$ is a matrix that computes first order difference of estimated coefficients by differentiating the associated B-spline basis for each age over the years.

This way, it is possible to constrain future mortality to lie within a certain interval of the observed rate of ageing δ,[10] the choice of which is conveniently highly dependent on the forecaster's professional judgement based on past mortality trends. These opinions can be incorporated into forecasting by constructing appropriate confidence limits (see Camarda, 2019, and references therein for a more detailed discussion).

Generally, infant mortality would normally be treated differently when constructing a lifetable (Chiang, 1984). Therefore, in this thesis, infant mortality is separated from other ages by using the modified basis

$$\boldsymbol{B}_a = \begin{bmatrix} 1 & \boldsymbol{0}_{1\times k_a} \\ \boldsymbol{0}_{(m-1)\times 1} & \boldsymbol{B}_a^{\star} \end{bmatrix} \tag{2.19}$$

where $\boldsymbol{B}_a^{\star}$ does not include age zero and hence an $(m-1)\times k_a$ matrix. The first entry of $\boldsymbol{D}_a$ is replaced with a zero to indicate the non-inclusion of infant mortality. This way, infant mortality development is separated from the other ages.

The above CPS model implies that rather than modelling mortality rates, we model the rates of change[11] of mortality in two dimensions: across ages and years. Consequently, the model allows us to restrict the historic mortality data that is used to the data where the projected first derivative of mortality is within a specific range based on observed derivatives. These

[10] δ is the derivative of the linear predictor $\boldsymbol{\eta}$.

[11] First derivative.

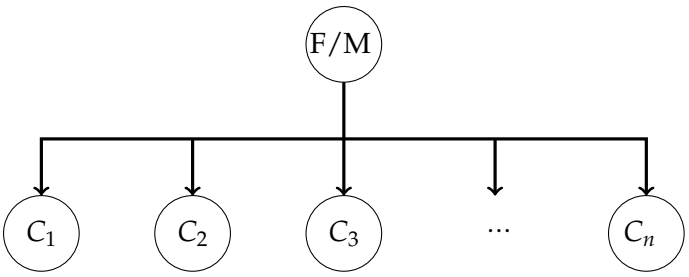

FIGURE 2.2: A hierarchy of mortality rates

restrictions are applied by using asymmetric penalties. The model is estimated iteratively, where at each iteration we check if the forecasted derivative is outside the selected interval. If it is, a penalty is applied, and re-estimation is undertaken. This process is repeated until the derivatives lie within the limits in both the age and time dimensions.

2.2.5 Hierarchical Modelling and Forecasting

A time series is said to form a hierarchy if it can be clustered into groups with a certain rank. If the rank is unimportant,[12] the cluster would result in a grouped time series. Hierarchical modelling attempts to model these series by fitting models to each hierarchy while preserving the overall structure (Wickramasuriya et al., 2018).

When considering CoDs, mortality forms a natural hierarchy since individual CoD mortality would add to the total mortality for a given gender. Figure 2.2 shows a two-level mortality hierarchy. C_i represents mortality for cause i for either female or male (F/M). At the lower level are the mortalities from n causes, $C_1, C_2, \cdots, C_n$, summing up to the mortality for either male (M) or female (F).

Several forecast reconciliation approaches have been proposed to ensure that the structure of the forecasted hierarchical time series is maintained. In this research, we considered three approaches: The top-down proportional reconciliation method, the bottom-up proportional reconciliation method, and the trace minimisation method.

We discuss each of these approaches in the subsections below. It is however noteworthy that, while an assumption on independence of the causes of death while fitting the mortality models to each cause may be implied, the application of forecast reconciliation approach incorporates the competing nature of the different causes, as illustrated by Li et al. (2019). Therefore, the forecasts obtained from this approach incorporates competing mortality.

[12] That is, it does not have a literal or statistical meaning.

2.2.5.1 Top-Down Proportional Reconciliation Method

Here, the assumption is that the top series contains sufficient information, and therefore the forecasts obtained from this series are considered more accurate (Panagiotelis et al., 2021). This method proceeds by first forecasting the top and bottom series, then adjusting the lower hierarchy series to ensure the hierarchical structure is maintained.

2.2.5.2 Bottom-Up Proportional Reconciliation Method

Here, the models are fitted to individual bottom series, and then the forecasts are summed up to obtain the aggregate series above it (Hyndman & Khandakar, 2008). The summation is repeated for each hierarchy. The forecasts can be expressed as follows:

$$\hat{y}_h = \boldsymbol{S}\hat{y}_{k,h}$$

where $\boldsymbol{S}$ is a summing matrix, and $y_{k,h}$ and y_h represent the bottom- and top-level series, respectively (Shang & Hyndman, 2017).

2.2.5.3 MinT Combination by Trace Minimisation

The $h-$step ahead forecasts is assumed to take the form:

$$\hat{y}_h = S\beta_h + \varepsilon_h$$

where S is the structure of the hierarchical series and $\varepsilon_h \sim N(0, \Sigma_h)$. Assuming that the forecast conforms to the hierarchical structure, then

$$\varepsilon_h \approx S\varepsilon_{K,h}$$

Hence, per Hyndman et al. (2011),

$$\hat{\beta}_h = \left(S'\Sigma_h^{\dagger}S\right)^{-1} S'\Sigma_h^{\dagger}\hat{y}_n(h)$$

is the best unbiased estimator of $\hat{\beta}_h$, producing the reconciled forecasts:

$$\hat{y}_h = S\left(S'\Sigma_h^{\dagger}S\right)^{-1} S'\Sigma_h^{\dagger}\hat{y}_n(h)$$

$\Sigma_h^{\dagger}$ is neither known nor identifiable. When $\Sigma_h^{\dagger} = \mathbb{I}$, it reduces to an ordinary least squares (OLS) estimator (see Shang & Hyndman, 2017). However, it can be approximated by W_h

(Wickramasuriya et al., 2018) such that

$$\mathbb{E}\left[\hat{e}_{t+h}\hat{e}'_{t+h}|y_1, y_2, \cdots, y_t\right] \qquad \text{and} \qquad \mathbb{VAR}\left[\tilde{e}_{t+h}|y_1, y_2, \cdots, y_t\right] = SPW_hP'S \tag{2.20}$$

By minimising the trace of $SPW_hP'S$ where P is the projection matrix, the calculation becomes

$$P = \left(S'\Sigma_h^{\dagger}S\right)^{-1}S'\Sigma_h^{\dagger}\hat{y}_n(h)$$

where $\hat{e}_{t+h} = y_{t+h} - \hat{y}_{t+h}$ and $\tilde{e}_{t+h} = SP\hat{e}_{t+h}$.

These methods can be implemented using the *hts* R package, with the implementation procedure outlined in (Hyndman et al., 2021). In summary:

a) For bottom up reconciliation approach, the reconciled forecasts are just the sum of the bottom series.

b) For top down approach, we first create a hierarchical series, after which the *hts* package is used to calculate the respective proportions and use them to reconcile the forecasts.

c) For MinT method, we first create a hierarchical series, and then the residuals are used to reconcile the forecasts as outlined by (Hyndman et al., 2021).

Chapter 3

Results

This chapter presents the results of the preliminary analysis and the mortality modelling using Kenyan data. To begin, we present preliminary analysis results in Section 3.1 from exploring the Kenyan mortality data. Next, we present the results of the models we evaluated in Section 3.2 and use them to forecast mortality. The results of the mortality forecasting are outlined in Section 3.3. This chapter concludes by illustrating how the chosen model can be used to project the population in Section 3.4.

3.1 Preliminary Analysis

This section undertakes an exploratory analysis of the data obtained and the data preprocessing procedures undertaken. We first describe the CoD classifications used in the research in Section 3.1.1. We then proceed in Section 3.1.2 and outline our exploratory data analysis to understand the historical mortality patterns. In Section 3.1.3, we conclude with a detailed discussion of the procedures undertaken to prepare the data for modelling.

3.1.1 Cause-of-Death Classification

In this research, the main aim was to illustrate that CoD modelling leads to a general improvement in forecasting ability. Thus, we used the officially published Top Ten CoDs published by KNBS.

The CoD data were checked to ensure that the cause categories were consistent with the International Classification of Diseases (ICD) for consistency with the existing CoD modelling literature. ICD-10[1] was adopted for this research. Reclassifications of the obtained CoD data were essential to align with ICD-10 reporting.

Additionally, garbage codes, a case where a significant number of deaths are assigned to a given CoD (not the actual CoD) have been cited for introducing biases in CoD modelling over time (Naghavi et al., 2020). These can cause a significant change in the pattern of a country's mortality from one year to another (Foreman et al., 2012). Some causes, such as HIV, have been more affected than others (Yudkin et al., 2009).

[1]The 10th edition of the international classification of diseases.

A variety of methods have been proposed to readjust or redistribute these mortalities to reflect actual mortality patterns over time (see Foreman et al., 2016; Johnson et al., 2021, and the references therein for examples). The GBD has developed methods for dealing with these issues. Thus, our data for this analysis were previously adjusted (Vos et al., 2020).

For completeness, ICD-10 codes for the diseases considered under each category are provided in Table (3.1). The ten categories were lower respiratory infections (LRI), malaria, cancer, HIV/AIDS, nutritional deficiencies, tuberculosis (TB), cardiovascular diseases, transport accidents, meningitis and others.[2]

The data were checked for consistency with basic reasonableness checks to ensure the total tally with the total mortality numbers for each year and each age category using aggregate-level death data. A second consistency check on age-specific death rates was completed, which involved checking that the age-specific death rates for each cause summed to the overall death rates for each gender.

3.1.2 Historical Observations

This section provides insight into the historical patterns of Kenyan mortality and population over time by analysing various summary statistics. First, we computed basic summary statistics to provide insight into the general structure of the Kenyan population and its evolution, as presented in Figure 3.1. The data were derived from the four most recent censuses, as reported by KNBS (2020), to construct the historical Kenyan population pyramid shown in Figure 3.1. Below is a summary of the insights:

a) The proportion of males and females reaching age 65 has consistently increased, indicating an ageing population.[3] Improved census accuracy over time may explain the decline in male proportions observed between 1989 and 1999.

b) The growth in the 65+ population has outpaced that of the working-age group (15–64),[4] with a more pronounced effect among females. This trend raises concerns about economic and policy implications, including increased healthcare costs and heightened pension funding risks under pay-as-you-go (PAYG) systems.

c) While the overall dependency ratio (people under 14 and over 65) significantly declined between 1989 and 1999, it has since stabilized, reflecting possible stagnation or decline in fertility rates due to improvements in maternal and neonatal care.

[2]Which included all other causes, not in this list.

[3]The WHO attributes this to declining fertility rates and rising life expectancy.

[4]ILO and OECD definitions (Harasty & Ostermeier, 2020; The Organisation for Economic Co-operation and Development [OECD], 2017).

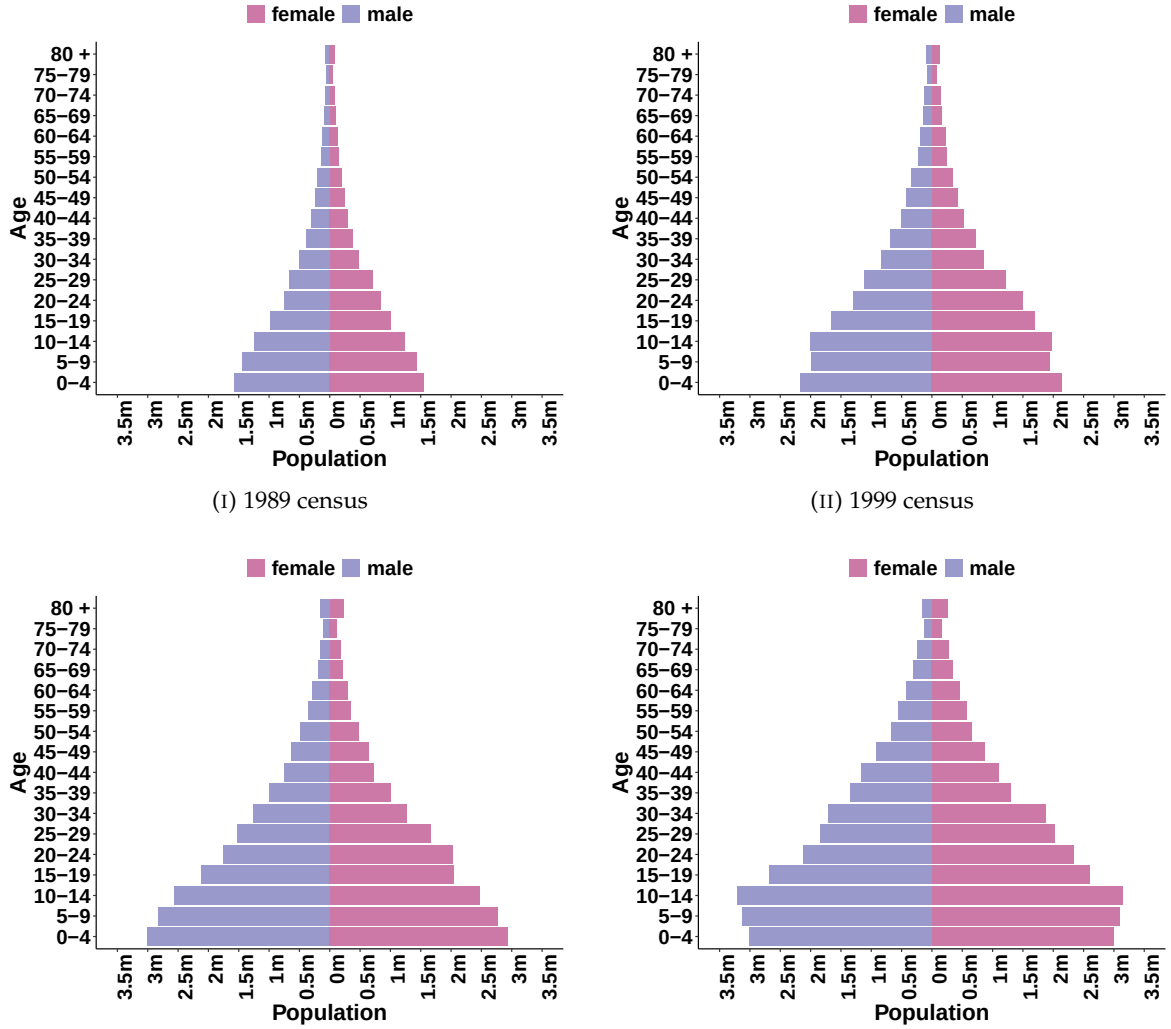

(I) 1989 census

(II) 1999 census

(III) 2009 census

(IV) 2019 census

FIGURE 3.1: Historical population pyramids for Kenya

TABLE 3.1: List of ICD-10 codes mapped to the causes of death considered in the study

Cause	ICD-10 Codes
Lower respiratory infections (LRI)	A48.1, A70, B97.4-B97.6, J09-J15.8, J16-J16.9, J20-J21.9, P23.0-P23.4, U04-U04.9
Malaria	B50-B53.8
Cancer	C00-C97, D00.1, D00.2, D01.0-D01.3, D02.0-D02.3, D03-D07.2, D07.4-D07.5, D09.0, D09.2-D09.3, D09.8, D10.0-D10.7, D11-D13.7, D14.0-D14.3, D15-D16.9, D22-D24.9, D26.0-D28.1, D28.7, D29.0-D29.8, D30.0-D30.8, D31-D31.9 , D34-D35.2, D35.5-D36.7, D37.1-D37.5, D38.0-D38.5, D39.1-D39.2, D39.8, D40.0-D40.8, D41.0-D41.8, D44.0-D44.8, D48.0-D48.6, D49.2-D49.4
HIV/AIDS	B20-B24.9

Cause	ICD-10 Codes
Nutritional deficiencies	D50.1-D50.8, D51-D52.0, D52.8-D53.9, E00-E02, E40-E46.9, E51-E61.9, E63-E64.0, E64.2-E64.9, M12.1
Tuberculosis (TB)	A15-A19.9, B90-B90.9, K67.3, K93.0, M49.0, N74.1, P37.0, U84.3
Cardiovascular diseases	B33.2, G45-G46.8, I01-I01.9, I02.0, I05-I09.9, I11-I11.9, I20-I25.9, I28-I28.8, I30-I31.1, I31.8-I37.8, I38-I41.9, I42.1-I42.8, I43-I43.9, I47-I48.9, I51.0-I51.4, I60-I63.9, I65-I66.9, I67.0-I67.3, I67.5-I67.6, I68.0-I68.2, I69.0-I69.3, I70.2-I70.8, I71-I73.9, I77-I83.9, I86-I89.0, I89.9, I98, K75.1
Transport accidents	V00-V86.9, V87.2-V87.3, V88.2-V88.3, V90-V98.8
Meningitis	A39-A39.9, A87-A87.9, G00.0-G00.8, G03-G03.8
Others	Everything else not included above

d) Females consistently exhibit higher longevity than males, with the gap widening over time. This differential is reflected in the dependency ratio, suggesting possible trends in younger male mortality, further explored in Section 3.2.

e) The decreasing proportion of the under-14 population and the ageing demographic are evident in Figure 3.1. This highlights a shifting population structure. As shown in Figures 3.1iii and 3.1iv, the ageing trend and rising dependency ratio are expected to reshape Kenya's population dynamics significantly.

Kenya has experienced significant improvements in mortality, consistent with trends observed in many African countries (United Nations [UN], 2017). Life expectancy increased from 46.8 years in 1960 to 59.1 years in 1984,[5] an average annual increase of 0.51 years. Although life expectancy declined sharply during the HIV epidemic, reaching 50.9 years in 2000, it recovered to 65.9 years by 2017, an accelerated annual increase of 0.81 years.

Key drivers of these trends include:

a) *Decline in infant mortality:* Infant mortality decreased from 118.2 per 1,000 live births in 1960 to 30.6 per 1,000 in 2018, aided by improved healthcare access and government-subsidised antiretroviral treatments (Demombynes & Trommlerová, 2012; Odhiambo et al., 2014).

b) *Impact of HIV/AIDS:* The epidemic led to a sharp mortality increase post-1985, affecting all age groups but especially mid-age populations (Lupia & Chien, 2012; Waruru et al., 2021).

c) *Post-2000 recovery:* Mortality improvements accelerated after the epidemic, though signs of waning progress are emerging (Waruru et al., 2021).

[5] Prior to the HIV epidemic (Kagaayi & Serwadda, 2016).

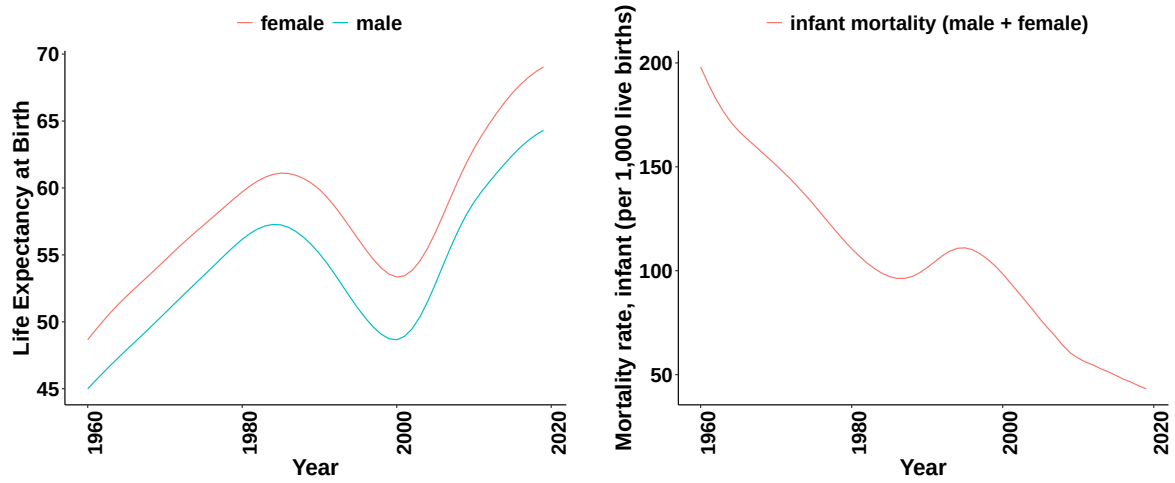

(I) Life expectancy at birth (II) Infant mortality

FIGURE 3.2: Life expectancy at birth and the combined infant mortality per 1,000 live births in Kenya. Data source: WB (2020)

These mortality fluctuations present challenges for government budgeting, particularly in the context of universal health coverage (UHC) initiatives. Accurate modelling is essential to understand these patterns and mitigate future risks.

Unlike developed countries, where mortality trends are stable and linearity assumptions such as that of Lee and Carter (1992) holds, Kenya's mortality patterns remain irregular as reflected in Figures 3.2i and 3.2ii. Therefore, such assumptions as those made by Booth et al. (2002) and others may not hold. This study seeks to examine these irregularities and adapt modelling approaches to Kenya's unique context.

Moreover, recent reports indicate a 48% decline in HIV/AIDS incidence between 2010 and 2020 (Young et al., 2023), suggesting that the sharp mortality increases observed in the past are unlikely to persist. However, questions remain regarding the long-term trajectory of mortality trends and when they will stabilise.

Figures 3.3 show the top ten CoDs for females and males over the study period. These categories were derived from the second level of CoDs obtained from the GBD, as shown in Table 2.1. We make the following observations:

a) In the early 1990s, HIV/AIDS was not in the top three CoDs in Kenya. Respiratory infections and TB had caused the highest number of deaths for males and females. However, within 5 years, HIV/AIDS had substantially surpassed all other causes to be the highest CoD.

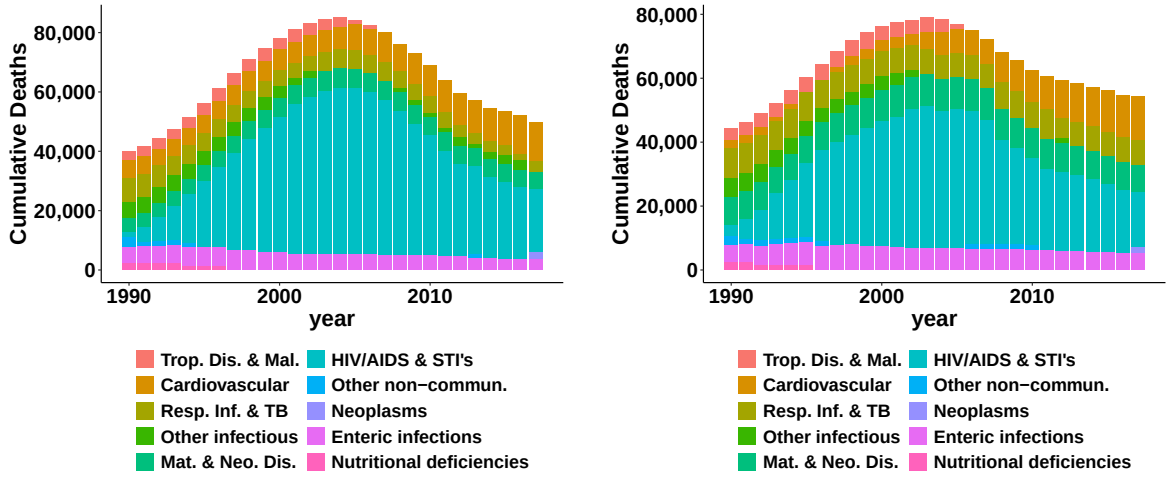

(I) Top 10 CoD, females

(II) Top 10 CoD, males

FIGURE 3.3: CoD evolution in Kenya

By 2000, HIV/AIDS had caused more deaths than respiratory infections and TB, cardiovascular diseases, and maternal and neonatal disorders combined for females and respiratory infections and TB and cardiovascular diseases combined for males.

The Kenyan government's striving to provide antiretroviral therapy drugs produced fruit, as seen in the decline in HIV/AIDS deaths, with male deaths in 2017 not significantly different from other causes. It is noteworthy that the CoD reclassification and increased awareness contributed to such trends.

b) However, as we celebrate the achievement of reducing HIV/AIDS deaths, it is important to note how it has impacted genders differently. It is clear in Figure 3.3 that HIV/AIDS still caused substantially more deaths in females than males in Kenya. This difference may indicate the stigma attached to females seeking sexual health services (Camlin et al., 2017), which can lead to late diagnosis and higher mortalities.

c) Cardiovascular diseases rapidly increased over the last 2 decades of the study period. In fact, for females, it was the second-highest CoD by death count in 2017, surpassing respiratory infections and TB. This finding indicates a global trend in the burden of cardiovascular diseases (Roth et al., 2020).

   This big challenge was caused by such risk factors as diet and lifestyle (Dahlöf, 2010). Therefore, we hope that increased campaigns and public education can increase awareness of these risk factors and teach how to avoid them to significantly reduce premature deaths in Kenya.

d) The rapid increase in neoplasm cases is noteworthy. The Kenyan government made an effort to reduce deaths, especially those cancer-related. This effort can be seen through the government's extension of national health coverage to include cancer treatments (Mbau et al., 2020). However, despite these efforts, cancer has not shown sign of slowing.

   The consistent increase in neoplasm cases may partly indicate the stigma associated with the disease, consequently leading to more people not seeking proper formal treatments (Sayed et al., 2019). This is more common among older people, who are also the most vulnerable.

   Therefore, the government may consider investing more in public education about early diagnosis and formal treatment benefits. The government can also invest in research and development to investigate the efficacy of the traditional herbal medication commonly used in rural Kenya. It may be the case that some herbal remedies are effective for some form of neoplasm, as discussed elsewhere (Gakuya et al., 2020; Omara et al., 2022).

The main advantage of exploring CoD data at this high-level aggregation is that we can easily see the key drivers of mortality within the population. As the disaggregation becomes more granular, it becomes more challenging to pick the main drivers of mortality.

However, these disaggregated CoD are useful for modelling, especially targeted modelling. Hence, if we are interested in analysing the impact of a specific cause and how it has changed over time, for example, malaria, then the disaggregated data becomes more valuable.

Aggregation also gives an immediate visual impact on the progress towards achieving high-level targets such as MDGs, for example, eradicating deaths due to communicable diseases.

Nevertheless, it is easy to miss the main drivers of mortality in the aggregation. For example, the majority of deaths occurring under the "tropical diseases and malaria" category were actually due to malaria, as we display shortly. Another example is the "respiratory infections and TB" category, which includes granular causes with almost equal death counts. Hence, disaggregating these two categories can lead to a different picture.

3.1.3 Data Preprocessing

Given the aggregate CoD data obtained, we then applied the constrained cubic splines to estimate the age specific mortality as described in Section 2.2.1. The main advantage of the cubic splines was their flexibility of constraining totals at the knots to be unchanged after smoothing, which ensured we still had the sum of age-specific death counts similar to the sum of the ungraduated death rates. We used this fact as a consistency check in our derived data. The death counts estimated via constrained cubic splines are denoted as $D_E(x,t)$ in Figure 2.1.

We then employed the extinct cohort method to estimate exposures. However, due to data limitations, this method was only applicable to cohorts up to 1906. For later cohorts, we utilised projected SRs to estimate exposures, assumming a limiting age of 100.

Due to the use of the extinct cohort method in estimating populations at 90+ and the explicit assumption of ω = 100, it was possible to estimate complete SR only up to 2007 with the data. For the other years, the following linear models were used to extrapolate the SRs.

a) For females, we fitted the model:

$$SR_x = \beta_0 + y\beta_1 + x\beta_2 + x^2\beta_3 + x^3\beta_4 \tag{3.1}$$

b) For males, the model was

$$SR_x = \beta_0 + y\beta_1 + y^2\beta_2 + y^3\beta_3 + x\beta_4 + x^2\beta_5 + x^3\beta_6 \tag{3.2}$$

In both these models, y represents the year, while x represents the current age.

Contrary to the literature suggesting a simple linear model for survival ratios at old ages, the data suggested a third-order polynomial. Indeed, a third-order polynomial led to survivor ratios that approached 0.5 at ω, in line with the existing literature using other potentially more accurate datasets (see Terblanche & Wilson, 2015b).

From our results, the mortality improvement rate in females appeared to be much more linear than for males. However, this finding was unsurprising because male deaths at these ages would have a higher impact on the few lives alive at that age. A single death would rapidly increase the roughness of the mortality curve and, hence, SRs at these ages.

Notably, given the formula used to estimate exposures, we inevitably ended up with a year's less of data.

3.1.4 By-Cause Exploratory Analysis

Once the period deaths, $D(x,t)$, and exposures, $E(x,t)$, were estimated, the central death rate, $m(x,t)$,[6] were estimated as:

$$m(x,t) = \frac{D(x,t)}{E(x,t)} \approx \mu_x \tag{3.3}$$

Subsequently, our aim was to study mortality patterns over the investigation period.

Kenyan mortality trends analysed by CoD reveal distinct historical patterns (Figure 3.4). Modeling mortality using all-cause data would overlook these nuances and the underlying drivers of

[6] Henceforth referred to as mortality rates, used as an estimator for μ_x.

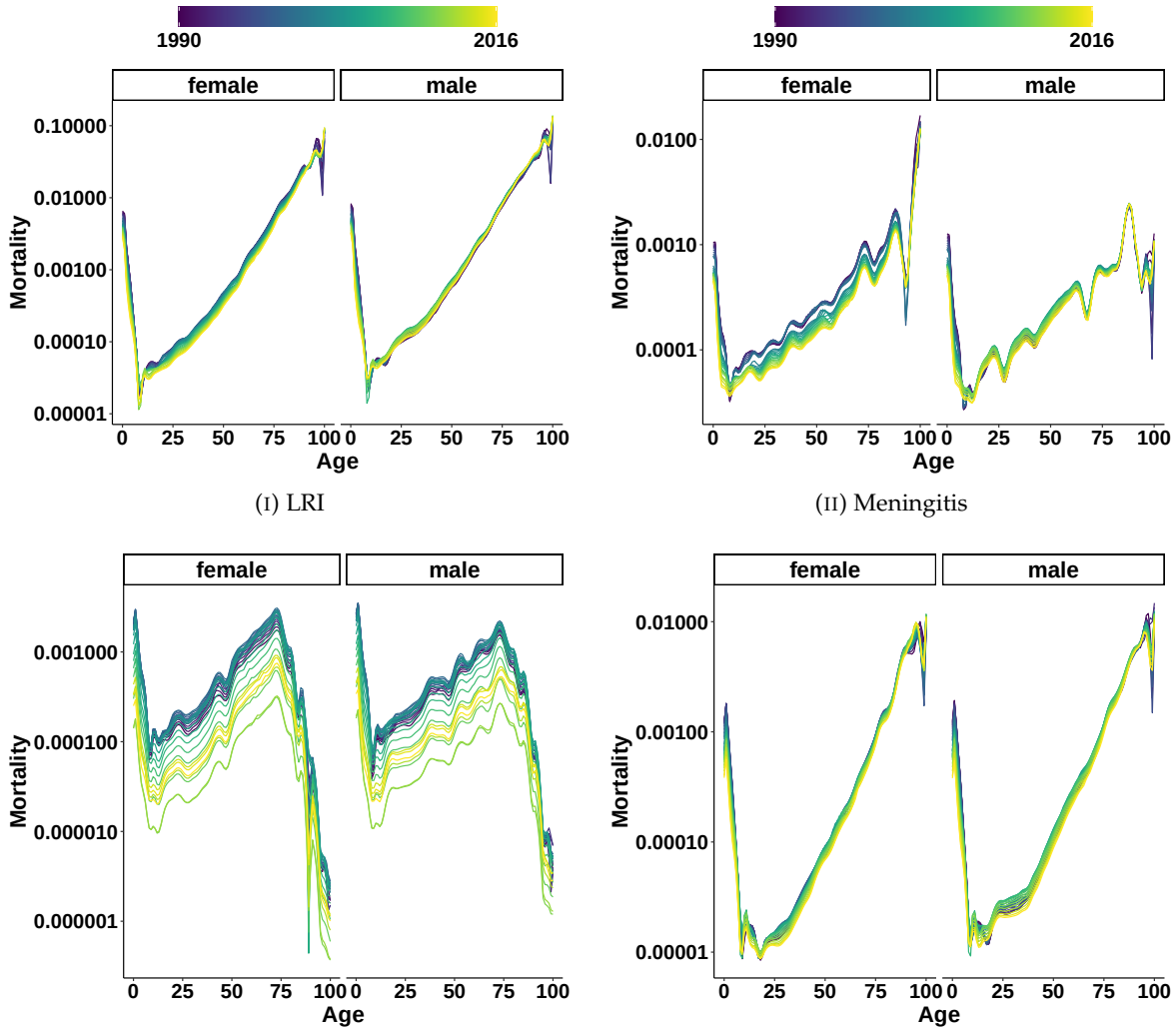

(I) LRI

(II) Meningitis

(III) Malaria

(IV) Deficiencies

FIGURE 3.4: Cause of mortality in Kenya

mortality. Additionally, mortality patterns in developing countries like Kenya often diverge from the "expected" patterns derived from developed nations, where socio-economic factors influence mortality differently across ages and CoDs (Li et al., 2021). This highlights the need for methods incorporating uncertainties and expert opinions for more accurate estimates, as discussed in Chapter 4.

Key observations from historical CoD-specific mortality data include:

a) Among the top ten CoDs, LRI caused the highest child mortality, followed by HIV/AIDS. High mother-to-child HIV transmission rates, exacerbated by limited access to antiretroviral treatments during pregnancy and postpartum prophylaxis, were likely significant contributors. Studies indicate fewer than 75% of HIV-positive pregnant women received

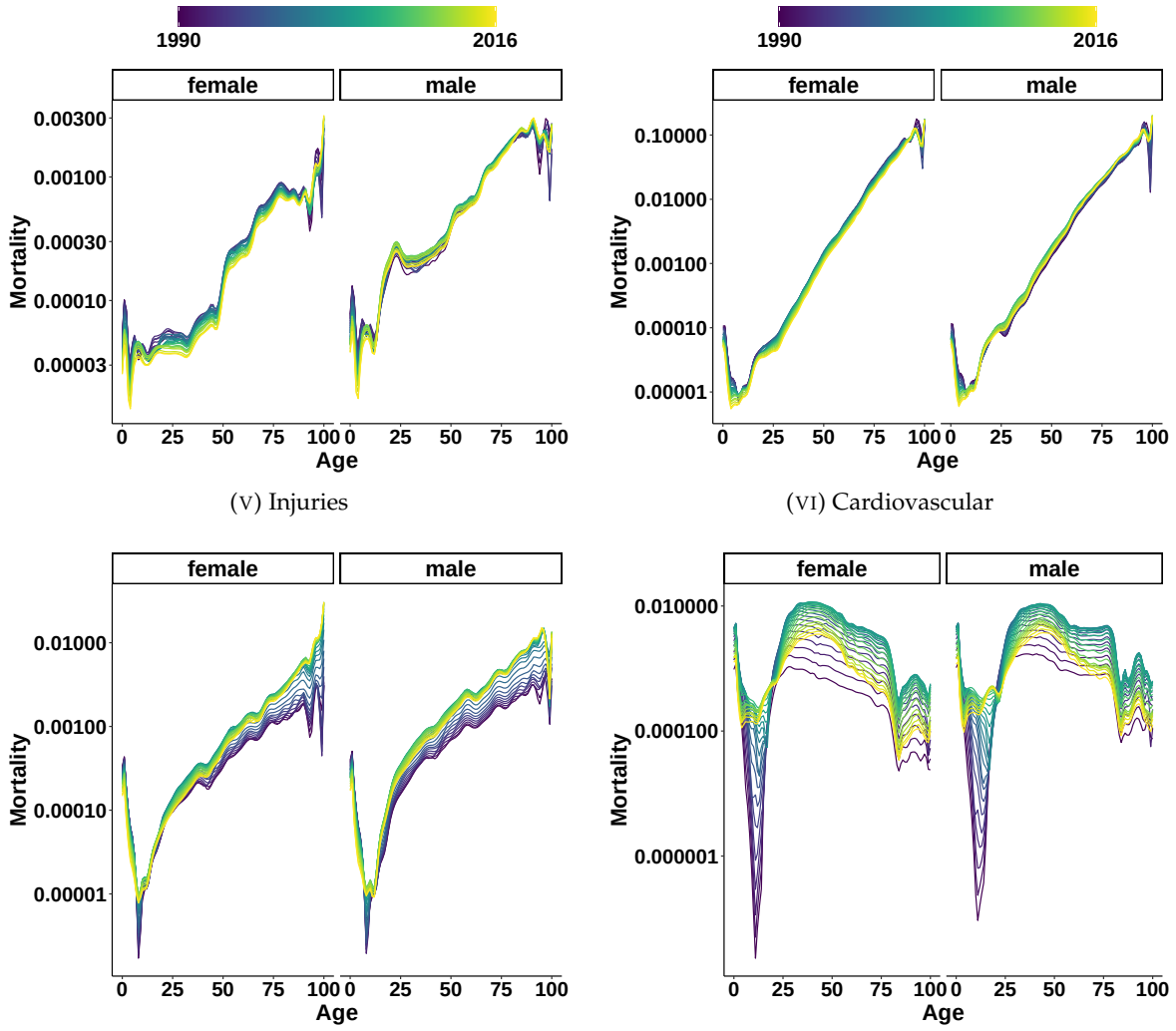

(V) Injuries

(VI) Cardiovascular

(VII) TB

(VIII) HIV

FIGURE 3.4: Cause of mortality in Kenya

necessary treatments, with higher transmission rates observed among female children (Mwau et al., 2017; Sirengo et al., 2014).

b) While overall mortality from injuries declined, it increased among males aged 20–50. This trend may reflect risky behaviors linked to early employment and affluence, such as binge drinking of illicit alcohol (Mkuu et al., 2018). Despite government efforts to curb unrecorded alcohol, it remains a significant risk factor for this demographic (Chaka et al., 2020; Mwangi, 2018).

c) Males generally had higher mortality rates for most CoDs and ages, except for meningitis and malaria at older ages.

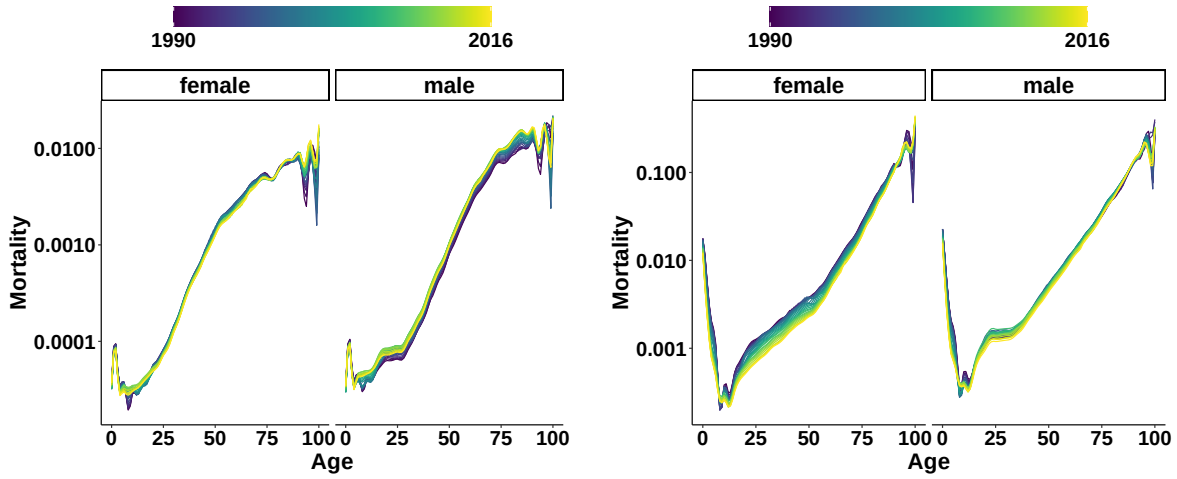

(IX) Cancer (X) Others

FIGURE 3.4: Cause of mortality in Kenya

d) HIV-related deaths among teenagers rose significantly, attributed to stigma around prevention and treatment (McHenry et al., 2016). TB-related deaths in this age group also increased, suggesting further public health challenges.

e) Malaria deaths peaked at age 75 and declined thereafter, possibly due to diagnostic errors. Symptoms such as fever and headache are often misattributed to malaria without proper testing, leading to incorrect CoD records (Choge et al., 2014).

f) Mortality from cardiovascular diseases and LRI has remained high, with little sign of decline for males. Females have shown marginal improvements in recent years.

g) Cancer mortality exhibited a consistent increase at middle ages but significant improvement at older ages. Delayed medical treatment due to cultural superstitions often results in patients seeking hospital care in advanced stages, where recovery chances are minimal (Nyarigoti et al., 2017). Enhanced community education, and stricter regulations on treatment practices are essential (Gakuya et al., 2020; Omara et al., 2022).

h) Recent declines in cancer mortality at older ages likely reflect informed healthcare decisions by children caring for their elderly parents. Enhanced cancer treatment facilities and early diagnoses have also contributed to better outcomes.

i) Irregular mortality improvements at older ages can be partly attributed to improved healthcare access and familial caregiving, as children often provide primary care for elderly parents, enabling quicker diagnoses and better health outcomes (Kimamo, 2018).

These findings underscore the complex interplay of socio-economic, cultural, and healthcare

factors in shaping mortality trends, emphasizing the need for tailored interventions and improved healthcare access and education. These findings may also signify the need for increased research and development in these areas.

3.1.5 Structural Changes in Mortality Pattern

This section examines whether structural changes in mortality patterns occurred over time, as suggested by Figure 3.2. Structural changes in mortality are critical for ensuring appropriate model selection, which involves assessing trends in mortality improvements over time. The procedure outlined by Booth et al. (2002) was used, employing the LC model for this investigation.

The model fitting process involved three approaches:

a) without any adjustments to $k(t)$,

b) adjusting $k(t)$ as per Lee and Miller (2001) and Lee and Carter (1992), and

c) adjusting $k(t)$ using the Poisson count deaths method by Booth et al. (2001).

Figure 3.5 shows the structural changes in Kenyan mortality over time, represented by the time component $k(t)$, mean deviance, and deviance ratios. Figures 3.5i and 3.5ii reveal deteriorating mortality before 2000, followed by significant improvements afterward, suggesting structural changes post-2000. Female mortality was unaffected by adjustment procedures, while for males, adjustments to total deaths had minimal impact.

Analysis of mean deviances relative to the base and total lack of fit aimed to identify periods where these statistics were small, nearly constant, and approximately equal. Figures 3.5iii and 3.5iv indicate that after 2003 for females and 2000 for males, mean deviances from the two fits became nearly indistinguishable, suggesting a structural shift in mortality patterns.

However, Figures 3.5v and 3.5vi present a nuanced view. The deviance ratio for females showed a marked increase post-2003, implying potential misinterpretation of the data if earlier years were excluded. In contrast, for males, the deviance ratios remained stable, particularly post-2000.

These findings align with reforms in Kenya's healthcare system, including the expansion of the civil servants' healthcare scheme to subscription-based health coverage, attracting participants from formal and informal sectors (Barasa et al., 2018).

Given the limited dataset, discarding pre-2000 data would have reduced the available data by 40%, leaving only 15 years for model fitting and cross-validation. To balance these constraints, a compromise approach was adopted, detailed in Section 3.2.

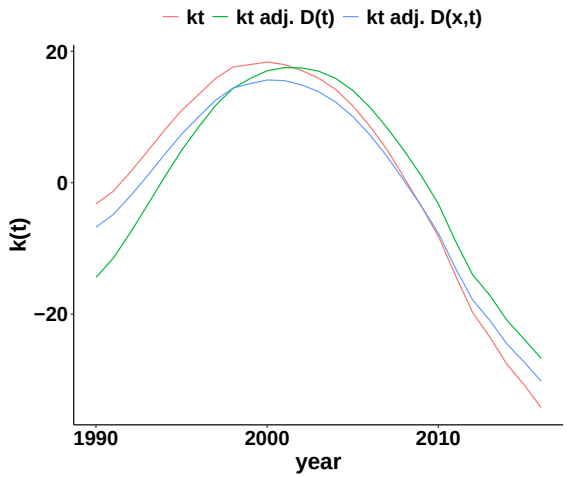

(I) Female, k(t)

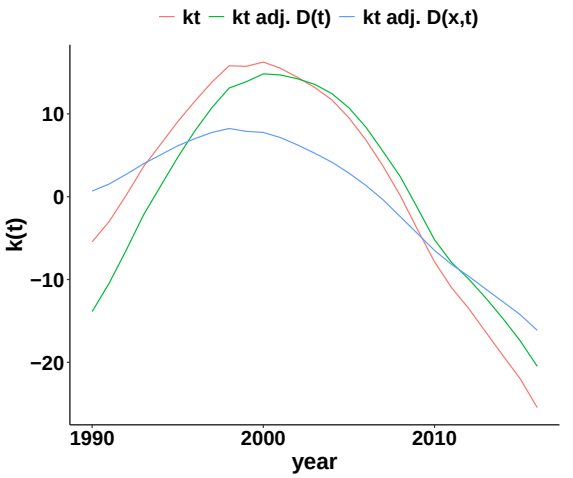

(II) Male, k(t)

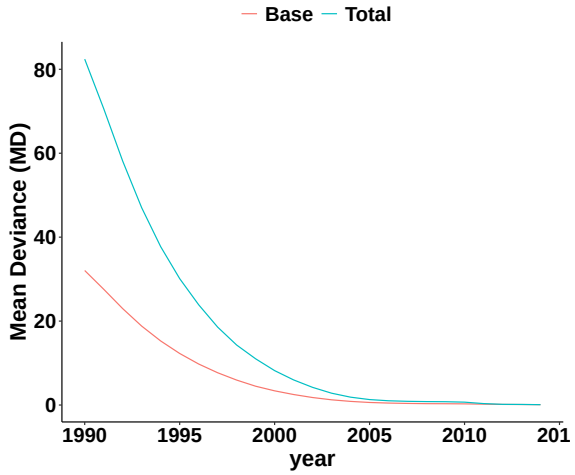

(III) Female, mean deviance

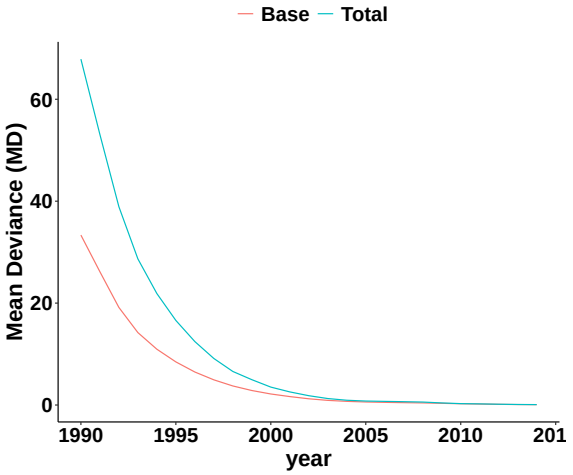

(IV) Male, mean deviance

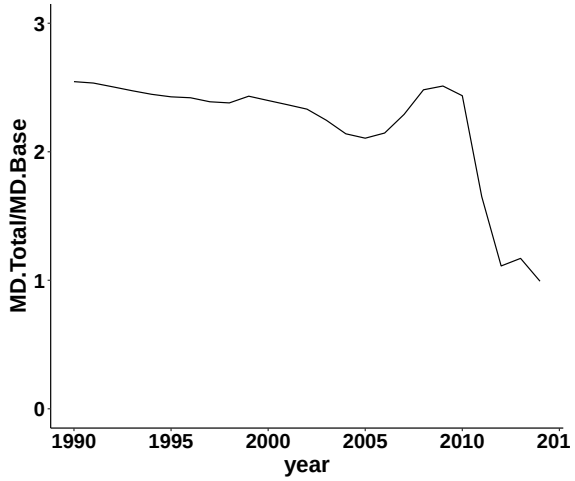

(V) Female, deviance ratios

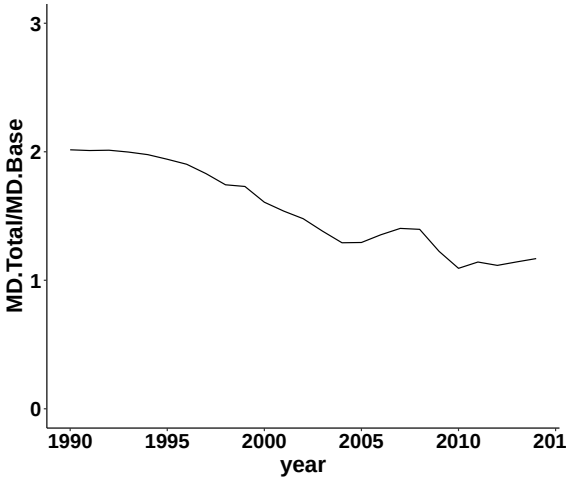

(VI) Male, deviance ratios

FIGURE 3.5: Structural changes in Kenyan mortality pattern

A comprehensive discussion of the methods used for fitting, evaluating, and selecting the most appropriate mortality model follows in the next section.

3.2 Cause-of-Death Mortality Modelling

In this research, we modelled $m(x,t)$ since it was observable in tandem with our constant mortality assumption. Additionally, central exposure to risk rather than initial exposures were used. Given any country with similar demographic and socioeconomic profiles, we hope the proposed methodologies and models can also be applied to them.

First, we explore age-specific mortality, $m(x,t)$. Figure 3.6 shows the evolution of historical age-specific female mortality for selected ages between 1990 and 2016.[7] It shows that historically, observed mortality generally declined over time, with the highest mortality improvements occurring at younger ages. Thus, we made the following additional observations for both females and males:

a) Infant mortality consistently improved, with under 5-year-old mortalities experiencing the most significant improvements post-2000, showing an almost linear downward trend. For example, Figure 3.6i shows the historical mortality trend for 1-year-olds over the investigation period.

b) Mortality seems to have worsened between ages 6 and 9. For example, Figure 3.6ii shows that mortality at age 7 worsened. However, a general linear improvement was seen again for pre-teenagers[8] in all years (see, e.g. Figure 3.6iii), after which it became erratic at mid-adolescence[9] (see, e.g. Figure 3.6iv).

   In Figure 3.3, we observed that the highest causes of death in Kenya have been HIV/AIDS and other sexually transmitted infections (STIs), followed by respiratory infections and TB. A recent study by Osano et al. (2017) reported that HIV/AIDS, respiratory tract infections, and malaria were the major causes of death for people between 5 and 17 years old in Kenya.

   In another study, Abuga et al. (2019) observed an increase in mortality in Kenya between the ages of 6 and 9. Therefore, considering these observations by Abuga et al. (2019) and Osano et al. (2017), the observations from Figure 3.6ii can be attributed to high mortality rates due to HIV/AIDS, respiratory tract infections, and malaria, as aligned with the observations in Figure 3.3.

[7] Males depicted similar patterns and therefore for presentation purposes, we have only shown graphs for females.
[8] Between ages 10 and 12, also early adolescence.
[9] Ages 13 to 16.

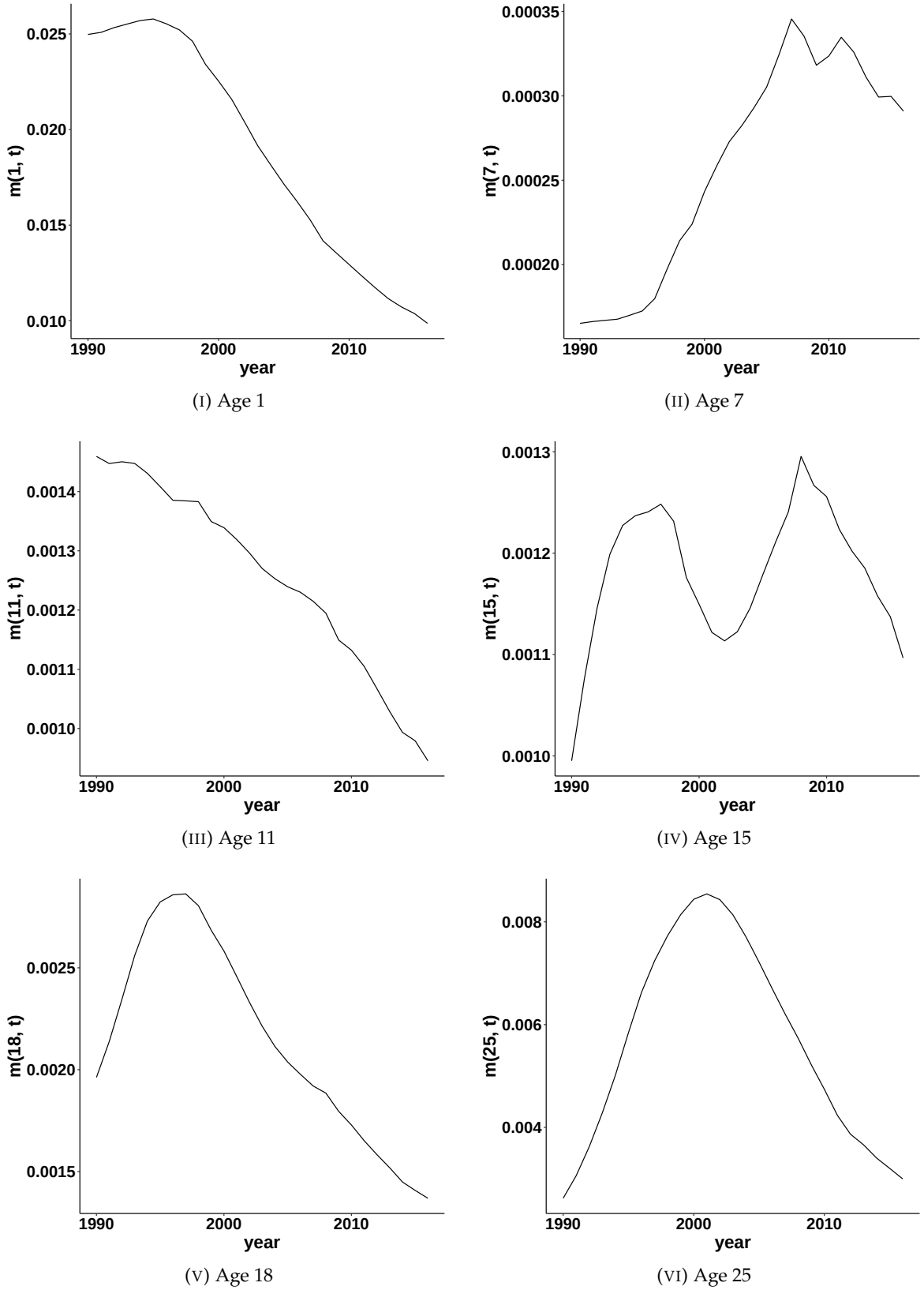

(I) Age 1

(II) Age 7

(III) Age 11

(IV) Age 15

(V) Age 18

(VI) Age 25

FIGURE 3.6: Historical age-specific female mortality trend between 1990 and 2016

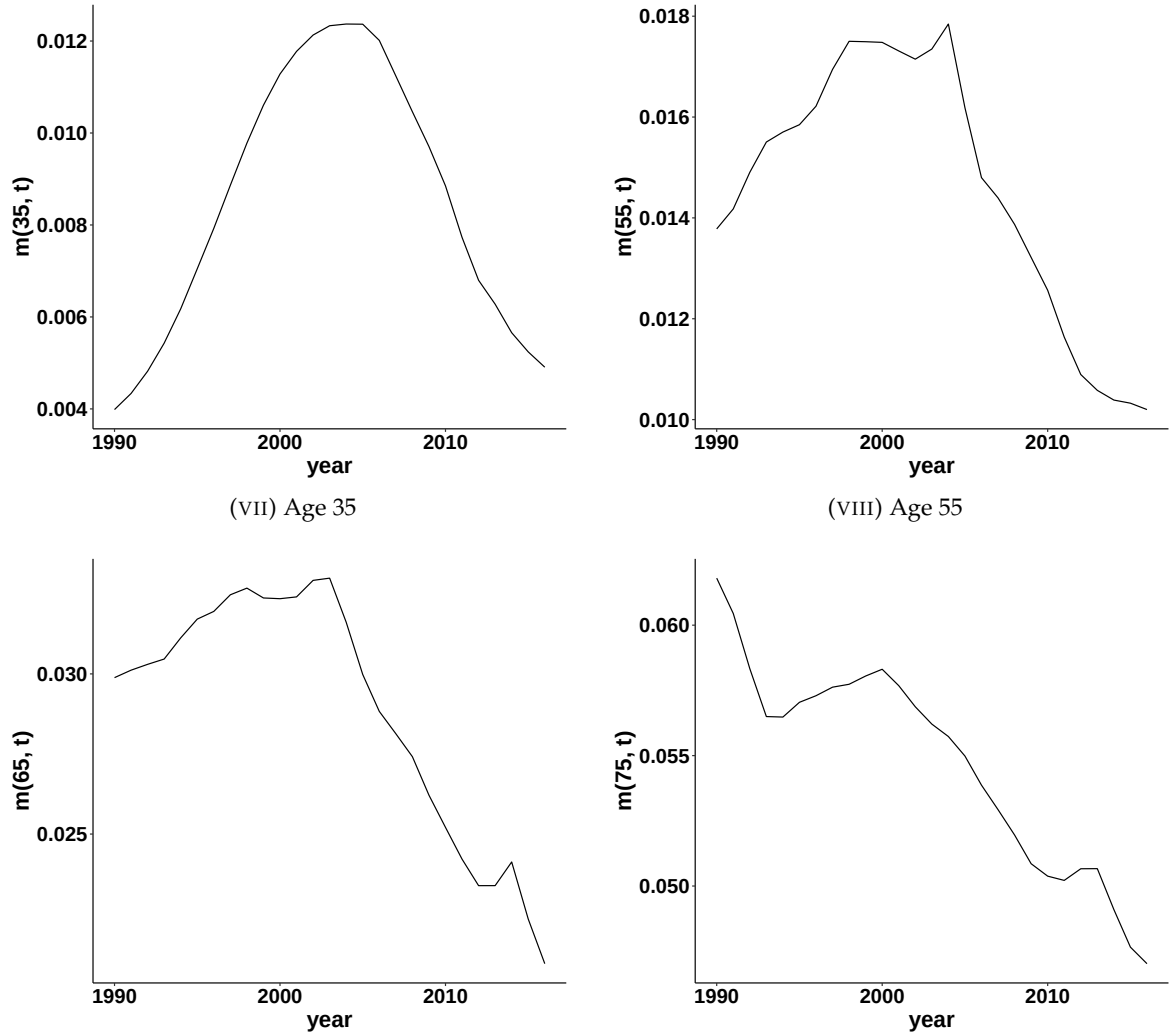

(VII) Age 35 (VIII) Age 55

(IX) Age 65 (X) Age 75

FIGURE 3.6: Historical age-specific female mortality trend between 1990 and 2016

c) Although there was general improvement after age 17, it was inconsistent. Notably, mortality worsened in the first 7 years with linear improvement afterwards (e.g. see Figures 3.6v - 3.6viii). This mortality shape over the sexually active years coincided with the HIV/AIDS epidemic. There appeared to be a shift across these ages in 2003 (Figures 3.6v - 3.6vii), coinciding with the commencement of the subsidised ARV[10] provision by the Kenyan government (Katana et al., 2020). This period was also the childbearing age.

d) After the childbearing age, mortality regained its almost linear decline over all years (e.g. see Figures 3.6viii & 3.6x), until older ages when mortality improvements were noticeably lower and erratic due to sparse and unreliable data. Other than mid-adolescence, mortality improvement rates seemed approximately linear over the years.

[10] Antiretroviral drugs.

The rest of this section is organised into three sections: Section 3.2.1 investigates the appropriate fitting period, and Section 3.2.2 describes the models fitted to the data. This Section then concludes by evaluating the out-of-sample performance of the models we fitted to the Kenyan mortality data.

3.2.1 Fitting Period

From Figure 3.5, and based on the discussion by Booth et al. (2002) on choosing the optimal fitting period, we identified the following periods as possibilities:

a) For females, the possible data periods were either the full 1990 to 2016 data range or a reduced range identified in the previous section, from 2003 to 2016.

b) For males, it was either the full range or the period between 2000 and 2016.

Hence, we fitted all models under investigation and evaluated their out-of-sample performance. Next, we present the out-of-sample performance of the fitted LC models for the following periods.

a) For female mortality:

   i) fit LC using data from 1990 to 2006 and forecast for 10 years,

   ii) fit LC using data from 1990 to 2010 and forecast for 6 years, and

   iii) fit LC using data from 2003[11] to 2010 and forecast for 6 years.

b) For male mortality:

   i) fit LC using data from 1990 to 2006 and forecast for 10 years,

   ii) fit LC using data from 1990 to 2010 and forecast for 6 years, and

   iii) fit LC using data from 2000[12] to 2010 and forecast for 6 years.

Table 3.2 summarises the out-of-sample measures for the three windows. The key observations are as follows:

a) Fitting the model to data from 1990-2010, 2003-2010 (for females), and 2000-2010 (for males) resulted in better overall model performance. This improvement was anticipated, as reducing the prediction period from 10 to 6 years generally enhances model fit.

   Comparing the second[13] and third windows,[14] the third window showed consistent improvements for all causes of death (CoD). This suggests that data prior to 2000 contained

[11] This is the point at which the mortality structure seem to have changed for females.
[12] This is the year in which the mortality structure seem to have changed for males.
[13] 1990-2010 fitting period.
[14] 2003-2010 for females and 2000-2010 for males.

TABLE 3.2: Out-of-sample forecasts for different fitting periods

		Female			Male		
Period	**CoD**	RMSE[15]	MPE[16]	MAPE[17]	RMSE	MPE	MAPE
1990-2006	Total	0.010709	-62%	62%	0.009853	-43%	44%
	LRI	0.000920	-14%	16%	0.001149	-17%	20%
	Meningitis	0.000036	-3%	6%	0.000050	-18%	19%
	Malaria	0.000310	-179%	179%	0.000274	-176%	176%
	Deficiency	0.000162	-15%	17%	0.000197	-23%	25%
	Injuries	0.000024	-8%	11%	0.000095	-13%	15%
	Cardiovascular	0.002453	-15%	17%	0.001778	-18%	19%
	TB	0.001040	-48%	48%	0.001624	-56%	56%
	HIV/AIDS	2.097583	-105914%	105917%	0.397173	-13738%	13743%
	Cancer	0.000205	-2%	7%	0.000555	-11%	15%
	Others	0.004451	-6%	10%	0.003503	-9%	12%
1990-2010	Total	0.005458	-40%	41%	0.004692	-23%	26%
	LRI	0.000465	-9%	11%	0.000729	-16%	19%
	Meningitis	0.000027	-4%	5%	0.000040	-17%	18%
	Malaria	0.000086	-9%	53%	0.000071	-14%	51%
	Deficiency	0.000114	-17%	17%	0.000175	-28%	28%
	Injuries	0.000016	-5%	7%	0.000055	-10%	11%
	Cardiovascular	0.001044	-9%	10%	0.000760	-12%	13%
	TB	0.000323	-26%	27%	0.000634	-30%	30%
	HIV/AIDS	0.002840	-234%	240%	0.001169	-88%	102%
	Cancer	0.000099	-1%	4%	0.000383	-11%	13%
	Others	0.002260	-5%	7%	0.002075	-9%	11%
2003-2010 (Female)/ 2000-2010 (Male)	Total	0.002869	-5%	9%	0.002367	-6%	8%
	LRI	0.000276	0%	6%	0.000318	-11%	13%
	Meningitis	0.000014	0%	4%	0.000024	-11%	13%
	Malaria	0.000134	32%	60%	0.000089	13%	55%
	Deficiency	0.000071	-10%	11%	0.000118	-24%	25%
	Injuries	0.000011	-2%	5%	0.000037	-6%	9%
	Cardiovascular	0.000826	-3%	6%	0.000577	-9%	11%
	TB	0.000129	-7%	8%	0.000274	-17%	18%
	HIV/AIDS	0.000749	-48%	49%	0.000299	-17%	23%
	Cancer	0.000096	0%	4%	0.000286	-8%	11%
	Others	0.001607	1%	5%	0.001017	-5%	8%

little useful information for predicting future mortality. Figures 3.5i and 3.5ii in Figure 3.5 highlight a noticeable change in the annual rate of mortality improvement post-2000.

b) Including data from 1990-2000 led to consistent underestimation of mortality for both males and females, as indicated by the all-negative values of the mean percentage error (MPE).

c) Excluding pre-2000 data improved model performance for most causes, except for malaria (females) and deficiencies (males), where performance worsened slightly in the third window compared to the second. Despite this, the marginal decline did not justify the added complexity of fitting separate models for these causes.

[15]Root mean squared error.
[16]Mean percentage error.
[17]Mean absolute percentage error.

The findings suggest that the optimal data period is post-2000 for males and post-2003 for females. Considering factors affecting mortality structure in Kenya such as healthcare reforms and improved access to medications like ARVs,[18]discarding earlier data was reasonable. Balancing data availability and model improvement further justified this approach, as shown in Table 3.2.

Although malaria and deficiencies did not benefit from excluding pre-2000 data, forecast reconciliation techniques, as outlined in later sections, were expected to mitigate the slight prediction decline. For consistency and simplicity, data from 2000-2016 were ultimately used for both males and females, rather than adopting different fitting windows.

3.2.2 Model Fitting

The models fitted included those proposed by Lee and Carter (1992, p. LC), Renshaw and Haberman (2006), Plat (2009, PL), and Currie et al. (2004, PS). As expected, the initial projections did not align with the overall projected mortality, necessitating the application of forecast reconciliation to ensure consistency while preserving the structure of CoD mortality projections.

Two special cases of Renshaw and Haberman's model were also considered: The RH model, where $\beta_x^{(0)} = 1$ and the APC model, where $\beta_x^{(0)} = \beta_x^{(1)} = 1$. While the RH model fit the data well due to its higher number of parameters, it failed to produce reasonable cross-validated forecasts, particularly for the more variable CoD data. This demonstrated that a good fit does not always translate to reliable forecasts.

Overfitting by the RH model caused nonsensical results when used with bottom-up and MinT reconciliation approaches, which rely on accurate lower-series forecasts. However, the RH model performed well for all-cause mortality and when top-down reconciliation was applied, as this approach leverages the accuracy of the top-series forecasts. Due to these limitations, RH model results are excluded from subsequent sections.

Additionally, we evaluated the constrained penalised spline (CPS) approach introduced by Camarda (2019). This novel methodology offers a flexible framework, balancing the overly adaptive nature of traditional P-spline models with the rigidity of stochastic models like the LC model. The CPS approach allows for incorporating prior knowledge about mortality, making it an intuitive and versatile option for modellers.

3.2.3 Out-of-Sample Measures

We fit the models described in Section 3.2.2 to Kenyan mortality data (2000–2016) and evaluated their performance using out-of-sample measures. The models were fit using data from 2000

[18]See Section 3.1.4 for details.

to 2010, then used to predict mortality up to 2016. To ensure forecast coherence, three reconciliation approaches were applied: top-down, bottom-up, and optimal combination by trace minimisation (MinT). For brevity, we present the results for females only.

Table 3.3 summarises the results. Results from five of the six models fitted are shown, excluding one for previously discussed reasons. The measures were calculated for forecasting horizons ranging from 1 to 6 years. For readability purposes, we highlighted the lowest values under each reconciliation approach for each out-of-sample measure and CoD. Key observations from Table 3.3 include:

(a) First, the LC model generally fit well to the all-cause mortality data. This observation supported our choice to use the LC model in selecting the optimal period to fit the models, as discussed in Section 3.2.1. It was also aligned with various studies analysing the appropriateness of the LC model in modelling and forecasting mortality (see, e.g. Ibrahim et al., 2017; Neves et al., 2017, and the references therein).

(b) Additionally, the LC model performed considerably well in modelling various CoDs based on the various LC model outputs highlighted in Table 3.3, further supporting the observation above.

(c) Notably, irrespective of the reconciliation method applied, the forecasting performance of the CPS model fell consistently between the performances of the more restrictive LC model and the more flexible PS model. This observation was in line with the discussions of Camarda (2019), the developer of the CPS model. According to Camarda, the CPS model can be used as a sliding scale between these two models, depending on the amount of confidence in the historical data, as further discussed in Chapter 4.

(d) When modelling and forecasting overall mortality, CoD mortality modelling techniques can improve the model and the forecasts. Additionally, applying some form of reconciliation can help improve the forecasts. As seen in Table 3.3, both the MinT and bottom-up approaches resulted in better forecasts of total mortality than the top-down approach. It is noteworthy that the application of the bottom-up approach to all-cause mortality implied summing the forecasts for the individual CoDs considered.

(e) MinT method performed well for mortality conforming to the typical mortality shape. For example, the application of the MinT method in reconciling malaria mortality forecasts resulted in a significant overestimation of future malaria mortality. Similar observations were made for male mortality. Therefore, we did not expect that the MinT would be appropriate for modelling mortalities with atypical patterns.

However, these observations may contradict the extant, research such as that by Li et al.

(2019), since these researchers applied these methods to mortality with a regular shape.[19] However, Wickramasuriya et al. (2018) appreciated that the bottom series often give important insights into the drivers of mortality (see also Alai et al., 2014; Li & Lu, 2018).

(f) The out-of-sample forecasting performance of malaria show that it would benefit from some form of reconciliation. This was the case because of the irregular nature of malaria mortality, especially at the tail ages. Therefore, at the mid-age range, the predictions from malaria mortality were more accurate than in the tail ends. Forcing the forecasts to have a similar structure as the overall observed mortality by reconciling deviations from the tail ages was expected to rectify the significant underestimation of mortality at this age.

(g) A closer look at the out-of-sample measures showed that of all the causes we investigated, HIV/AIDS and malaria significantly impacted overall mortality. It was valid that if a single model was to be chosen to fit all causes, then requiring it to fit well to HIV/AIDS and malaria mortality was appropriate and justified. However, it was challenging to achieve this given the irregular pattern of these mortalities, so judgement was applied.

(h) Due to meagre mortality rates for some causes at given age ranges, a slight change in mortality resulted in a considerable mortality deviation, as observed in Table 3.3. Therefore, it was imperative to interpret these measures carefully alongside the observed mortalities, as shown in Figure 3.4.

(i) Finally, we observed that no single model accurately fit all CoDs. However, the PL model consistently performed well on many CoDs, followed by the CPS model. We further noted that the LC model's overall performance was thwarted by its forecasting performance on malaria. Otherwise, it performed well when fitted to other causes. Moreover, no single model consistently performed well across all CoDs for male mortality. Additionally, the MinT reconciliation method was significantly compromised by the more irregular mortalities, especially malaria.

These results highlighted some of the advantages of CoD mortality modelling and the importance of model selection. For example, while the MPE indicated that the LC fit well to female all-cause mortality, this accuracy resulted from the model overestimating most of the other causes while considerably underestimating HIV/AIDS mortality.

When selecting models to be fitted, it is essential to know what drives the observed mortality patterns. Additionally, with such irregular mortality patterns as observed here, no one reconciliation approach would fit all, so it was essential to test as many approaches as possible.

[20] Optimal combination by trace minimisation.

[19] That is, higher mortality at birth which slightly declines after birth until teenage years where it rises again, exhibits an accident hump towards the end of teenage and increases almost linearly after this.

TABLE 3.3: Out-of-sample measures for females for the models fitted and reconciliation approaches used

		MinT[20]			Bottom-Up			Top-Down		
Cause	**Model**	**RMSE**	**MPE**	**MAPE**	**RMSE**	**MPE**	**MAPE**	**RMSE**	**MPE**	**MAPE**
Total	APC	0.004454	-6%	17%	0.001755	-10%	15%	0.004208	**-6%**	16%
	CPS	0.002441	**-5%**	**11%**	0.002277	-9%	13%	0.002349	-7%	**12%**
	LC	0.003805	-10%	13%	0.003944	-12%	14%	0.003804	-10%	13%
	PL	0.002221	-8%	15%	**0.001459**	-9%	13%	0.002135	-8%	15%
	PS	**0.001721**	-8%	16%	0.002926	**-5%**	**12%**	**0.001302**	-7%	13%
LRI	APC	0.000579	13%	27%	0.000268	2%	7%	0.000556	5%	12%
	CPS	0.000314	8%	29%	0.000278	-11%	21%	0.000287	-9%	21%
	LC	0.000391	**7%**	**17%**	0.000405	80%	**6%**	0.000384	**1%**	**6%**
	PL	**0.000270**	76%	32%	**0.000159**	**1%**	**6%**	0.000292	2%	10%
	PS	0.000392	-39%	85%	0.000281	-33%	42%	**0.000173**	-40%	50%
Meningitis	APC	0.000362	126%	145%	0.000025	6%	7%	0.000046	9%	12%
	CPS	**0.000076**	**11%**	**31%**	0.000059	-8%	22%	0.000058	-6%	24%
	LC	0.000122	39%	47%	**0.000023**	97%	**5%**	**0.000021**	**5%**	**6%**
	PL	0.000141	96%	52%	**0.000023**	**5%**	7%	0.000037	6%	10%
	PS	0.000318	-123%	159%	0.000085	-15%	27%	0.000091	-19%	32%
Malaria	APC	0.000325	46660%	46691%	0.000117	21%	57%	0.000119	24%	**56%**
	CPS	0.000196	1738%	**7508%**	0.000122	**-11%**	84%	0.000123	**-9%**	84%
	LC	**0.000161**	19045%	19103%	**0.000111**	97%	58%	**0.000113**	17%	58%
	PL	0.000183	**97%**	10331%	0.000120	24%	**56%**	0.000120	25%	**56%**
	PS	0.000535	-67385%	71577%	0.000155	-28%	120%	0.000155	-33%	124%
Deficiency	APC	0.000306	55%	128%	0.000071	**-9%**	11%	**0.000061**	**-6%**	**10%**
	CPS	0.000098	24%	50%	0.000078	-23%	29%	0.000078	-20%	27%
	LC	**0.000096**	5%	**46%**	0.000104	95%	14%	0.000093	-11%	12%
	PL	0.000133	97%	126%	**0.000052**	**-9%**	**10%**	0.000068	-8%	12%
	PS	0.000341	**4%**	117%	0.000091	-46%	50%	0.000115	-50%	54%
Injuries	APC	0.000379	40%	131%	0.000008	**0%**	**4%**	0.000023	3%	10%
	CPS	**0.000017**	**3%**	**7%**	0.000017	**0%**	6%	0.000017	2%	6%
	LC	0.000111	20%	37%	0.000014	93%	**4%**	**0.000013**	2%	**5%**
	PL	0.000135	94%	92%	**0.000007**	**0%**	**4%**	**0.000013**	**1%**	8%
	PS	0.000052	-7%	16%	0.000019	-1%	6%	0.000021	-2%	9%
Cardiovascular	APC	0.000779	-16%	44%	0.000541	**-3%**	6%	0.001307	**0%**	10%
	CPS	0.000757	**2%**	**10%**	0.000756	-5%	8%	0.000772	-2%	7%
	LC	0.001150	11%	20%	0.001146	98%	6%	0.001185	-1%	**6%**
	PL	**0.000493**	100%	56%	**0.000451**	**-3%**	**5%**	0.000572	-2%	10%
	PS	0.000811	-17%	23%	0.000901	-6%	9%	**0.000298**	-7%	10%
TB	APC	0.000267	-3%	33%	0.000181	**-11%**	**12%**	**0.000093**	**-7%**	**10%**
	CPS	**0.000166**	-12%	21%	**0.000177**	-23%	25%	0.000169	-20%	22%
	LC	0.000167	**2%**	**20%**	0.000237	98%	13%	0.000206	-10%	11%
	PL	0.000183	100%	38%	0.000197	-12%	13%	0.000177	-11%	14%
	PS	0.000314	-44%	48%	0.000209	-25%	26%	0.000237	-29%	31%
HIV/AIDS	APC	0.001018	222%	317%	0.001017	-79%	84%	0.001022	-70%	76%
	CPS	0.000592	-12%	148%	0.000623	-70%	73%	0.000578	-67%	70%
	LC	0.001083	**-5%**	112%	0.001084	60%	71%	0.001113	-66%	67%
	PL	0.000888	75%	**80%**	0.000881	-57%	61%	0.000960	-54%	60%
	PS	**0.000425**	-400%	485%	**0.000221**	**-49%**	**54%**	**0.000207**	**-51%**	**56%**
Cancer	APC	0.000247	-6%	28%	**0.000088**	-4%	5%	0.000154	**0%**	7%
	CPS	**0.000100**	**4%**	**10%**	0.000099	**-1%**	7%	0.000109	1%	7%
	LC	0.000133	8%	11%	0.000114	96%	**4%**	0.000119	2%	**5%**
	PL	0.000127	97%	32%	0.000092	-4%	5%	**0.000108**	-2%	8%
	PS	0.000140	-7%	13%	0.000124	-2%	8%	0.000119	-3%	9%
Others	APC	0.001180	3%	7%	0.000882	2%	6%	0.002206	5%	10%
	CPS	0.001379	-4%	16%	0.001322	-8%	16%	0.001392	-5%	16%
	LC	0.002016	**1%**	**6%**	0.002043	59%	**5%**	0.001943	**2%**	**6%**
	PL	**0.000835**	65%	**6%**	**0.000764**	**1%**	**5%**	0.001161	3%	9%
	PS	0.001040	-19%	32%	0.001879	-16%	26%	**0.001083**	-20%	30%

For completeness, we calculated Theil's U to assess the accuracy of our forecasts. Figure 3.7 presents Theil's U for all-cause mortality across three reconciliation methods: MinT, bottom-up, and top-down.

Theil's U measures the randomness of forecasts, effectively evaluating whether predictions are better than random guesses. Its decision rules are as follows:

a) $U < 1$: Forecasts are better than random guesses.

b) $U = 1$: Forecasts are as good as random guesses.

c) $U > 1$: Forecasts are worse than random guesses.

As shown in Figure 3.7, all models produced forecasts significantly better than random guesses ($U < 1$), confirming their strong mortality forecasting capabilities.

Theil's U generally increased over longer forecast horizons, reflecting the growing uncertainty over time. Consistent with previous findings, the CPS model demonstrated intermediate performance between the LC and PS models. Mortality forecasting also benefitted from forecast reconciliation, as previously discussed.

Building on prior observations, certain CoDs exhibited mortality patterns closer to regular expectations.[21] Motivated by Li et al. (2019), we attempted to cluster CoDs with similar patterns for joint modeling. This approach aimed to smooth irregularities in the data without losing essential information from the bottom series.[22]

However, except for the CPS model, this clustering approach did not yield significant improvements in out-of-sample performance. As a result, we opted not to adopt this method, and it is not discussed further.

Finally, to be consistent with the demographic literature, we tested our models' out-of-sample accuracy using commonly used demographic measures (see, e.g. Camarda, 2019). Specifically, two measures were calculated: Life expectancy at birth (e_0) and the average number of life years lost measured at birth ($e_0^\dagger$), which are the two most commonly used measures of lifespan (Camarda, 2019).

e_0 was used to measure the mean lifespan, while $e_0^\dagger$ estimated lifespan variations. They could also monitor the overall population health (Permanyer et al., 2022). As noted by Tuljapurkar et al. (2000), healthcare financing is primarily driven by a sustained increase in human lifespan. Therefore, ensuring that the models accurately modelled and forecasted the human lifespan was essential. To measure the out-of-sample accuracy of our models when used to predict these two measures,we used the RMSE. The results are summarised in Table 3.4.

[21] Relatively smooth and less irregular mortality trends.

[22] The individual causes of death.

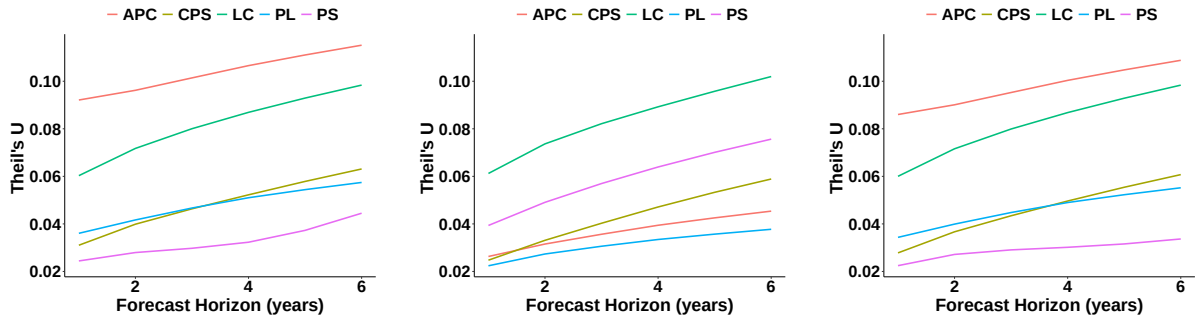

(I) MinT (II) Bottom-Up (III) Top-Down

FIGURE 3.7: Theil's U for female total mortality using the three reconciliation methods

TABLE 3.4: Out-of-sample RMSE for e_0, $e_0^\dagger$ and η

		Female			Male		
Model	**Approach**	η	e_0	$e_0^\dagger$	η	e_0	$e_0^\dagger$
APC	MinT	0.0045	1.5477	2.1088	0.0038	0.8520	1.5726
	bottom-up	0.0018	1.8029	0.9359	0.0018	1.3819	0.7570
	top-down	0.0042	1.5735	2.0060	0.0036	0.9013	1.4988
CPS	MinT	0.0024	0.5012	**0.1744**	**0.0015**	0.4948	0.1161
	bottom-up	0.0023	1.2980	0.6487	**0.0017**	1.0000	0.4212
	top-down	0.0023	0.7684	0.3467	**0.0014**	**0.1048**	0.2023
LC	MinT	0.0038	1.6344	0.4603	0.0024	0.7584	**0.0697**
	bottom-up	0.0039	2.0465	0.3765	0.0022	1.4771	0.1612
	top-down	0.0038	1.6679	0.4523	0.0024	0.8146	**0.0525**
PL	MinT	0.0022	2.4267	1.5647	0.0018	1.4659	1.0886
	bottom-up	**0.0015**	1.7208	0.8163	0.0018	1.2362	0.7469
	top-down	0.0021	2.3639	1.4976	0.0018	1.4427	1.0551
PS	MinT	**0.0017**	**0.4870**	0.2530	0.0023	0.7313	0.4961
	bottom-up	0.0029	**0.2642**	**0.0604**	**0.0017**	**0.1431**	**0.0367**
	top-down	**0.0013**	**0.3496**	**0.1388**	0.0018	**0.4871**	0.3267

For ease of discussion, we highlighted the three lowest RMSEs in any given column in bold. For females, for example, the three lowest mortality RMSEs were those obtained from the PS model using the top-down approach, the PL model using the bottom-up reconciliation approach, and the PS model using the MinT reconciliation approach, in that order. The following observations were made from Table 3.4:

a) In general, when forecasting the measures of the lifespan, the more restrictive class of models performed poorly compared to other models, such as the PS and the CPS, because of the ability of the latter models to capture the variability in the irregular mortality pattern better than the former.

b) We also observed that, the MinT reconciliation approach generally tended to worsen the predictions. Table 3.4 shows that the bottom-up reconciliation approach was the most appropriate technique when forecasting lifespan measures. Notably, the forecasts could have been affected if the bottom series was volatile, as remarked by Li et al. (2019), which is often cited as the downside of the bottom-up approach. In such cases, choosing appropriate models for the given scenario is essential.

c) The results in Table 3.4 were consistent with the results discussed thus far. For example, Table 3.4 shows that the LC model was less sensitive to the reconciliation approach than the other models.

d) Additionally, we observed that the PS model performed considerably better than most of the other models due to its flexibility in capturing most features in a mortality series with irregular patterns. This observation highlighted the importance of choosing a model based on the mortality pattern experienced.

e) Finally, while no single model fit all, the CPS model maintained a relatively stable fit regardless of the reconciliation approaches or metrics employed. Furthermore, its performance remained consistent across genders, aligning with prior findings. This characteristic can be attributed to its adaptability, allowing it to filter out mortality data fluctuations less likely to persist in the future while effectively capturing the primary irregularities.

   As previously noted, the CPS model consistently generated outcomes that struck a balance between the more rigid LC model and the more flexible PS model. The insights gleaned from the data presented in Table 3.4 further bolstered our observation of the CPS model being a sliding scale between the restrictive and flexible class of mortality models.

Figure 3.8 shows the out-of-sample forecasts obtained from the five fitted models using the three reconciliation approaches over the 6-year projection horizon. The PS model generally produced reasonable projections, especially for life span variations measure $e_0^\dagger$. However, for longer period predictions, the PS model was likely to overestimate the life expectancy at birth. Here, the CPS model closely matched the life expectancy trend. Unsurprisingly, the CPS model benefitted most from the MinT reconciliation approach when predicting lifespan measures, which was consistent with previous observations.

We concluded that the PS model performed better while modelling all-cause mortality, the PL model performed better at modelling CoD data, and the CPS model benefitted most from some form of reconciliation (see Table 3.3).

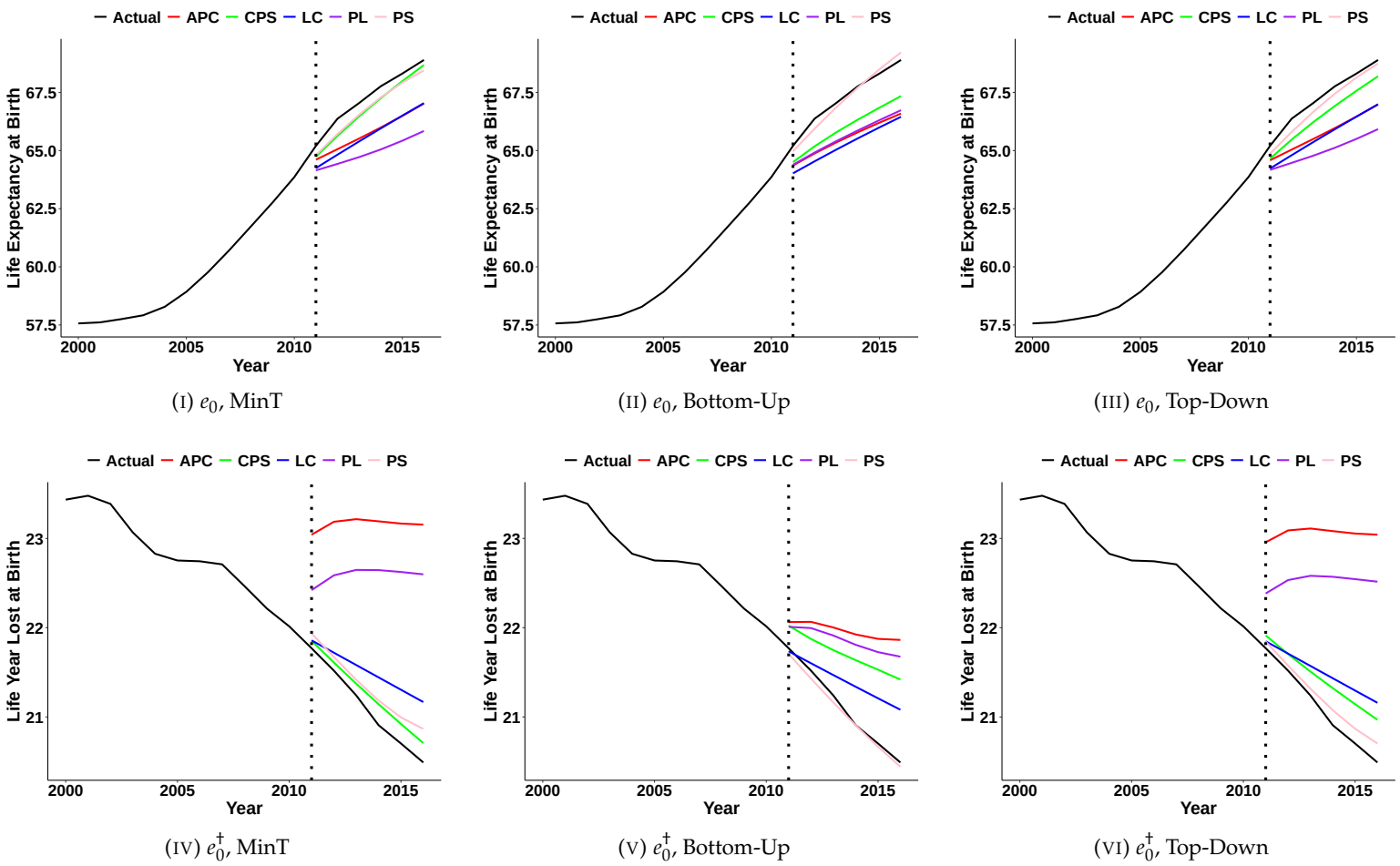

(I) e_0, MinT (II) e_0, Bottom-Up (III) e_0, Top-Down

(IV) $e_0^\dagger$, MinT (V) $e_0^\dagger$, Bottom-Up (VI) $e_0^\dagger$, Top-Down

FIGURE 3.8: Out-of-sample mean lifespan (e_0) and life expectancy variation ($e_0^\dagger$) results

Additionally, the CPS model was a stable model that accurately captured the variations in mortality data. As seen in Chapter 4, the CPS model could be adjusted to reproduce the results from either the restrictive class of models, such as the LC model, or the more flexible model, such as the PS model, by changing the penalty parameters.

3.2.4 Mortality Model Selection

To summarise the results from this section, we scored the five models we fitted using the following parameters: COD out-of-sample performance, model stability and measures of lifespan out-of-sample performance. We then summarised the results in Table 3.5[23] and made the following main observations:

a) Overall, the LC model was a good model for modelling mortality. This conclusion supported the existing literature on applying the LC model in modelling mortality, and our choice to use the LC model in selecting the fitting period in section 3.2.1.

b) An extension of the LC model, the PL model, outperformed the LC model as expected because of its additional parameters. Recall that we defined the PL model as

$$\texttt{log}(m(x,t)) = \alpha_x + k_t^{(1)} + (x-\bar{x})k_t^{(2)} + (x-\bar{x})^+ k_t^{(3)} + \gamma_{t-x}$$

This model performed better for the following reasons.

i) The PL model is a combination of the Cairns-Blake-Dowd (CBD) model (Cairns et al., 2006) and the LC model. Therefore, it combines the features of the CBD and the LC model to model mortality for the full age ranges.

It also adds a cohort term. This combination of models leads to a general improvement in model performance in line with studies such as Shang and Booth (2020), who demonstrated improvements in results when more than one model was combined.

ii) Through the $k_t^{(2)}$ term, the model models mortality improvements in younger ages[24] relative to older ages. This is an important factor when modelling mortality from diseases such as malaria, which disproportionately affects children compared to adults.

[23] In this table, the lower the score, the poorer the model in modelling and predicting Kenyan mortality. The full detail on the scoring algorithm has been exhaustively discussed by **Rotich2024<empty citation>**, with full details available here.

[24] Below the average age.

TABLE 3.5: Summary of Model selection for COD mortality modelling.

		Female					Male				
		APC	**CPS**	**LC**	**PL**	**PS**	**APC**	**CPS**	**LC**	**PL**	**PS**
Cause	**Approach**										
Summary by Reconciliation Approach											
Overall	MinT	105	211	182	134	122	108	205	178	144	123
	BU	172	141	136	213	113	181	144	139	201	119
	TD	139	153	186	171	121	163	157	175	160	116
Summary by Mortality Data Used											
All-cause	All	51	110	65	77	113	53	116	80	78	91
COD	All	365	395	439	441	243	399	390	412	427	267
Summary by Reconciliation Approach and Mortality Data Used											
All-cause	MinT	15	41	25	23	35	17	43	29	24	24
	BU	20	32	16	34	37	19	32	22	30	39
	TD	16	37	24	20	41	17	41	29	24	28
COD	MinT	90	170	157	111	87	91	162	149	120	99
	BU	152	109	120	179	76	162	112	117	171	80
	TD	123	116	162	151	80	146	116	146	136	88
OVERALL											
		416	505	504	518	356	452	506	492	505	358

iii) Finally, the $k_t^{(3)}$ term improves the model's accuracy when measuring mortality at older ages by introducing an additional term for mortality at older ages.

We fitted both the model shown above and the reduced model

$$\texttt{log}(m(x,t)) = \alpha_x + k_t^{(1)} + (x - \bar{x})k_t^{(2)} + \gamma_{t-x}$$

and observed that the inclusion of the term $k_t^{(3)}$ overall improved our model. Therefore, our mortality data had cohort effects, which the PL model better captured where mortality patterns at lower ages differed from older ages.

c) As observed, the CPS model benefitted from reconciliation. In particular, it performed well when the MinT method was applied. It was also a stable model since the reconciliation approach did not adversely affect its performance.

d) Additionally, the CPS model was good for modelling all-cause mortality. However, the PL model outperformed it when applied to CoD modelling. As discussed in Chapter 4, by appropriately choosing the penalty parameters of the CPS model, we produced similar results with the CPS model and the PL model. Therefore, the CPS model presented a versatile model.

Generally, these results showed that the CPS and PL models were the most appropriate for modelling the Kenyan mortality data. We compared the results of the PL model, the PS model, and the CPS model to show that with appropriately chosen penalty parameters, the PS and PL models could be replicated.

We retained and further evaluated the PS model since it showed good performance when applied to data with stable mortality patterns and short-term mortality forecasting. Finally, the PS model tended to overfit the mortality and perform poorly for longer-term predictions, as presented in Table 3.5.

3.3 Cause-of-Death Mortality Forecasting

When forecasting mortality, selecting the model with the best out-of-sample performances does not always suffice. Thus, we also wanted to check that the forecasts produced by the model were sensible. For example, in Figure 3.9, we showed short-term and long-term forecasts of the malaria mortality model using the three models selected. Figures 3.9i, 3.9iii and 3.9v were obtained using the bottom-up approach, while Figures 3.9ii, 3.9iv, and 3.9vi were derived from the top-down reconciliation approach.

In Figures 3.9i and 3.9ii, we saw that the PS model produced reasonable forecasts in the short term but quite unreasonable forecasts in the long run due to the PS's model flexibility, providing another example that just because a model performs well in out-of-sample forecasting does not mean it will perform well when applied to forecasting. Therefore, the reasonableness of forecasts should always be checked.

The CPS model made it possible to check and adjust the model based on the reasonableness of the forecasts. Since we could change the constraint parameters to replicate the PS and PL models' results, it was possible to calibrate them based on the modeller's need. We only evaluated the PL and the CPS models for these reasons. However, we show in Chapter 4 that CPS constraints could be appropriately chosen to produce results similar to the PL and PS models.

From the discussions in Section 3.2, we established that the PL model best modelled Kenyan CoD mortality by assessing the out-of-sample performances of the six selected models. We also observed that the CPS model presented a stable model among all the models we considered.

We also saw that the top-down and bottom-up approaches generally performed substantially better than the MinT reconciliation method. In Table 3.5, we observed that the PL performed better with the bottom-up reconciliation approach. In contrast, the CPS model would produce better results if the top-down reconciliation approach were applied. As already outlined, the PL was the best for modelling individual causes.

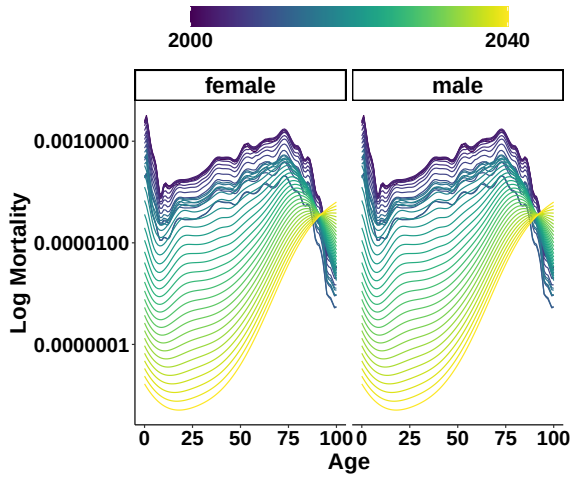

(I) PS model, BU

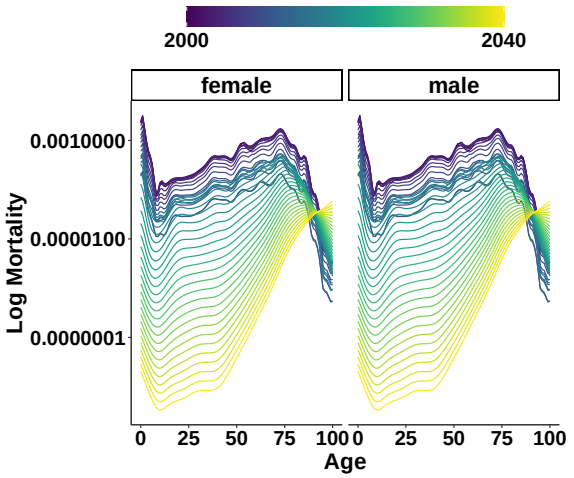

(II) PS model, TD

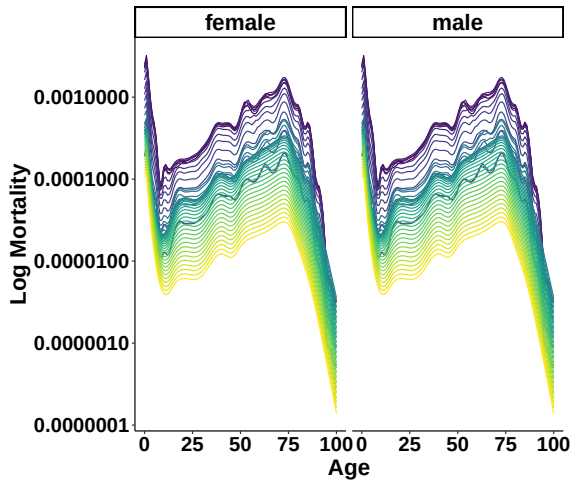

(III) CPS model, BU

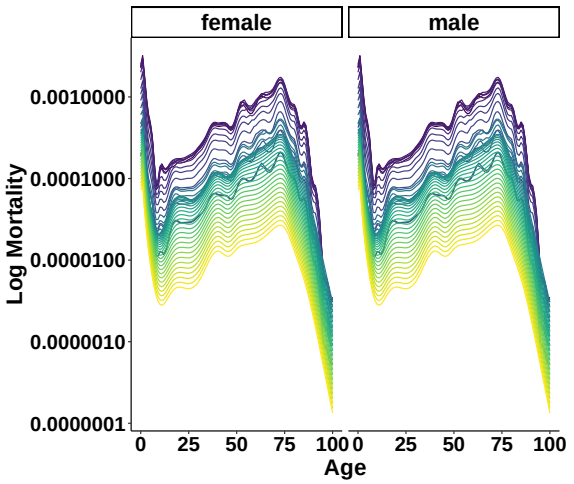

(IV) CPS model, TD

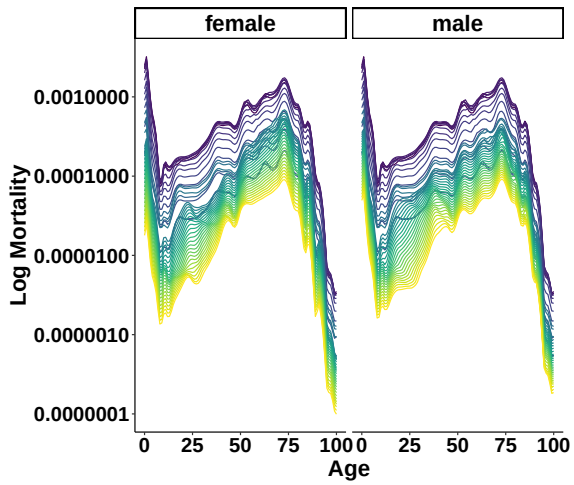

(V) PLAT model, BU

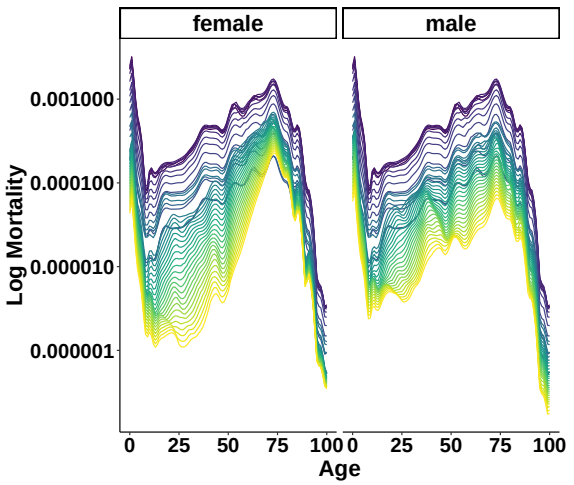

(VI) PLAT model, TD

FIGURE 3.9: Projected malaria mortalities for Kenya using the PS, CPS and PL models

We also observed that the irregular mortality series were better modelled using the PL model and the top-down reconciliation approaches. This observation was expected because, compared to the APC model for example, the PL model had two additional parameters, as discussed in Section 3.2.4. These additional parameters enhanced the capability of the PL model to capture more mortality features.

It is noteworthy that, for irregular series, the differences in mortality at older and younger ages may not have been consistent. This irregularity may have made estimating these parameters harder or resulted in overfitting. However, the actual differences were not substantial. Therefore, we still opted to use the PL and CPS models for consistency.

Additionally, we observed from Table 3.4 and Figure 3.8 that of the two models, the CPS model outperformed the PL model on male and female mortality. However, we fitted these models to both male and female mortality.

We then used them to project female and male mortality up to 2040. For presentation purposes, we only present the projections obtained from the CPS model for females and the CPS model for males using the top-down reconciliation approach in Figure 3.10.

Mortality was projected to continue improving over the years, as expected. Some causes had higher mortality improvements than others. The projected improvements depended on the rate of improvements over the previous years. The malaria mortality improvements were noticeable due to increased efforts towards the fight against malaria. However, these improvements were likely to be curtailed by the emergence of antimalarial resistance (Lu et al., 2017). If this is not swiftly addressed, the mortality improvements from malaria are likely to be significantly less in the future, or even wholly reversed.

Additionally, it is noteworthy that more than the projected mortality improvements are needed to achieve SDG goal 3.3, which aims to end the malaria endemic by 2030 (see United Nations General Assembly [UN-GAOR], 2015, Goal 3.3). Even more worrying is the meagre mortality improvements projected for infants most affected by the malaria endemic. Therefore, to be on track with SDG goals, more effort and innovative methods must be applied in the fight against malaria. Otherwise, this goal may not be achieved.

As expected, most mortality improvements occurred at older ages. While this result could have been due to improved care-seeking at these older ages, these improvements were also driven by fewer people attaining these ages. As such, minor mortality improvements in the past are likely to significantly impact the trend in mortality improvements.

For example, say the number of people alive at age 90 increases from two to three. That is a 50% increase. However, if the number increased from four to five, it would be a 25% increase. Therefore, a slight improvement would disproportionately show a significant mortality improvement if the numbers are lower.

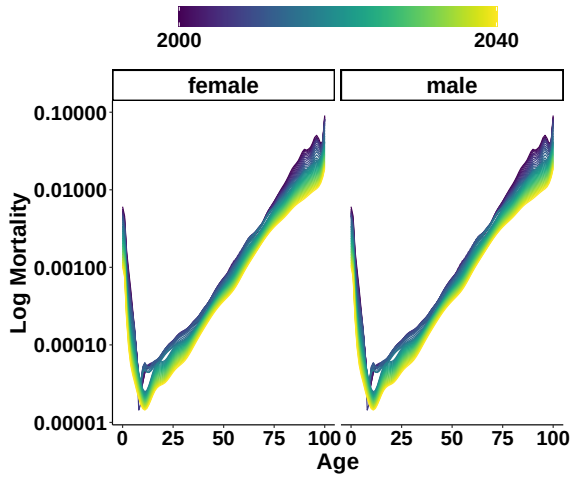

(I) LRI

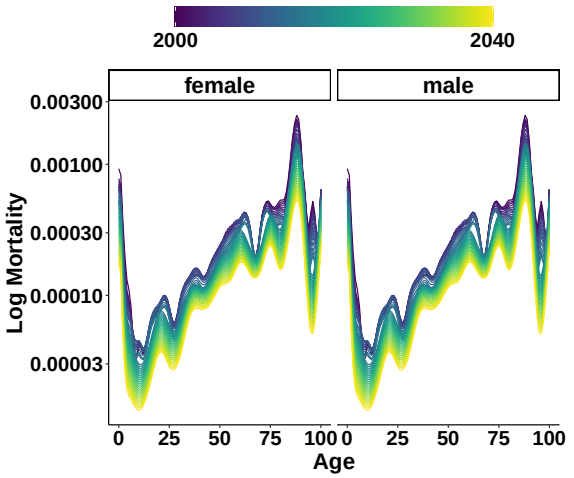

(II) Meningitis

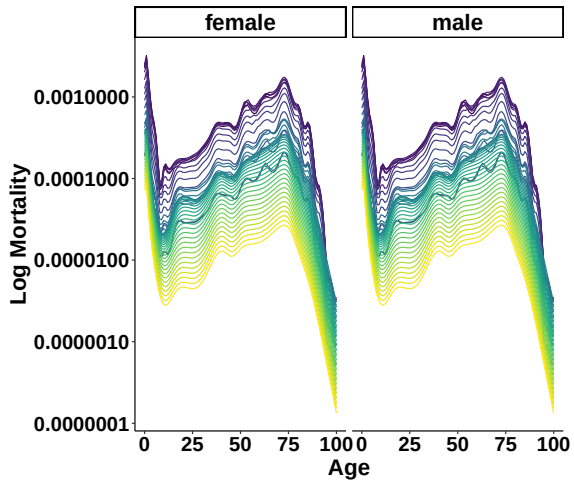

(III) Malaria

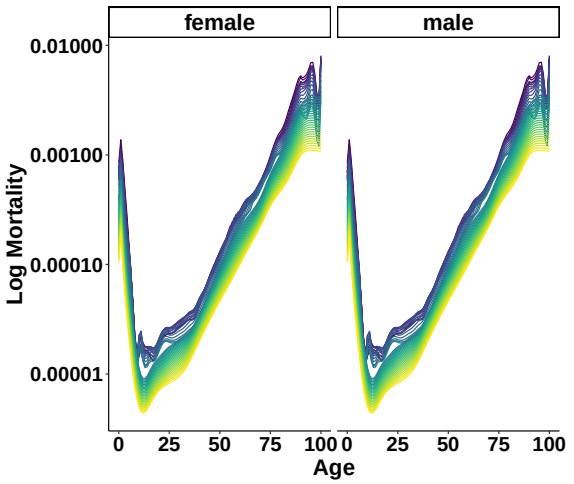

(IV) Deficiencies

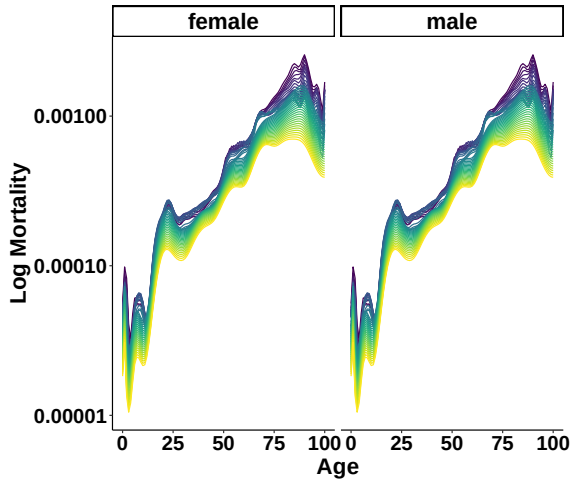

(V) Injuries

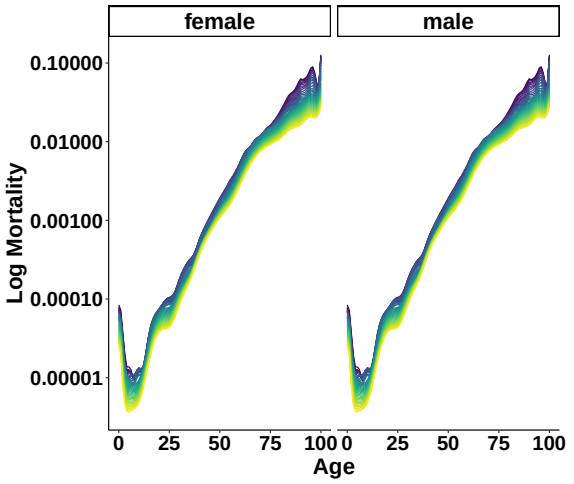

(VI) Cardiovascular

FIGURE 3.10: Projected CoD mortality for Kenya

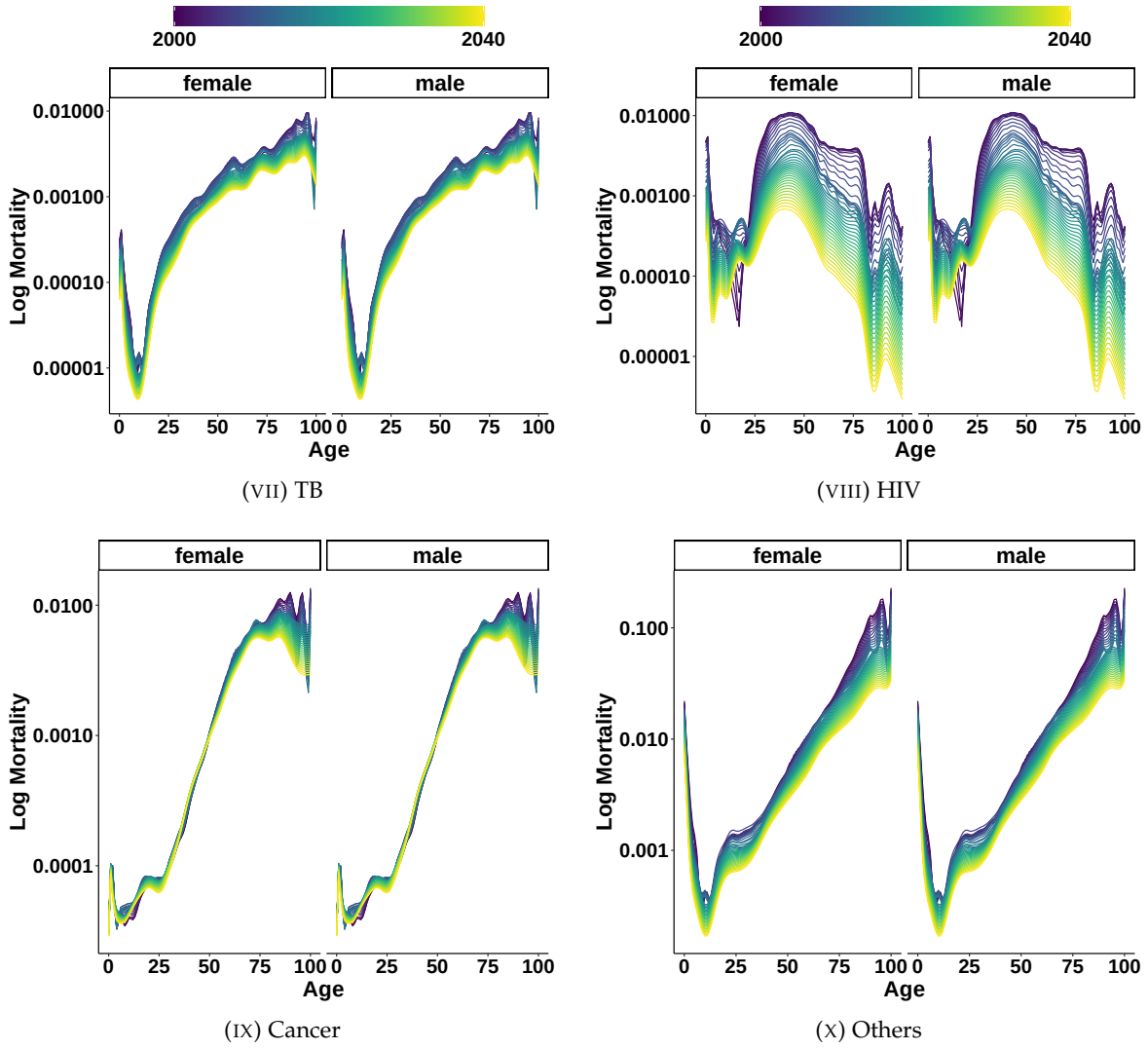

(VII) TB (VIII) HIV

(IX) Cancer (X) Others

FIGURE 3.10: Projected CoD mortality for Kenya

Cardiovascular diseases and LRI significantly affect the older generations. While cardiovascular diseases affect males more than females, LRI affect females to a larger extent. Moreover, the mortality improvements for these two CoDs are lower than for other causes, and all other age groups.

Mortality improvements from cancer are almost unnoticeable except at younger and older ages. We believe this indicates a lack of early diagnosis and prompt treatment. Therefore, it is essential to emphasise the need for civic education on cancer treatment.

Despite the government's expansion of its health coverage to include cancer treatment and medication (Makau-Barasa et al., 2020), the stigma attached to formal cancer treatment (Makau-Barasa et al., 2018) has not been sufficiently addressed. The government must put more effort

into educating its citizens on the importance of seeking cancer treatment early.

Unfortunately, despite the Kenyan government declaring cancer a national disaster, little has been done to build citizens' confidence in formal treatment. It is pointless to have the best facilities if no one uses them. If nothing is urgently done, then the considerable investment the government is pumping into state-of-the-art cancer centres would all be for nothing.

A recent study by Wambalaba et al. (2019) cited a strain in current healthcare facilities: most of the cancer-related health facility demand was from patients in later stages, who ended up requiring admission for optimal care. A more serious and proactive approach to addressing the cancer menace needs to be realised, beginning with the state. Therefore, early diagnoses and interventions are needed, with enough resources to treat it quickly before it progresses to later terminal stages.

We also observe a pattern in the age domain in some causes, particular malaria and meningitis, as shown in Figures 3.10ii and 3.10iii. Maternal immunity can be acquired for both of these causes (Cohn et al., 2010; Gonzales et al., 2020) but wane after sometime, which might partially explain the shape of the mortality curve over the first few year. As the immunity wane, the individual become more vulnerable to the disease hence the increase in mortality. However, for meningitis, this is boosted through vaccination which also wane over time (Gituro et al., 2017), which explains the mortality pattern. For malaria, the pattern is slightly different as the immunity acquired from exposure to mosquitoes is gradual. It is also important to note that mortality data for malaria are derived through vector[25] and human population dynamic analyses (Bakary et al., 2018) which may affect the mortality pattern.

Historically, per Figure 3.10viii, we observed an increase in HIV mortality among young adults,[26] although it was projected to improve in future. From the graphs, HIV has affected females more than their male counterparts, except at younger ages.

The observed higher mortality among females could be attributed to delayed diagnosis. A study by Kako et al. (2013) indicated that Kenyan women, especially those residing in rural areas, were often diagnosed only after displaying AIDS-related symptoms.[27] Furthermore, the research highlighted that women in Kenya, in general, tended to delay seeking treatment for their symptoms. These findings align with previous research underscoring missed opportunities for early HIV diagnosis, particularly among women.

It is also known that the risk of HIV seroconversion among females is significantly higher compared to their male counterparts (Scully, 2018). As expected, this disparity would translate to higher prevalence and higher mortality.

[25] Here, vector refers to the mosquito carrying the malaria parasite.
[26] Between ages 18 and 30.
[27] This are symptoms manifasted after HIV progresses to AIDS.

In addition, most cases of HIV female mortality in Kenya were reported among sex workers who intentionally do not take antiretroviral treatment, citing adverse side effects affecting their daily lives (Mantell et al., 2022). However, this trend is expected to change with improvements in antiretroviral therapy. This example reniforces that mortality patterns require flexible models for choosing which historical patterns to include in the modelling.

Finally, we presented the projected all-cause mortality curves in Figure 3.12 for males and females, based on the models we selected. As discussed, the models were selected based on their out-of-sample performances and the sensibleness of the forecasts.

The volatility in male mortality, especially in old age, was still evident in the projections, irrespective of our method. In Figure 3.12, mortality rates above age 50 for females remained relatively stable as expected since they were less sensitive to the model.

However, mortality around the accident age, spilling into young adulthood, was highly sensitive to model selection, especially for females. This result was attributable to an earlier note that mortality exhibited an upward trend around young adulthood ages.

Therefore, Figure 3.12 indicates an opportunity for the hybridisation of models to capture all the trends at different age ranges. While several models in the literature could be evaluated, this study aimed to apply the universally accepted models to CoD modelling while retaining the academic rigour required for such a study. In this regard, testing the newer entrants into the mortality modelling literature was not part of the main objective and, therefore, beyond the scope of the current research.

Notably, small extensions of the models were attempted. A partially parametric extension of the LC model was promising, which can be an avenue for further research, especially when using noisy mortality data as used in this research.

Given that there was no significant departure from the mean mortality level of the projections from all the models, we are convinced that new models may not significantly impact the overall mortality level, except for female mortality in young adulthood.

When smoothness is preferred, as is always the case, the CPS model is recommended as a good choice. While other models showed an unexpected mortality decline at older ages, the CPS model seemed consistently fair. The PL model was close in both cases, particularly with female mortality.

We also investigated projected mortality improvements over the years for the selected ages and found that other than for very young ages, a deceleration in mortality improvements was observed in the recent past, and this trend is projected to continue.

We also fitted stochastic mortality models to quantify the uncertainty within our estimates. Thus, we applied the residual bootstrap algorithm to construct confidence intervals for these

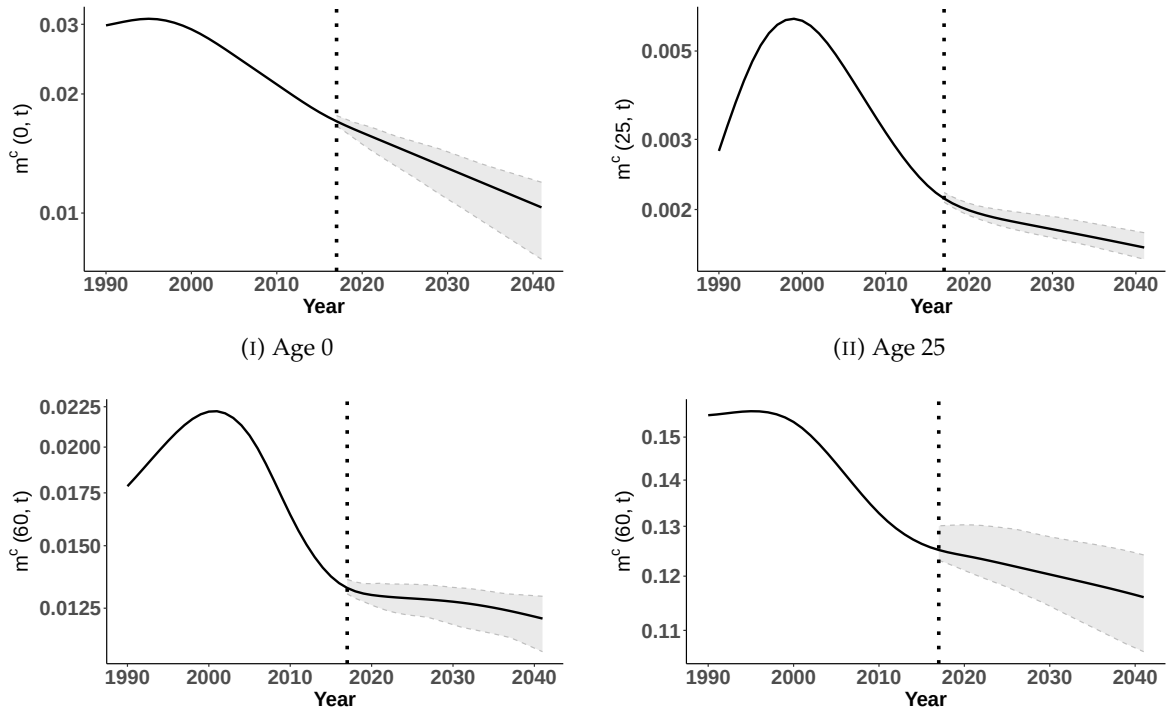

(I) Age 0 (II) Age 25

(III) Age 60 (IV) Age 85

FIGURE 3.11: Female mortality forecasts at selected ages and their confidence interval

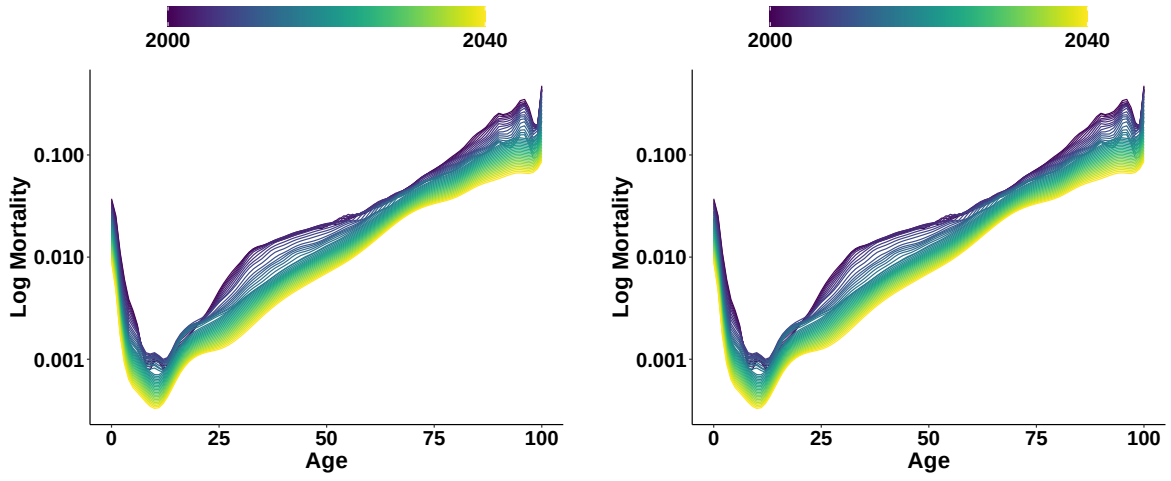

(I) Female (II) Male

FIGURE 3.12: Projected Kenyan mortality upto 2040 for females and males

projections. For example, Figure 3.11 shows the mortality improvements for females at selected ages, including the point estimates and the confidence intervals.

Generally, we observed that, at older ages, the uncertainty around mortality estimates increased (see Figures 3.11i to 3.11iv) due to the decline in the amount of available data at these ages. This observation was true for both males and females.

We then used these projections to calculate the projected mean lifespan and lifespan variations. Our model projected a female life expectancy of 73.3 years [[95% prediction interval (PI): 72.4, 74.1] in 2042, compared to the UN's 70.0 years (UNPD, 2022). It also projected male life expectancy as 65.12 years [95% PI: 64.78, 65.54] in 2042 compared to the UN's 64.54 years. We attributed this improvement to the more flexible modelling ability of the CPS model to capture diverse mortality patterns across the different CoDs.

The model also projected that the average number of life years lost at birth would smoothly decline from 15.9 years in 2016 to 13.8 years [95% PI: 13.6, 14.0] in 2042. Kenya's population is, therefore, predicted to age more quickly under our model than previously projected. This finding has potentially significant implications for healthcare, aged care, and government welfare financing. An older population will likely increase healthcare and demand for elderly services, so proper planning is essential.

3.4 Application to Population Projections

One of the applications of mortality modelling in demography is in population projections that are often produced for various reasons, including government planning for social services, budgetary requirements, health care planning, and financing (Thomas, 2018), including providers of these services. Commonly used as the denominator in most economic, demographic, and epidemiological indicators, the accuracy in estimating and modelling this denominator can never be over-emphasised.

To construct a population projection model, the classical demographic equilibrium equation,

$$N(T) = N(0) + B(0,T) + G(0,T) - D(0,T) \tag{3.4}$$

was applied, where $N(T), N(0), B(0,T), G(0,T)$, and $D(0,T)$ were the population at time T, initial population, number of live births in $(0,T)$, net migration in $(0,T)$ and the number of deaths in $(0,T)$, respectively (Preston et al., 2000).

In this research, models were fitted for each component of the demographic equilibrium equation, except for $N(0)$, which was readily available. Then, Equation 3.4 was used to project the population to some future time T, $N(T)$. The individual elements of this model were developed as follows:

a. $D(0,T)$ was obtained from the projected mortalities through a recursive process by implementing the theory discussed in Section 3.1 on lexis diagrams. The projected mortality was then used to estimate yearly deaths, from which cohort deaths were derived. The cohort deaths were plugged into Equation 3.4.

b. $B(0,T)$ was estimated from fertility rates. For consistency, the CPS model used to model mortality was also used to model and project fertility rates. These were multiplied by the estimated mid-year population to estimate the number of expected live births at time T, $B(0,T)$.

c. Net migration rate $G(0,T)$ was finally projected using the simple linear regression model,

$$G(0,T) = 10706 - 0.255 \times G(0,0) \tag{3.5}$$

was used, where $G(0,0)$ was the net migration for the base year, obtained from the KNBS (2020).

However, using this formula only provided a point estimate, the best estimate (BE). It did not indicate the uncertainties of these estimates. It is important to incorporate these uncertainties in the population projections. Since policymakers often use population projections to make policy decisions that are arguably more used than mortality projections, it is valuable to give policymakers a range of possible scenarios. Hence, we applied non-parametric bootstrap techniques to produce the estimates' associated uncertainty. In particular, the residual bootstrap method was applied.

Additionally, we applied similar concepts as those in CPS modelling to ensure we obtained sensible outcomes. For example, we defined the acceptable male-female sex ratio to be between 0.85 and 1.3 at birth, which was within the expected sex ratio of 103 to 107 male births per 100 females (Goodkind, 2015). Higher sex ratios have been reported elsewhere (Edvardsson et al., 2018) but still within our chosen interval.

Briefly, every time a bootstrap was conducted and a projection produced, we checked the sex ratio. If the sex ratio was not within this interval, another estimate was produced. This process was repeated until a defined number of stochastic population projections at birth in a particular year were achieved. This way, we ensured we did not produce non-sensical projections where, for example, a male-female sex ratio of 0.5 was produced.

Population projections were then produced up to 2040. Using the BEs of these projections, we assessed how the population was expected to change by constructing population pyramids, as shown in Figure 3.13.

Most noticeable were the increases in dependency ratios and the proportion of the population retiring. According to the projections, the total dependency ratio is set to decrease from 75.2% in

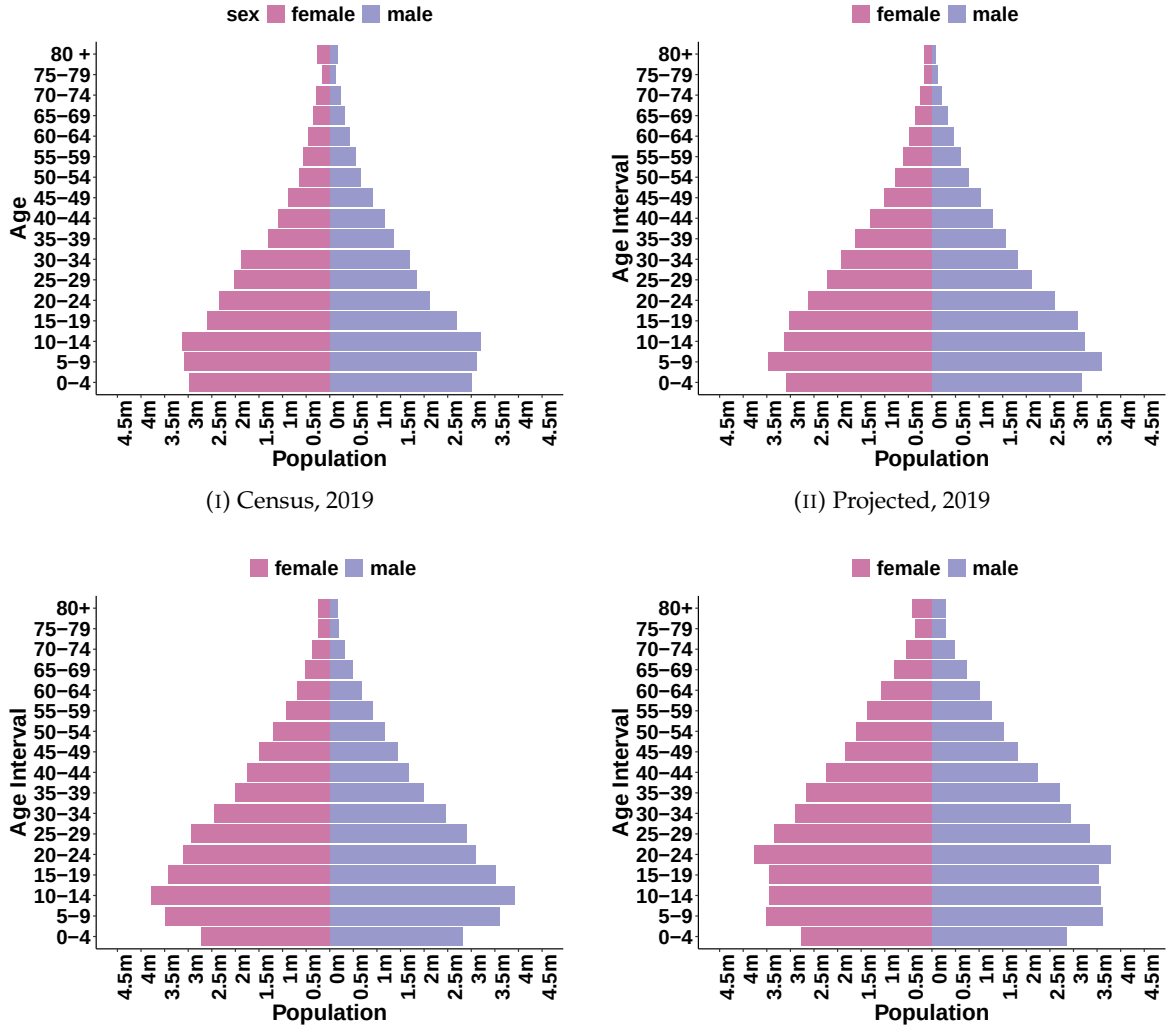

(I) Census, 2019

(II) Projected, 2019

(III) Projected, 2029

(IV) Projected, 2039

FIGURE 3.13: Projected population pyramids upto 2039 for Kenya

2019 to just over 50% in 2039, partly due to the shrinking birth rate and a reduction in mortality over the years. This trend consequently leads to increased life expectancy.

Notably, these projections did not consider technological advancements, including advances in medicine and medical research. Although they may be implicit in past mortality improvements, technological advances have significantly increased over the last few years, so it may not be easy to quantify and incorporates these in our current models.

With all these external factors held constant, the number of working-age people is set to increase significantly. With a significant cohort set to enter the labour market, wages will likely plummet due to increased competition unless there is an intervention. Without one, living standards may decrease and cause mortality to rise. The proportion of people retiring is also likely to increase

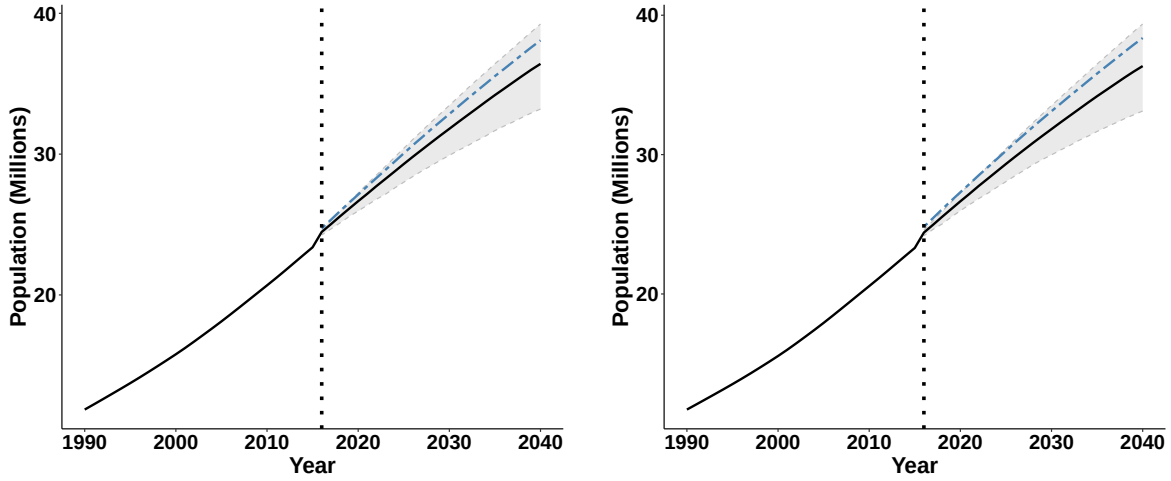

(I) Projected Population, Female

(II) Projected Population, Male

FIGURE 3.14: Projected population estimates upto 2040 for females and males

TABLE 3.6: How our population projections compared to different official estimates at different times

	Year	Males	Females	Intersex	Total
UNDOP Estimates	2017	24,950,142	25,271,004	-	50,221,146
KNBS Estimates	2017	23,298,547	23,608,248	-	47,006,795
Our Estimate	2017	23,620,867	24,492,905	-	48,113,772
UNDOP Estimates	2019	26,122,382	26,451,585	-	52,573,967
2019 Census	2019	23,548,056	24,014,716	1,524	47,564,296
Our Estimate	2019	23,973,048	25,583,937	-	49,556,985
UNDOP Estimates	2029	32,363,444	32,777,764	-	65,141,208
Our Estimate	2029	26,725,009	28,043,203	-	54,768,212
UNDOP Estimates	2039	38,803,084	39,394,937	-	78,198,021
Our Estimate	2039	31,046,582	31,371,060	-	62,417,642

substantially.

Generally, we observed that Kenya's population has started to show signs of ageing. The fiscal burden will be felt, so without proper planning, the wellbeing of those attaining retirement will be jeopardised.

Moreover, as the Kenyan government rolls out UHC, the financing question must be accurately assessed. The consequences of not having a forward-looking approach can never be overemphasised.

Due to the complex relationship between the different model parameters, the residual bootstrap approach was preferred to estimate the uncertainty. We, therefore, conclude this section by providing population projections and their associated uncertainties.

Figure 3.14 shows the projected population and the associated 95% prediction interval alongside the estimates provided by the UN's population division. The solid black line is our estimates, the gray area is the 95% prediction interval for our estimates, and the steel-blue dotted line shows the UN population division's estimates. Although the UN estimates fall within our prediction interval, they are noticeably greater than our best estimate projections, exceeding our best estimates by over 20% by 2039.

We also compared our projection estimates with official estimates, as shown in Table 3.6. Our estimates compared well with actual[28] and official estimates.

Additionally, we compared the projections when the CPS and the PS models were used. We established that for the PS model, the prediction intervals widened faster than the CPS model and remained wider over the projection period. This result further showed the usefulness and flexibility of the CPS model. Areas of further improvement to this model have been exhaustively discussed by Camarda (2019).

[28] Results from recent 2019 census.

Chapter 4

Implications of CPS Model Constraints

In this chapter, we discuss the implications of using the CPS model for modelling mortality data.

We fitted various stochastic mortality models and applied forecast reconciliation approaches to model and forecast CoD data from Kenya. By evaluating model fits and their forecasting performances through out-of-sample forecasting measures, we identified the CPS as the optimal model for Kenyan CoD mortality data. We now consider the implications of this choice.

To provide a comprehensive discussion, we compare the CPS model with two other models: one from the more restrictive APC class and another from the more flexible PS class.[1] In the APC class, we selected the APC model, an extension of the LC model that includes a cohort component, as there is evidence of cohort effects in the Kenyan data.

As outlined in Section 2.2, the CPS model implies that instead of modeling mortality rates directly, we model the rates of aging[2] in two dimensions: across ages and years. This approach allows us to apply restrictions to mortality modeling such that the projected first derivative of mortality falls within a specific range based on observed derivatives. Applying a similar restriction directly to mortality data results in a significant loss of mortality information that could be valuable for modeling and forecasting.

To illustrate this, consider Figure 4.1, which presents HIV/AIDS mortality in Kenya. The first column are plots of log mortality, while the second column shows rates of aging. The first row represents a case where only 95% of fluctuations in the data are considered.

As shown in Figure 4.1i, directly applying quantiles to mortality data to limit the prior information considered results in a greater loss of mortality data compared to analysing the relative derivative. The latter approach preserves most of the information, discarding only extreme fluctuations, as illustrated in Figure 4.1ii.

To illustrate this further, consider the second row of Figure 4.1, which demonstrates the effect of cutting off 50% of prior information. As shown in Figure 4.1iii, directly applying quantiles

[1] See Appendix A.1 and Figure A.1 for a detailed discussion on model classification.
[2] First derivative of mortality. See Section 2.2 for details.

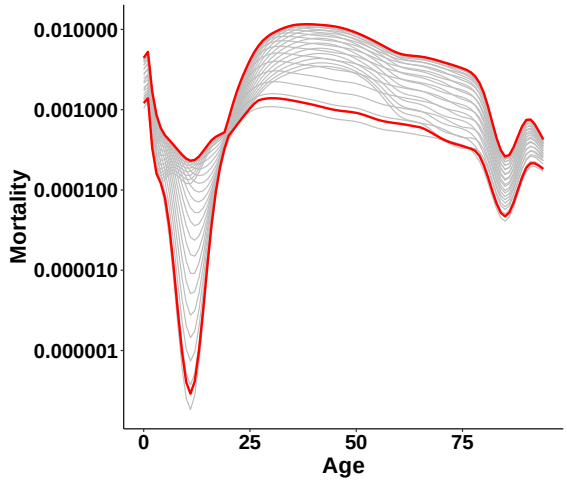

(I) log Mortality, 95% C.I

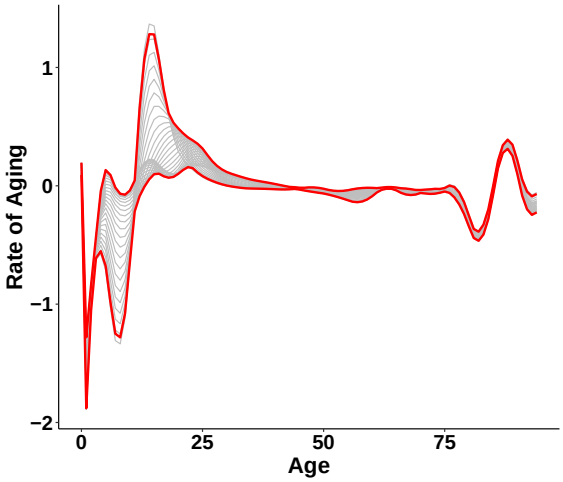

(II) Relative Derivative, 95% C.I

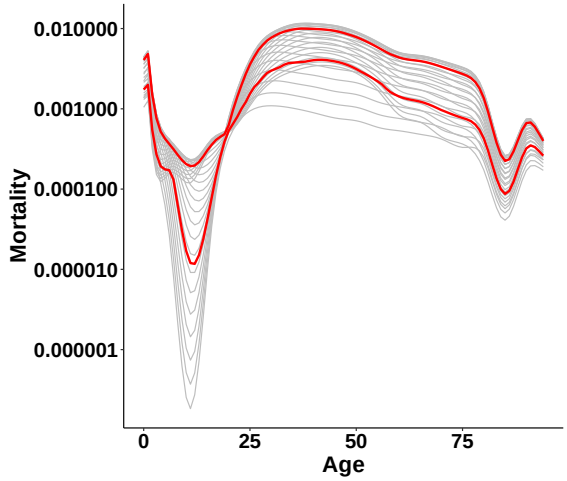

(III) log Mortality, 50% C.I

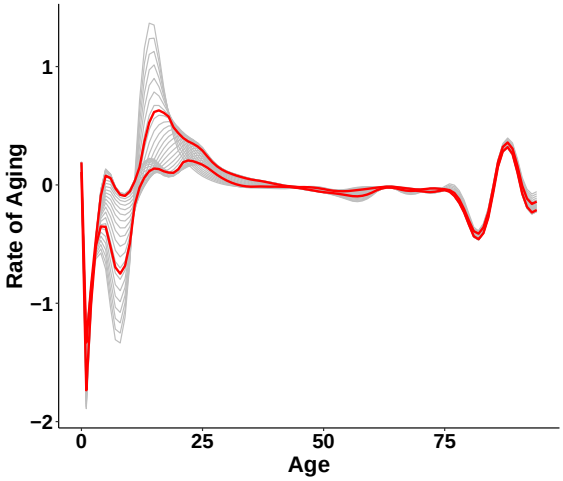

(IV) Relative Derivative, 50% C.I

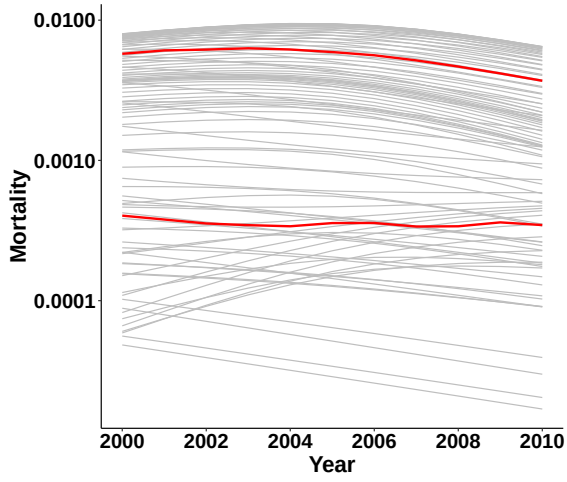

(V) log Mortality, 50% C.I

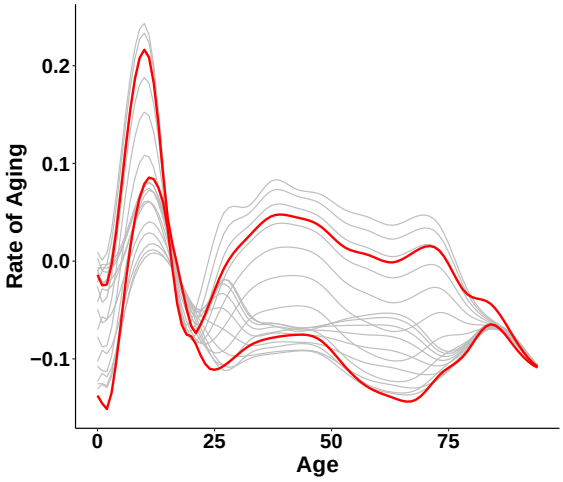

(VI) Relative Derivative, 50% C.I

FIGURE 4.1: Motivation for the CPS model

to mortality data results in consistent data loss across all ages. The primary objective of this restriction is to remove sharp fluctuations that, in the modeller's professional judgment, are unlikely to recur.

Applying this approach to the rate of aging instead (Figure 4.1iv) effectively eliminates sharp HIV/AIDS-related mortality fluctuations at specific ages – particularly among teenagers and young adults, who were the most affected by the HIV/AIDS epidemic in the early 1990s (Waruru et al., 2021) – while preserving the overall mortality structure. This method successfully achieves the objective without discarding excessive mortality data.

Thus far, we have considered cases where these restrictions are applied in the age domain. However, it is also possible to apply them in the time domain, as shown in Figures 4.1v and 4.1vi. Figure 4.1vi shows that applying the restriction in the time domain "cuts off" fluctuations across all ages for specific years,[3] in this case, the HIV/AIDS-related mortality observed in the 1990s.[4]

Formally, using the notation from Section 2.2, the flexibility of the CPS model stems from the ability to constrain future rates of aging within a certain interval, say δ_L^t and δ_U^t, representing the lower and upper bounds, respectively. This enables the model to disregard past mortality patterns that are unlikely to recur.[5]

The choice of confidence intervals for δ reflects the forecaster's judgment on how past mortality should inform future projections. Different values of δ_L^t and δ_U^t may be used based on varying perspectives on historical mortality and future trends.

Moreover, the researcher could choose past mortality patterns to include in the modelling based on anticipated future developments. A more pessimistic belief about the past could be expressed by utilising less information in determining future mortality, while a more optimistic belief would usually have wider confidence intervals.

This flexibility, explored in this thesis, demonstrates that appropriately chosen restrictions can replicate results from different classes of mortality models. Figure 4.2 illustrates this, using mortality data up to 2006 to fit the models and data from 2007 to 2016 for cross-validation. We use RMSE and MAPE for cross-validation, where CPS-5% denotes a 5% constraint level on the time dimension and 50% on the age dimension, CP-50% represents a 50% constraint on time and 95% on age, and CP-95% applies a 95% constraint on both dimensions.

[3]This is unlike Figure 4.1iv, which targets only ages with high fluctuations. Specifically, the rate of aging in Figure 4.1vi has been calculated using Equation 2.18, while that in Figure 4.1iv is calculated using Equation 2.17. Calculating the rate of aging on the time domain is useful when the goal is to exclude mortality for specific years entirely, which based on professional judgment are unlikely to recur.

[4]See Section 3.1.4 for a detailed discussion.

[5]For instance, the high HIV mortality in Kenya in the early 90s, prior to widespread antiretroviral treatment availability, is unlikely to be observed in future.

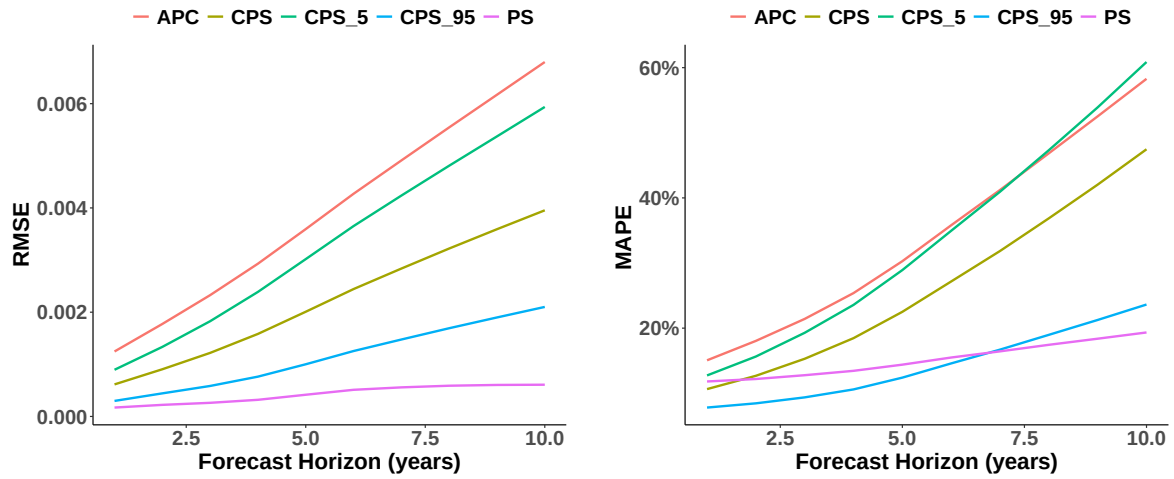

(I) RMSE, HIV/AIDS (h=6)

(II) MAPE, all-cause (h=6)

FIGURE 4.2: Out-of-sample forecasting using APC and PS models, and CPS model at three constraint levels

As shown in Figure 4.2i, CPS effectively models irregular mortality patterns, such as those observed in HIV/AIDS. Generally, the more irregular the pattern, the more valuable expert judgment becomes, as not all information in irregular mortality is useful.

In our case, HIV/AIDS mortality data prior to the availability of ARVs—particularly for teenagers and individuals around the age of 25—was not valuable for predicting future HIV/AIDS mortality in Kenya. Consequently, the modeling process could be improved by eliminating this information. The CPS methodology allowed us to achieve this without discarding excessive data. As demonstrated in Figure 4.2i, applying this approach enhances the model's forecasting ability.

For a mortality curve with a "typical" mortality pattern and almost unidirectional[6] mortality improvements, CPS shows a very smooth sliding scale in performance between the more restrictive APC model and the more flexible PS model, as seen in Figure 4.2ii.

Since all-cause mortality has fewer irregularities than CoDs, the constraint parameters of the CPS model can be chosen to produce similar results as the APC and PS models. However, the information to be utilised for mortalities with irregular patterns can be subjective. The rule of thumb is to use similar figures as Figure 4.1 to select the appropriate level of information to include, as outlined by Camarda (2019).

For example, in modeling HIV/AIDS mortality, excluding early-age mortality data significantly improved model performance without affecting overall structure (Figure 4.1iv). Consequently, the CPS model provided a sliding scale model from the restrictive type of models, such as the

[6]Mortality that had consistently improved or worsened over time.

TABLE 4.1: MAPE for all-cause mortality for males and females

	Female			Male		
Model	BU	TD	MinT	BU	TD	MinT
APC	15%	16%	17%	19%	17%	18%
PS	12%	13%	16%	15%	14%	19%
CP-5%	16%	14%	14%	14%	15%	17%
CP-50%	13%	12%	11%	12%	14%	13%
CP-95%	11%	11%	10%	12%	13%	11%

TABLE 4.2: RMSE for selected summary measures for the different CPS model constraint levels

	Female			Male		
Model	η	e_0	$e_0^\dagger$	η	e_0	$e_0^\dagger$
APC	0.103	0.483	0.873	0.040	0.879	1.041
PS	0.022	0.251	0.112	0.016	0.396	0.342
CPS-5%	0.108	0.464	0.574	0.035	0.747	0.928
CPS-50%	0.027	0.313	0.388	0.039	0.588	0.900
CPS-95%	0.023	0.297	0.183	0.014	0.464	0.588

LC class, to the more flexible PS models. To further illustrate, we calculated the MAPE for all-cause mortality, the results of which are presented in Table 4.1.

The RMSE for out-of-sample forecasts for the life expectancy and life span variation based on the three restriction levels was also calculated and the results presented in Table 4.2. As expected, we can closely replicate the results of the PS and APC models by adjusting the restriction levels of the CPS model. Additionally, it allowed us to flexibly incorporate prior information about mortality without changing overall mortality patterns.

It is important to note that, the choice of the constraints must be justified, whether in the age or time domain. For example, from Figure 4.1, a tighter restriction on the time domain corresponds to an assumption that the improvements over time[7] were linear, implying that the researcher believed that the time component could be sufficiently modelled using models such as a simple RWD model.

[7] Typically k_t in APC class of models.

Chapter 5

Conclusion

5.1 Summary of Findings

Most African countries have experienced a sharp decline in mortality rates. As part of the Sustainable Development Goals (SDGs), all UN member states have unanimously agreed to strive for and achieve Universal Health Coverage (UHC) by 2030. Since most African countries are UN member states, they are also committed to this goal. However, achieving UHC poses a significant financial challenge for these nations, given their already stretched financial budgets.

Additionally, the ageing population and high fertility rates present further challenges, especially as the global push for UHC continues. Without a comprehensive understanding of mortality trends and their long-term implications, it may be difficult to accurately predict the financial consequences of such policy decisions and effectively plan for them.

Therefore, we fitted mortality models that can help us understand mortality trends, and these mortality models can be used to improve population projections.

First, we introduced methodologies for developing mortality data, particularly in cases where data limitations are pronounced. Using these methodologies, we constructed mortality data for Kenya by integrating information from various population data sources and estimating mortality rates at older ages where data was sparse. Given the scarcity of mortality analyses in Kenya and the broader region, we aim to make our data publicly available to encourage further research and help bridge this gap. Additionally, these data could serve as proxy estimates for countries with similar socio-economic and geopolitical profiles.

Next, we analysed Kenya's historical mortality data to understand trends and their underlying causes. Our analysis demonstrated how such data could be used to evaluate government policies. For instance, we found evidence suggesting that policies such as the expansion of free primary healthcare coverage in Kenya[1] contributed to improved mortality outcomes. We also observed trends consistent with findings reported elsewhere, such as rising cardiovascular mortality (Roth et al., 2020) and stagnation in malaria control progress (Noor & Alonso, 2022), reinforcing the need for renewed global efforts against malaria (Elnour et al., 2023).

[1] Such as the expansion of the civil servants' healthcare scheme. See section 3.1.4 for details.

Further exploration of historical mortality data allowed us to draw inferences that could inform policy changes. For example, we noted that some persistent trends, particularly in neoplasms, were likely driven by low uptake of formal healthcare services (Sayed et al., 2019). Without strategic intervention, these trends were projected to continue. As discussed elsewhere (Gakuya et al., 2020; Omara et al., 2022), regulating and legislating traditional medicine could help mitigate these trends, particularly as its widespread use is influenced not only by socio-economic factors but also by deep-rooted cultural beliefs that could be addressed through educational campaigns.

We then evaluated various mortality models, including Camarda's recent model (Camarda, 2019), as well as reconciliation methodologies to ensure that mortality forecasts remain within a plausible range. After assessing these models and reconciliation approaches, we concluded that the novel CPS model was the most appropriate for our cause-of-death (CoD) mortality modeling.

The CPS model allowed us to integrate constraints based on past observed CoD mortality fluctuations. We explored different constraint levels and determined that the 50% constraint, as suggested by Camarda, was most suitable for Kenyan mortality data. Furthermore, for causes with noisy mortality patterns, such as HIV and malaria, incorporating expert judgment to select appropriate constraints significantly improved our model's performance.

Specifically, we applied the CPS model to Kenyan mortality data from 1990 to 2016 and generated projections through 2040. We demonstrated that the CPS model produces superior forecasts compared to the APC and PS models and used reconciliation methods to ensure coherence. Out-of-sample results indicated that the CPS model was stable and not highly sensitive to the reconciliation approach used.

The CPS model allowed us to constrain the selection of data used in modeling based on observed fluctuations. While applying constraints without justification can be subjective, expert-informed judgments make the CPS model a transparent tool for excluding data deemed unsuitable for predictions.

For example, temporary changes in healthcare practices, population risk factors, or specific events may lead to fluctuations that are not expected to persist in the future. Imposing constraints in the CPS model to exclude such fluctuations can improve forecasting accuracy.

This methodology was particularly useful for CoD mortality data, where identifying the cause of specific fluctuations is more feasible than with aggregate data. This provides greater opportunities to incorporate expert judgment when selecting parameter constraints.

We showed that constraint parameters for models using Kenyan CoD data could be adjusted to yield results similar to either restrictive models, such as the APC model, or flexible models like the PS model. Thus, the CPS model can also function as a "what-if" tool for modeling mortality

data with erratic patterns, effectively serving as a sliding scale between restrictive and flexible models. Adjusting age constraints had minimal impact on forecasting outcomes.

Using the CPS model, we projected life expectancy increases by 3.3 years beyond the UN's projections. In a resource-limited country like Kenya, where many nations are striving to achieve UHC, this finding has significant implications for healthcare budgeting.

Three forecast reconciliation approaches were assessed, and we found that applying reconciliation improved forecasting accuracy. While modeling individual causes offers advantages, challenges remain in handling noisy and irregular patterns, especially with commonly used models. Low mortality rates contributed to significant out-of-sample errors, affecting interpretability. However, out-of-sample model performance evaluations indicated that the CPS model was consistent across different reconciliation approaches.

Finally, we concluded by applying these models to generate population projections for Kenya. Our population projections by age and sex aligned well with official estimates. To incorporate uncertainty, we used the residual bootstrap methodology to construct prediction intervals for our point estimates. These intervals, derived using the residual bootstrap algorithm, demonstrated reasonable prediction uncertainty.

5.2 Application of Findings

Although this research has primarily utilised Kenyan data, its findings offer valuable insights and methodologies that hold relevance for other African countries. Across the continent, nations grapple with similar challenges in mortality modeling, as already discussed earlier.

Firstly, the methodologies employed here, particularly in generating mortality data and evaluating mortality models, can be adapted and applied to other African countries facing limited mortality data availability. With sub-Saharan Africa witnessing notable increases in life expectancy, challenges related to aging populations have escalated (WB, 2020). The scarcity of mortality research and data exacerbates these challenges (Haakenstad et al., 2019; Micah et al., 2020). Given the importance of accurate data for measuring progress towards global goals such as the SDGs (UN-GAOR, 2015), the methods and results outlined here serve as a valuable benchmark for researchers in other African countries.

Secondly, the potential impact of government interventions, such as free primary health coverage, on mortality trends has been highlighted. Similar analyses can be conducted in other African countries to assess the effectiveness of governmental policies and interventions in improving health outcomes.

5.3 Limitations

The following were the main limitations of this research.

a) While our research focused on developing mortality models to capture the evolving mortality landscape in Kenya, we acknowledge that various factors beyond those explicitly modeled can influence mortality trends. For instance, lifestyle factors such as smoking status have been shown to impact mortality rates. Despite acknowledging these factors in our literature review, we did not incorporate them into our models due to data availability constraints and the complexity of integrating additional variables into our framework. Future research should explore methodologies for incorporating such factors into mortality models to enhance their predictive accuracy.

b) A key aspect of our methodology involved using survivor ratios (SRs) to extrapolate mortality patterns at older ages. However, during the calculation of SRs, we observed roughness in the estimates, which we attributed to unmodeled mortality improvements over time. Notably, we did not explicitly account for these mortality improvements when estimating historical SRs, assuming that such trends would be smoothed out during the modeling and projection process. However, this approach may introduce bias into our estimates, particularly if mortality improvements vary significantly across age groups. Future research should explore methods for explicitly incorporating mortality improvements into SR calculations to improve the accuracy of mortality projections.

c) Our analysis revealed significant changes in the mortality structure of Kenya over the past three decades, posing challenges when applying mortality models within the APC class of models. To address these challenges, we had to discard a substantial amount of mortality data, potentially introducing bias into our analysis. While we attempted to mitigate this bias through rigorous model validation and sensitivity analyses, the impact of data selection bias on our results cannot be entirely ruled out. Future research should explore alternative methodologies for handling changes in mortality structure over time, such as dynamic modeling approaches that can adapt to shifting demographic trends more effectively.

5.4 Further Research

Building on our findings and addressing the aforementioned limitations, we propose several avenues for further research:

a) In Section 3.1.4, our analysis identified a significant increase in HIV-related deaths among teenagers. We have also observed a similar trend for TB-related deaths among this age group, raising questions about potential interactions between HIV and other causes of

death within this age group. Future research should investigate the potential comorbidities, and its implications for cause-of-death classification and mortality forecasting.

b) In this research, we have shown that incorporating expert opinion into mortality modelling can improve the accuracy of the forecasts. We have compared different models and applied reconciliation approaches to ensure coherence in forecasts. Shang and Booth (2020) have explored model averaging methods and applied them to fertility forecasting. There is, therefore, scope to combine the concepts outlined in this research with those described by Shang and Booth.

c) In Section 3.3, we have noted the possibility of testing hybrid models that can better capture mortality patterns at different ages. Such methods, as explored by Dodd et al. (2020) and Hong et al. (2020), are promising. Building on this work, future research could explore such advanced model averaging methods.

d) We have also explored the CoD stochastic mortality modelling alongside approaches that ensure coherence in the forecasts. We have discussed reconciliation approaches that can be used to achieve coherence. We have then applied some of these concepts to population projection. One of the sources of incoherence is the fact that these series are projected independently. Another promising field when projecting series that require coherence is functional data analysis (FDA) which has been applied in such studies as that of Erbas et al. (2010) and Lam and Wang (2022). Here is an opportunity to apply FDA to model these rates and project, say, the population.

e) When fitting mortality models, we fitted the models that are widely accepted for mortality modelling in literature. However, there are newer mortality models that have been proposed, such as those that combine various models. For example, in this research, we tested a partially parametric extension of the LC model which showed promising results. Therefore, application of such models to Kenyan mortality is an avenue for future research, especially testing these extensions on mortality data with irregular patterns.

f) Another possible area of further research is the application of the CPS model within functional mortality data analysis (see for example Shang & Hyndman, 2017, and the references therein).

Appendix A

Appendices

A.1 Classification of mortality models

Mortality forecasting methods encompass a diverse range of statistical, actuarial, and demographic techniques designed to capture the complex dynamics of mortality rates over time (Booth et al., 2002; Raftery et al., 2013). These methods often draw upon historical mortality data, socio-economic indicators, and epidemiological insights to develop robust models capable of predicting future mortality trends.

Central to the analysis of mortality rate evolution is the utilisation of models that analyse mortality rates across age, period, and cohort dimensions. And as discussed by Hunt and Blake (2020), these dimensions provide a natural framework for scrutinising how mortality rates evolve as individuals age, the influence of temporal medical and social advancements, and the lifelong mortality effects associated with individuals' birth year. Therefore, by extrapolating the impacts of period and cohort, valuable insights into the potential trajectory of mortality rates in the future can be gleaned.

For the current research, mortality models within the age-period-cohort (APC) structure are of interest, and the simple classification of mortality models presented by Hunt and Blake (2020) is adopted.

Generally, the APC class of models can be written in the form

$$\eta_{x,t} = \alpha_x + \sum_{i=1}^{N} \beta_x^{(i)} \kappa_t^{(i)} + \beta_x^{(0)} \gamma_{t-x} \tag{A.1}$$

where the left-hand side (LHS) is the link function, and the right-hand side (RHS) is the (bi)linear predictor. The predictor consists of three components: age (x), period[1] and cohort.[2]

The link function is some form of transformation of mortality rates with the following components:

a) the age component, α_x, for capturing the overall mortality pattern across ages and

[1] Or year, t.
[2] Or year of birth, $t - x$.

b) the period component, $\sum_{i=1}^{N} \beta_x^{(i)} \kappa_t^{(i)}$, showing the mortality pattern from the interaction of two functions:

   i) the age function $\beta_x^{(i)}$ and

   ii) the period function $\kappa_t^{(i)}$.

c) A cohort component, $\beta_x^{(0)} \gamma_{t-x}$, which illustrates how mortality varies based on year of birth through an interaction of age and cohort functions, $\beta_x^{(0)}$ and γ_{t-x}, respectively.

For this study, it is important to take note of the following:

a) First, the link function in Equation A.1 is a function of mortality rates, not, for example, mortality improvements as defined in such studies as that of Haberman and Renshaw (2013), among others.

b) Secondly, the representation in Equation A.1 allows for the natural inclusion of other regressors to demonstrate the impact of other factors on mortality, including smoking prevalence and macroeconomic factors, which impact overall mortality, as shown in such studies as Kleinow and Cairns (2013) and Hanewald (2011), respectively, among others. While such factors can naturally be incorporated into the model, the emphasis of the current research is on CoD mortality modelling, in which case such models may not be considered and are therefore not discussed further.

c) Thirdly, some mortality models have been calibrated to fit specific age ranges, such as Cairns et al. (2006) and its extensions, which are calibrated to fit mortality at older ages (Cairns et al., 2009). Since the primary objective of the current study is to investigate mortality trends over all ages, such models are also not considered further.

d) Finally, new research has emerged on the application of model averaging techniques in modelling such data as fertility rates, as shown by Shang and Booth (2020). These methods aim to produce better forecasts by averaging forecasts from various models using predefined weights based on the forecasting horizon. Although such methods have been applied in other research (see Bates & Granger, 1969; Clemen, 1989; Hoeting et al., 1999), their application in demographic research is limited (Shang & Booth, 2020). Since there is limited literature on evaluating such models in mortality modelling, they are not considered any further in this study.

APC models can be classified based on how the period component is modelled. Most of the models in this class have allowed for a stochastic period function, which has been desirable in most pragmatic modelling and projection applications. In particular, the allowance of this class of models for the period component to vary over time without any smooth constraints,

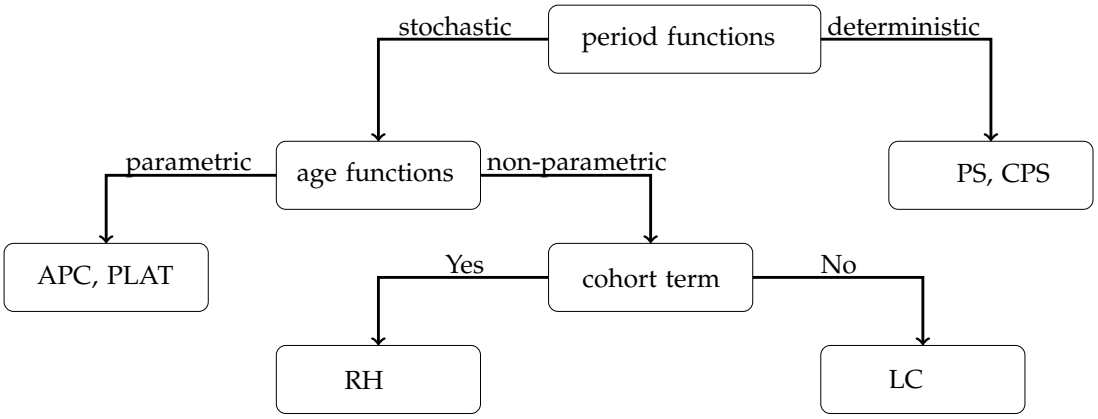

FIGURE A.1: Classification of mortality models, adopted from Hunt and Blake (2020, figure 3)

allowing stochastic and, hence, probabilistic mortality projections, is an attractive feature of most of these discrete-time mortality models.

In contrast, models that apply deterministic functions in estimating the period component have been widely used for historical smoothing and short-term projections of mortality (Hunt & Blake, 2020).

The appeal of APC models is the ability to attach a demographic significance to each estimated parameter. They can be interpreted as explaining the changes in mortality levels through age, time and year of birth based on underlying medical, biological and socio-economic factors. Additionally, the possible representation of this class of models, as in Equation A.1, allows for a more natural inclusion of other parameters that influence mortality levels.

Figure A.1 illustrates the classification of models that we evaluated in this study. Based on their period functions, we classified the models into either deterministic or stochastic. The models outlined in Figure A.1 were evaluated in this research. These models were either LC or PS model extensions or their variations. The LC model and its extensions were studied for stochastic models, while for deterministic models, PS and its variations were of interest.

There has been increased academic literature on functional data analysis (FDA) applications to mortality (Lam & Wang, 2022). However, from the mortality modelling-based industry reports that we have reviewed, there have been limited citations and applications of FDA in modelling mortality data (Boumezoued et al., 2019; Bozikas & Pitselis, 2018; Hunt & Blake, 2020). This fact was reiterated by Hunt and Blake (2020). In the spirit of producing academically defensible and overly acceptable pragmatic work, we elected not to dive into this side of modelling. Therefore, such models are not discussed further.

A.1.1 Stochastic Period Function Models

The work by Lee and Carter (1992) is considered the cornerstone of modern stochastic mortality models.[3] Lee and Carter (1992) fitted a linear model defined as

$$\log(m(x,t)) = a_x + b_x k_t + \varepsilon(x,t) \tag{A.2}$$

where:

i) $m(x,t)$ is the central rate of mortality,

ii) a_x and b_x were appropriately chosen vectors of age-specific constants,

iii) k_t was a time-varying mortality index at time t, which is an index indicating the level of mortality and hence can be rewritten as $k(t)$, and

iv) $\varepsilon(x,t)$ was an error term reflective of historical fluctuations that could not be incorporated in the model and has zero mean and some variance, σ_ε.

The model developed by Lee and Carter (1992) did not allow for such mortality intervening factors[4] as medical advances and social and behavioural influences. However, it was commonplace for most extrapolative mortality models. Neither did they attempt to capture all time and age mortality variations, citing high levels of irregularity due to historical circumstances, giving the 1918 epidemic influenza in the USA as an example. According to Lee and Carter (1992), such irregularities would diverge from the long-run trend and, therefore, should not be included in the model.

Although the LC model has been widely accepted and used in academic literature and empirical studies, it has received wide criticism over its inability to produce consistent estimates for the jump-off year[5] and the first year of the forecast. Another commonly cited drawback is in identifying the period to which to fit the LC model.

These drawbacks were explored by Tuljapurkar et al. (2000), who applied the LC model and SVD method to model mortality over 5 decades in G7 countries.[6] They observed an exponential decay of mortality over time at almost a constant rate.

In response, Wilmoth (1993) outlined two alternative methods of estimating the LC parameters: The use of the weighted least squares method through an iterative search procedure and the application of the maximum likelihood estimation method.

[3] More detailed and exhaustive discussions is outlined in the original paper by Lee and Carter (1992).

[4] In this context, mortality intervening factors are factors that improve mortality. For example, the impact of medical innovations have been documented (Goldman et al., 2005; Sunshine et al., 2019).

[5] That is, the final fitting year.

[6] The seven most economically developed countries, which are Germany, United Kingdom, Japan, Canada, United States, Italy and France.

Historically, Renshaw and Haberman (2006) were the first authors to introduce cohort effects to the basic LC model. The model,

$$\texttt{log}(m(x,t)) = \alpha_x + \beta_x^{(1)} k(t) + \beta_x^{(0)} \gamma_{t-x} \tag{A.3}$$

was proposed, where the bilinear factor $\beta_x^{(0)}\gamma_{t-x}$ was the cohort component of the model, while the other terms carried the same meaning as in the LC model. Some of the substructures considered were as follows:

a) the case where $\beta_x^{(0)} = 0$ and $\beta_x^{(1)} = \beta_x$,as the classic LC model,

b) the case where $\beta_x^{(0)} = \beta_x$ and $\beta_x^{(1)} = 0$, as a model without period effects,

c) the case where $\beta_x^{(0)} = 1$ and $\beta_x^{(1)} = 1$,as a classical APC model,

d) the case where $\beta_x^{(0)} = 1$ and $\beta_x^{(1)} = \beta_x$, and

e) the case where $\beta_x^{(0)} = \beta_x$ and $\beta_x^{(1)} = 1$.

The case where $\beta_x^{(0)} = 1$ and $\beta_x^{(1)} = \beta_x$ was found to be a stable substructure of the proposed models (Haberman & Renshaw, 2011).

By letting $\beta_x^{(1)} = 1$, we reduced the number of parameters to be estimated by 1, consequently making a more stable substructure. This reduction was particularly useful when investigating whether period and cohort effects existed in a given mortality dataset. It was accomplished by taking pairwise combinations of age-period-cohort and fitting the respective substructures to the data.

Several other attempts were made to improve this model, such as the study by Hatzopoulos and Haberman (2011), who generalised this model to include multiple bilinear period effects and cohort effect terms to obtain the model:

$$\texttt{log}(m(x,t)) = \alpha_x + k^{(1)}(t) + \sum_{i=2}^{N} \beta_x^{(i)} k^{(i)}(t) + \gamma_{t-x}^{(1)} + \sum_{j=2}^{M} \beta_x^{(j)} \gamma_{t-x}^{(j)} \tag{A.4}$$

Including multiple cohort effects has been cited not to significantly improve overall model precision while unnecessarily making model fitting more challenging. A special case study by van Berkum et al. (2014) extended Case (d) above to include two bilinear period effects. Both were arguably extensions of the LC model generalisation proposed by Booth et al. (2002).

A parametric extension of the LC model was given by Plat (2009). The study combined the LC model's static age properties with the Cairns-Blake-Dowd (CBD) model's parametric age

transformations to propose a model of the form:

$$\texttt{log}(m(x,t)) = \alpha_x + k_t^{(1)} + (x - \bar{x})k_t^{(2)} + (x - \bar{x})^+ k_t^{(3)} + \gamma_{t-x} \tag{A.5}$$

where $(x - \bar{x})^+ = \texttt{max}(0, x - \bar{x})$.

Some notable extensions of this model were studies by O'Hare and Li (2012) and Börger et al. (2013). However, these extensions have not been popular in practice due to their identifiability issues. Hence, they are not discussed further in this research.

A.2 Cause-of-Death Mortality Modelling

There has been an increase in research attention towards CoD mortality modelling in the recent past partly because of its potential to provide more insight into the drivers of mortality patterns. However, modelling mortality by cause increases the noise in the model (Li et al., 2019).

Therefore, a compromise on the amount of noise introduced by this low-level series into the modelling process and the amount of information harnessed by modelling by cause must be reached. Here, we briefly describe five main categories of CoD mortality modelling methodologies from recent literature (Boumezoued et al., 2019):

a) The first approach emanates from the classical LC model (Lee & Carter, 1992), as explored by Alai et al. (2018). Here, the causes of death are modelled using an appropriate stochastic mortality model to provide estimates of the time mortality index (see Equation A.2), which are then modelled using multivariate time series methods. Often, the time component is assumed to follow a random walk process with a drift.

   This method has been widely used in practice. The attractiveness of this type of modelling is its ability to reproduce the mortality structure of the by-cause data in its forecasts. It is also possible to incorporate expert by-cause opinions in the forecasts.

   However, the process of incorporating such opinions is not intuitive. Additionally, this method does not guarantee that the CoD forecasts will add up to the aggregate mortality forecasts, even if they are simultaneously modelled. In this method, mortality forecasts would be highly driven by the causes with the highest mortality.

b) A more recent approach to CoD mortality modelling, which can be thought of as an extension of the first approach, is utilising the dependency structure of the causes through application of copulas as seen in Li and Lu (2018). These methods utilise stochastic mortality models as well. However, in this modelling approach, instead of directly modelling the mortality rates, the estimated by-cause mortalities are first transformed into

marginal mortalities representing the marginal contribution of each cause to the overall mortality.

In contrast with the multivariate methods, the modelling and forecasting here are on the marginals. The actual mortalities are then imputed from the forecasted marginals by applying the same methodology used to estimate the marginals, but now in reverse order.

While these methods provide more insight into the by-cause mortality structures, the fact that they are modelling marginals has limited their practical applications due to difficulty in interpreting the results. Like the first approach, they do not guarantee consistent aggregation of mortality forecasts.

c) The third approach relies on expert opinion, where mortality forecasts are generated to align with expert clinical and public health opinions regarding future improvements. These methods have been explored in studies such as Canudas-Romo et al. (2016). This approach involves incorporating anticipated future changes in treatments and advancements in preventing various causes of death.

While this modelling technique addresses the shortcomings of the classical mortality modelling techniques, that is, the assumption that past clinical advancements will be the same in the future, it is subjective and resource-intensive. It requires input from a broad group of experts, and one expert's opinion may not be the same as another. It is still a good modelling approach, especially where, for example, the interest is in assessing the impact of different causes of death given a selection of possible future medical advancements.

d) The fourth approach involves modelling clinical factors as proxies of mortality. This differs from the third approach above which models mortality first, and then tries to adjust the mortality forecasts to align with medical expert opinion on by-cause future improvements (see, e.g. Foreman et al., 2012, 2018). Here, the aim is to assess the association between mortality and clinical indicators such as smoking status, physical activity and body mass index. Stochastic mortality models are then used to model and forecast these clinical indicators (see, e.g. Foreman et al., 2018, and references therein), which are used to impute future mortalities.

Such models are beneficial in modelling causes across jurisdictions and assessing the impact of different future health outcomes on mortality. However, this method heavily relies on opinions from a wide range of experts, making it an extremely resource-intensive exercise.

In addition, it requires much medical information, which may otherwise not be readily available. Even with the availability of such information, the reporting of the outcome may be impeded by confidentiality caveats, making its use difficult. Additionally, the development of such models may be too complex, so the model documentation clogs

the main aim of understanding mortality patterns, making it some black box. Notably, modelling and forecasting such clinical indicators may themselves be more difficult.

e) The last approach is the forecast reconciliation approach as applied in such studies as those of Li et al. (2019). This approach utilises the hierarchical structure of mortality models as described in Section 2.2.5.

   In the forecast reconciliation approach, appropriate stochastic mortality models are fitted to aggregate and by-cause mortalities and forecasted. The forecasts are then reconciled using an appropriate technique (see Sections 2.2.5.1-2.2.5.3) to ensure coherence in the forecasts.

   The most attractive feature of this approach is its ability to produce coherent mortality forecasts. Since mortality forms a natural hierarchy, interpreting and communicating the results from this method are easier and more intuitive. It also allows a simple approach of incorporating expert opinion and testing the impact of future medical changes such as cause elimination as discussed by Li et al. (2019).

Considering the benefits and downsides of the different approaches discussed above, we opted to use the forecast reconciliation approach in this research.

Bibliography

Abuga, J. A., Kariuki, S. M., Kinyanjui, S. M., et al. (2019). Premature mortality in children aged 6–9 years with neurological impairments in rural Kenya: a cohort study. *The Lancet Global Health*, *7*(12), e1728–e1735.

Alai, D. H., Arnold, S., Bajekal, M., et al. (2018). Mind the Gap: A Study of Cause-Specific Mortality by Socioeconomic Circumstances. *North American Actuarial Journal*, *22*(2), 161–181.

Alai, D. H., (-Gaille), S. A., & Sherris, M. (2014). Modelling cause-of-death mortality and the impact of cause-elimination. *Annals of Actuarial Science*, *9*(1), 167–186.

Andreev, K. F. (2004). A Method for Estimating Size of Population Aged 90 and over with Application to the U.S. Census 2000 Data. *Demographic Research*, *11*, 235–262.

Bakary, T., Boureima, S., & Sado, T. (2018). A mathematical model of malaria transmission in a periodic environment. *Journal of Biological Dynamics*, *12*(1), 400–432.

Barasa, E., Rogo, K., Mwaura, N., et al. (2018). Kenya National Hospital Insurance Fund Reforms: Implications and Lessons for Universal Health Coverage. *Health Systems & Reform*, *4*(4), 346–361.

Bates, J. M., & Granger, C. W. J. (1969). The Combination of Forecasts. *Journal of the Operational Research Society*, *20*(4), 451–468.

Booth, H., & Tickle, L. (2008). Mortality Modelling and Forecasting: a Review of Methods. *Annals of Actuarial Science*, *3*(1-2), 3–43.

Booth, H., Maindonald, J., & Smith, L. (2001). *Age-time interactions in mortality projection: Applying lee-carter to australia* (tech. rep. No. 85) [Working papers in demography]. Australian National University.

Booth, H., Maindonald, J., & Smith, L. (2002). Applying Lee-Carter under conditions of variable mortality decline. *Population Studies*, *56*(3), 325–336.

Börger, M., Fleischer, D., & Kuksin, N. (2013). MODELING THE MORTALITY TREND UNDER MODERN SOLVENCY REGIMES. *ASTIN Bulletin*, *44*(1), 1–38.

Boumezoued, A., Coulomb, J.-B., Klein, A., et al. (2019). *Modeling and forecasting cause-of-death mortality* (tech. rep.). Society of Actuaries.

Bozikas, A., & Pitselis, G. (2018). An Empirical Study on Stochastic Mortality Modelling under the Age-Period-Cohort Framework: The Case of Greece with Applications to Insurance Pricing. *Risks*, *6*(2), 44.

Cairns, A. J. G., Blake, D., & Dowd, K. (2006). A two-factor model for stochastic mortality with parameter uncertainity: theory and calibration. *The Journal of Risk and Insurance*, *73*(4), 687–718.

Cairns, A. J. G., Blake, D., & Dowd, K. (2008). Modelling and management of mortality risk: a review. *Scandinavian Actuarial Journal*, *2008*(2-3), 79–113.

Cairns, A. J. G., Blake, D., Dowd, K., et al. (2009). A Quantitative Comparison of Stochastic Mortality Models Using Data From England and Wales and the United States. *North American Actuarial Journal*, *13*(1), 1–35.

Camarda, C. G. (2019). Smooth constrained mortality forecasting. *Demographic Research*, *41*, 1091–1130.

Camlin, C. S., Ayadi, A. M. E., Kwena, Z. A., et al. (2017). High Mobility and HIV Prevalence Among Female Market Traders in East Africa in 2014. *JAIDS Journal of Acquired Immune Deficiency Syndromes*, *74*(5), e121–e128.

Canudas-Romo, V., DuGoff, E., Wu, A. W., et al. (2016). Life Expectancy in 2040: What Do Clinical Experts Expect? *North American Actuarial Journal*, *20*(3), 276–285.

Chaka, B., Gitari, A. T., Aloys, O., et al. (2020). Health Impacts of a Traditional Illicit Brew (Kaanga) Consumed in Meru County, Kenya. *European Journal of Environment and Public Health*, *5*(1), em0065.

Chiang, C. L. (1984). *The life table and its applications*. Malabar: Krieger.

Choge, J. K., Magak, N. G., Akhwale, W., et al. (2014). Symptomatic malaria diagnosis overestimate malaria prevalence, but underestimate anaemia burdens in children: results of a follow up study in Kenya. *BMC Public Health*, *14*(1).

Clemen, R. T. (1989). Combining forecasts: A review and annotated bibliography. *International Journal of Forecasting*, *5*(4), 559–583.

Cohn, A. C., MacNeil, J. R., Harrison, L. H., et al. (2010). Changes inNeisseria meningitidis-Disease Epidemiology in the United States, 1998–2007: Implications for Prevention of Meningococcal Disease. *Clinical Infectious Diseases*, *50*(2), 184–191.

Currie, I. D., Durban, M., & Eilers, P. H. C. (2004). Smoothing and forecasting mortality rates. *Statistical Modelling*, *4*(4), 279–298.

Dahlöf, B. (2010). Cardiovascular Disease Risk Factors: Epidemiology and Risk Assessment. *The American Journal of Cardiology*, *105*(1), 3A–9A.

Demombynes, G., & Trommlerová, S. K. (2012, May). *What has Driven the Decline of Infant Mortality in Kenya?* The World Bank.

Depoid, F. (1973). La mortalite des grands vieillards. *population*, *29*(4-5), 755–792.

Dodd, E., Forster, J. J., Bijak, J., et al. (2020). Stochastic modelling and projection of mortality improvements using a hybrid parametric/semi-parametric age-period-cohort model. *Scandinavian Actuarial Journal*, *2021*(2), 134–155.

Dowd, K., Cairns, A. J. G., Blake, D., et al. (2010). Evaluating the goodness of fit of stochastic mortality models. *Insurance: Mathematics and Economics*, *47*(3), 255–265.

Edvardsson, K., Axmon, A., Powell, R., et al. (2018). Male-biased sex ratios in Australian migrant populations: a population-based study of 1 191 250 births 1999-2015. *International Journal of Epidemiology*, *47*(6), 2025–2037.

Elnour, Z., Grethe, H., Siddig, K., & Munga, S. (2023). Malaria control and elimination in Kenya: economy-wide benefits and regional disparities. *Malaria Journal*, *22*(1).

Erbas, B., Akram, M., Gertig, D. M., et al. (2010). Using Functional Data Analysis Models to Estimate Future Time Trends in Age-Specific Breast Cancer Mortality for the United States and England-Wales. *Journal of Epidemiology*, *20*(2), 159–165.

Foreman, K. J., Lozano, R., Lopez, A. D., et al. (2012). Modeling causes of death: an integrated approach using CODEm. *Population Health Metrics*, *10*(1).

Foreman, K. J., Marquez, N., Dolgert, A., et al. (2018). Forecasting life expectancy, years of life lost, and all-cause and cause-specific mortality for 250 causes of death: reference and alternative scenarios for 2016–40 for 195 countries and territories. *The Lancet*, *392*(10159), 2052–2090.

Foreman, K. J., Naghavi, M., & Ezzati, M. (2016). Improving the usefulness of US mortality data: new methods for reclassification of underlying cause of death. *Population Health Metrics*, *14*(1).

Gakuya, D. W., Okumu, M. O., Kiama, S. G., et al. (2020). Traditional medicine in Kenya: Past and current status, challenges, and the way forward. *Scientific African*, *8*, e00360.

Gelman, A., & Auerbach, J. (2016). Age-aggregation bias in mortality trends. *Proceedings of the National Academy of Sciences*, *113*(7).

Gituro, C. N., Nyerere, A., Ngayo, M. O., et al. (2017). Etiology of bacterial meningitis: a cross-sectional study among patients admitted in a semi-urban hospital in Nairobi, Kenya. *Pan African Medical Journal*, *28*.

Global Burden of Disease Collaborative Network. (2017). *Global Burden of Disease Study 2017 (GBD 2017) Results* [data retrieved from Institute for Health Metrics and Evaluation, http://ghdx.healthdata.org/gbd-results-tool]. Institute for Health Metrics and Evaluation (IHME). Retrieved April 21, 2020, from http://ghdx.healthdata.org/gbd-results-tool

Goldman, D. P., Shang, B., Bhattacharya, J., et al. (2005). Consequences Of Health Trends And Medical Innovation For The Future Elderly: When demographic trends temper the optimism of biomedical advances, how will tomorrow's elderly fare? *Health Affairs*, *24*(Suppl2), W5-R5-W5–R17.

Gonzales, S. J., Reyes, R. A., Braddom, A. E., et al. (2020). Naturally Acquired Humoral Immunity Against Plasmodium falciparum Malaria. *Frontiers in Immunology*, *11*.

Goodkind, D. (2015). *International encyclopedia of the social & behavioral sciences* (J. D. Wright, Ed.; Second). Elsevier.

Haakenstad, A., Harle, A. C., Tsakalos, G., et al. (2019). Tracking spending on malaria by source in 106 countries, 2000–16: an economic modelling study. *Infectious Diseases*, *19*(7), 703–716.

Haberman, S., & Renshaw, A. (2011). A comparative study of parametric mortality projection models. *Insurance: Mathematics and Economics*, *48*(1), 35–55.

Haberman, S., & Renshaw, A. (2013). Modelling and projecting mortality improvement rates using a cohort perspective. *Insurance: Mathematics and Economics*, *53*(1), 150–168.

Hanewald, K. (2011). Explaining Mortality Dynamics. *North American Actuarial Journal*, *15*(2), 290–314.

Harasty, C., & Ostermeier, M. (2020). *Population ageing: alternative measures of dependency and implications for the future of work* (tech. rep.). International Labour Organization.

Hatzopoulos, P., & Haberman, S. (2011). A dynamic parameterization modeling for the age–period–cohort mortality. *Insurance: Mathematics and Economics*, *49*(2), 155–174.

Hoeting, J. A., Madigan, D., Raftery, A. E., & Volinsky, C. T. (1999). Bayesian model averaging: a tutorial (with comments by M. Clyde, David Draper and E. I. George, and a rejoinder by the authors. *Statistical Science*, *14*(4).

Hong, W. H., Yap, J. H., Selvachandran, G., et al. (2020). Forecasting mortality rates using hybrid Lee-Carter model, artificial neural network and random forest. *Complex & Intelligent Systems*, *7*(1), 163–189.

Horiuchi, S., & Wilmoth, J. R. (1997). Age Patterns of the Life Table Aging Rate for Major Causes of Death in Japan, 1951-1990. *The Journals of Gerontology Series A: Biological Sciences and Medical Sciences*, *52A*(1), B67–B77.

Hunt, A., & Blake, D. (2020). On the Structure and Classification of Mortality Models. *North American Actuarial Journal*, *25*(sup1), S215–S234.

Hyman, J. M. (1983). Accurate Monotonicity Preserving Cubic Interpolation. *SIAM Journal on Scientific and Statistical Computing*, *4*(4), 645–654.

Hyndman, R. J., Ahmed, R. A., Athanasopoulos, G., & Shang, H. L. (2011). Optimal combination forecasts for hierarchical time series. *Computational Statistics & Data Analysis*, *55*(9), 2579–2589.

Hyndman, R. J., Athanasopoulos, G., & Shang, H. L. (2021). *Hts: An r package for forecasting hierarchical orgrouped time series* [R package version 0.1.5].

Hyndman, R. J., & Khandakar, Y. (2008). Automatic Time Series Forecasting: TheforecastPackage for R. *Journal of Statistical Software*, *27*(3).

Ibrahim, R. I., Ngataman, N., & Abrisam, W. N. A. W. M. (2017). Forecasting the mortality rates using Lee-Carter model and Heligman-Pollard model. *Journal of Physics: Conference Series*, *890*, 012128.

Institute for Health Metrics and Evaluation. (2021). Gbd 2019 documentation [Accessed: 2023-03-09].

Johnson, S. C., Cunningham, M., Dippenaar, I. N., et al. (2021). Public health utility of cause of death data: applying empirical algorithms to improve data quality. *BMC Medical Informatics and Decision Making*, *21*(1).

Kagaayi, J., & Serwadda, D. (2016). The History of the HIV/AIDS Epidemic in Africa. *Current HIV/AIDS Reports*, *13*(4), 187–193.

Kako, P. M., Stevens, P. E., Mkandawire-Valhmu, L., et al. (2013). Missed opportunities for early HIV diagnosis: critical insights from the stories of Kenyan women living with HIV. *International Journal of Health Promotion and Education*, *51*(5), 267–275.

Katana, P. V., Abubakar, A., Nyongesa, M. K., et al. (2020). Economic burden and mental health of primary caregivers of perinatally HIV infected adolescents from Kilifi, Kenya. *BMC Public Health*, *20*(1).

Kenya National Bureau of Statistics. (2018). *Economic Survey 2018* (tech. rep.) [Working papers in demography]. Kenyan National Bureau of Statistics. Nairobi, Kenya.

Kenya National Bureau of Statistics. (2020, February 15). *2019 Kenya Population and Housing Census Results* [data retrieved from https://www.knbs.or.ke/?p=5621]. Retrieved April 21, 2020, from https://www.knbs.or.ke/?p=5621

Kimamo, C. (2018). Taking Care of the Aged in Kenya: The Changing Trends. *MOJ Gerontology & Geriatrics*, *3*(1).

Kleinow, T., & Cairns, A. J. G. (2013). Mortality and smoking prevalence: An empirical investigation in ten developed countries. *British Actuarial Journal*, *18*(2), 452–466.

Knoema. (2018, November 25). *Knoema enterprise data solutions* [data retrieved from https://kenya.opendataforafrica.org/aqxfiib/kenya-mortality]. Retrieved April 21, 2020, from https://knoema.com/

Lam, K. K., & Wang, B. (2022). Multipopulation mortality modelling and forecasting: the weighted multivariate functional principal component approaches. *Journal of Applied Statistics*, 1–22.

Lee, R., & Miller, T. (2001). Evaluating the performance of the lee-carter method for forecasting mortality. *Demography*, *38*(4), 537–549.

Lee, R. D., & Carter, L. R. (1992). Modeling and Forecasting U.S. Mortality. *Journal of the American Statistical Association*, *87*(419), 659–671.

Li, H., Li, H., Lu, Y., et al. (2019). A forecast reconciliation approach to cause-of-death mortality modeling. *Insurance: Mathematics and Economics*, *86*, 122–133.

Li, H., & Lu, Y. (2018). Modeling cause-of-death mortality using hierarchical Archimedean copula. *Scandinavian Actuarial Journal*, *2019*(3), 247–272.

Li, H., Lu, Y., & Lyu, P. (2021). Coherent Mortality Forecasting for Less Developed Countries. *Risks*, *9*(9), 151.

Lu, F., Culleton, R., Zhang, M., et al. (2017). Emergence of Indigenous Artemisinin-Resistant Plasmodium falciparum in Africa. *New England Journal of Medicine*, *376*(10), 991–993.

Lupia, R., & Chien, S.-C. (2012). HIV and AIDS Epidemic in Kenya: An Overview. *Journal of Experimental & Clinical Medicine*, *4*(4), 231–234.

Makau-Barasa, L. K., Greene, S. B., Othieno-Abinya, N. A., et al. (2018). Improving Access to Cancer Testing and Treatment in Kenya. *Journal of Global Oncology*, (4), 1–8.

Makau-Barasa, L. K., Greene, S., Othieno-Abinya, N. A., et al. (2020). A review of Kenya's cancer policies to improve access to cancer testing and treatment in the country. *Health Research Policy and Systems*, *18*(1).

Mantell, J., Franks, J., Zerbe, A., et al. (2022). MPrEP+ study protocol: a prospective cohort study assessing the feasibility and acceptability of an HIV pre-exposure prophylaxis (PrEP) strategy for male clients of female sex workers in Kisumu, Kenya. *BMJ Open*, *12*(11), e064037.

Mbau, R., Kabia, E., Honda, A., et al. (2020). Examining purchasing reforms towards universal health coverage by the National Hospital Insurance Fund in Kenya. *International Journal for Equity in Health*, *19*(1).

McHenry, M. S., Nyandiko, W. M., Scanlon, M. L., et al. (2016). HIV Stigma: Perspectives from Kenyan Child Caregivers and Adolescents Living with HIV. *Journal of the International Association of Providers of AIDS Care (JIAPAC)*, *16*(3), 215–225.

McNeil, D. R., Trussell, T. J., & Turner, J. C. (1977). Spline interpolation of demographic data. *Demography*, *14*(2), 245–252.

Micah, A. E., Su, Y., Bachmeier, S. D., et al. (2020). Health sector spending and spending on HIV/AIDS, tuberculosis, and malaria, and development assistance for health: progress towards Sustainable Development Goal 3. *The Lancet*, *396*(10252), 693–724.

Mkuu, R. S., Barry, A. E., Ishino, F. A. M., et al. (2018). Examining characteristics of recorded and unrecorded alcohol consumers in Kenya. *BMC Public Health*, *18*(1).

Mwangi, C. (2018). Media Influence on Public Policy in Kenya: The Case of Illicit Brew Consumption. *SAGE Open*, *8*(2), 215824401876424.

Mwau, M., Bwana, P., Kithinji, L., et al. (2017). Mother-to-child transmission of HIV in Kenya: A cross-sectional analysis of the national database over nine years (S. L. Pett, Ed.). *PLOS ONE*, *12*(8), e0183860.

Naghavi, M., Richards, N., Chowdhury, H., et al. (2020). Improving the quality of cause of death data for public health policy: are all 'garbage' codes equally problematic? *BMC Medicine*, *18*(1).

Neves, C., Fernandes, C., & Hoeltgebaum, H. (2017). Five different distributions for the Lee–Carter model of mortality forecasting: A comparison using GAS models. *Insurance: Mathematics and Economics*, *75*, 48–57.

Noor, A. M., & Alonso, P. L. (2022). The message on malaria is clear: progress has stalled. *The Lancet*, *399*(10337), 1777.

Nyarigoti, N., Awuor, Q. E., & Nyamasyo, E. (2017). The Role of Culture in Managing the Cancer Crisis in Kenya. *International Journal of Innovative Research and Development*, *6*(6).

Odhiambo, J. O., Kellogg, T. A., Kim, A. A., Ng'ang'a, L., Mukui, I., Umuro, M., Mohammed, I., Cock, K. M. D., Kimanga, D. O., & Schwarcz, S. (2014). Antiretroviral Treatment Scale-up Among Persons Living With HIV in Kenya. *JAIDS Journal of Acquired Immune Deficiency Syndromes*, *66*(Supplement 1), S116–S122.

of Washington, U. (2021). Institute for health metrics and evaluation [Accessed on March 8, 2023].

O'Hare, C., & Li, Y. (2012). Explaining young mortality. *Insurance: Mathematics and Economics*, *50*(1), 12–25.

Omara, T., Odero, M. P., & Obakiro, S. B. (2022). Medicinal plants used for treating cancer in Kenya: an ethnopharmacological overview. *Bulletin of the National Research Centre*, *46*(1).

openAFRICA. (2020, April 22). *African independent repository: Code for africa* [By code for africa] [by Code for Africa; data retrieved from https://open.africa/]. Code for Africa. Retrieved April 21, 2020, from https://open.africa/

Osano, B. O., Were, F., & Mathews, S. (2017). Mortality among 5-17 year old children in Kenya. *Pan African Medical Journal*, *27*.

Panagiotelis, A., Athanasopoulos, G., Gamakumara, P., et al. (2021). Forecast reconciliation: A geometric view with new insights on bias correction. *International Journal of Forecasting*, *37*(1), 343–359.

Permanyer, I., Spijker, J., & Blanes, A. (2022). On the measurement of healthy lifespan inequality. *Population Health Metrics*, *20*(1).

Plat, R. (2009). On stochastic mortality modeling. *Insurance: Mathematics and Economics*, *45*(3), 393–404.

Preston, S., Heuveline, P., & Guillot, M. (2000). *Demography: Measuring and modeling population processes*. Wiley.

Raftery, A. E., Chunn, J. L., Gerland, P., et al. (2013). Bayesian Probabilistic Projections of Life Expectancy for All Countries. *Demography*, *50*(3), 777–801.

Renshaw, A. E., & Haberman, S. (2006). A cohort-based extension to the Lee–Carter model for mortality reduction factors. *Insurance: Mathematics and Economics*, *38*(3), 556–570.

Roth, G. A., Mensah, G. A., Johnson, C. O., et al. (2020). Global Burden of Cardiovascular Diseases and Risk Factors, 1990–2019. *Journal of the American College of Cardiology*, *76*(25), 2982–3021.

Sayed, S., Ngugi, A. K., Mahoney, M. R., et al. (2019). Breast Cancer knowledge, perceptions and practices in a rural Community in Coastal Kenya. *BMC Public Health*, *19*(1).

Scully, E. P. (2018). Sex Differences in HIV Infection. *Current HIV/AIDS Reports*, *15*(2), 136–146.

Shang, H. L., & Booth, H. (2020). Synergy in fertility forecasting: improving forecast accuracy through model averaging. *Genus*, *76*(1).

Shang, H. L., & Hyndman, R. J. (2017). Grouped Functional Time Series Forecasting: An Application to Age-Specific Mortality Rates. *Journal of Computational and Graphical Statistics*, *26*(2), 330–343.

Sirengo, M., Muthoni, L., Kellogg, T. A., et al. (2014). Mother-to-Child Transmission of HIV in Kenya. *JAIDS Journal of Acquired Immune Deficiency Syndromes*, *66*(Supplement 1), S66–S74.

sourceAFRICA. (2018, November 25). *Kenya data portal: Demographics (kenya mortality)* [data retrieved from https://knoema.com/]. Retrieved April 21, 2020, from https://kenya.opendataforafrica.org/aqxfiib/kenya-mortality

Stevens, G. A., Alkema, L., Black, R. E., et al. (2016). Guidelines for Accurate and Transparent Health Estimates Reporting: the GATHER statement. *The Lancet*, *388*(10062), e19–e23.

Sunshine, J. E., Meo, N., Kassebaum, N. J., et al. (2019). Association of Adverse Effects of Medical Treatment With Mortality in the United States: A Secondary Analysis of the Global Burden of Diseases, Injuries, and Risk Factors Study. *JAMA Network Open*, *2*(1), e187041.

Terblanche, W., & Wilson, T. (2015a). Accuracy of Nearly Extinct Cohort Methods for Estimating Very Elderly Subnational Populations. *International Journal of Population Research*, *2015*, 1–16.

Terblanche, W., & Wilson, T. (2015b). An Evaluation of Nearly-Extinct Cohort Methods for Estimating the Very Elderly Populations of Australia and New Zealand (T. Leone, Ed.). *PLOS ONE*, *10*(4), e0123692.

Thatcher, A. R. Overview of methods for estimating population numbers at high ages from data on deaths. In: In *Old age mortality*. Old age mortality (February 8, 1993). Duke University. Duke University, 1993.

Thatcher, R., Kannisto, V., & Andreev, K. F. (2002). The Survivor Ratio Method for Estimating Numbers at High Ages. *Demographic Research*, *6*, 1–18.

The Organisation for Economic Co-operation and Development. (2017, November). Working age population.

The World Bank. (2019). *Life expectancy at birth, total (years) - Kenya.* [data retrieved from https://data.worldbank.org/indicator/SP.DYN.LE00.IN?locations=KE]. https://data.worldbank.org/indicator/SP.DYN.LE00.IN?locations=KE

The World Bank. (2020, September 22). *Life expectancy at birth, total (years) - Sub-Saharan Africa, Kenya*. The World Bank. Retrieved April 21, 2020, from https://data.worldbank.org/indicator/SP.DYN.LE00.IN?locations=ZG-KE

The World Bank. (2021). *Mortality rate, infant (per 1,000 live births) - Kenya*. Retrieved June 29, 2021, from https://data.worldbank.org/indicator/SP.DYN.IMRT.IN?locations=KE

Thomas, R. K. (2018). *Concepts, methods and practical applications in applied demography: An introductory book*. Springer International Publishing.

Tuljapurkar, S., & Boe, C. (1998). Mortality Change and Forecasting. *North American Actuarial Journal*, *2*(4), 13–47.

Tuljapurkar, S., Li, N., & Boe, C. (2000). A universal pattern of mortality decline in the G7 countries. *Nature*, *405*(6788), 789–792.

United Nations. (2017). *World Mortality 2017: Data Booklet - the United Nations*. United Nations. Retrieved April 21, 2020, from http://www.un.org/en/development/desa/population/publications/pdf/mortality/World-Mortality-2017-Data-Booklet.pdf

United Nations, Department of Economic and Social Affairs, Population Division. (2022). *World Population Prospects 2022*.

United Nations General Assembly. (2015). *Transforming our world: the 2030 Agenda for Sustainable Development* (U. Nations, Ed.; tech. rep. No. A/RES/70/1). United Nations. New York, USA.

United Nations' Population Division. (2019, November 26). *world population prospects 2019: methodology of the united nations population estimates and projections*. United Nations. Retrieved November 26, 2019, from https://www.un.org/development/desa/publications/world-population-prospects-2019-highlights.html

van Berkum, F., Antonio, K., & Vellekoop, M. (2014). The impact of multiple structural changes on mortality predictions. *Scandinavian Actuarial Journal*, *2016*(7), 581–603.

Villegas, A. M., Kaishev, V. K., & Millossovich, P. (2018). StMoMo: An R Package for Stochastic Mortality Modeling. *Journal of Statistical Software*, *84*(3).

Vincent, P. (1951). La mortalite des vieillards. *French Edition*, *6*(2), 181–204.

Vollset, S. E., Goren, E., Yuan, C.-W., et al. (2020). Fertility, mortality, migration, and population scenarios for 195 countries and territories from 2017 to 2100: a forecasting analysis for the Global Burden of Disease Study. *The Lancet*, *396*(10258), 1285–1306.

Vos, T., Lim, S. S., Abbafati, C., et al. (2020). Global burden of 369 diseases and injuries in 204 countries and territories, 1990–2019: a systematic analysis for the Global Burden of Disease Study 2019. *The Lancet*, *396*(10258), 1204–1222.

Wambalaba, F. W., Son, B., Wambalaba, A. E., Nyong'o, D., & Nyong'o, A. (2019). Prevalence and capacity of cancer diagnostics and treatment: A demand and supply survey of health-care facilities in kenya. *Cancer Control*, *26*(1), 1–12.

Waruru, A., Wamicwe, J., Mwangi, J., et al. (2021). Where Are the Newly Diagnosed HIV Positives in Kenya? Time to Consider Geo-Spatially Guided Targeting at a Finer Scale to Reach the "First 90". *Frontiers in Public Health*, *9*.

Wickramasuriya, S. L., Athanasopoulos, G., & Hyndman, R. J. (2018). Optimal Forecast Reconciliation for Hierarchical and Grouped Time Series Through Trace Minimization. *Journal of the American Statistical Association*, *114*(526), 804–819.

Wilmoth, J. R. (1993). *Computational methods for fitting and extrapolating the lee-carter model of mortality change* (tech. rep.). University of California, Berkeley.

Wilmoth, J. R., Andreev, K., Jdanov, D., et al. (2017, July 29). *Methods Protocol for the Human Mortality Database (version 6)* [Information retrieved from https://www.mortality.org/Public/Docs/MethodsProtocol.pdf on September 23, 2020.]. Retrieved December 18, 2019, from https://www.mortality.org/Public/Docs/MethodsProtocol.pdf

World Health Organisation. (2019, November 26). *Millennium Development Goals (MDGs)* (tech. rep.). World Health Organisation. Geneva, Switzerland.

World Health Organisation. (2020, February 15). *Global Health Observatory data repository* [data retrieved from https://apps.who.int/gho/data/node.home]. Retrieved April 21, 2020, from https://apps.who.int/gho/data/node.home

Young, P. W., Musingila, P., Kingwara, L., et al. (2023). HIV Incidence, Recent HIV Infection, and Associated Factors, Kenya, 2007–2018. *AIDS Research and Human Retroviruses*, *39*(2), 57–67.

Yudkin, P. L., Burger, E. H., Bradshaw, D., et al. (2009). Deaths caused by HIV disease under-reported in South Africa. *AIDS*, *23*(12), 1600–1602.